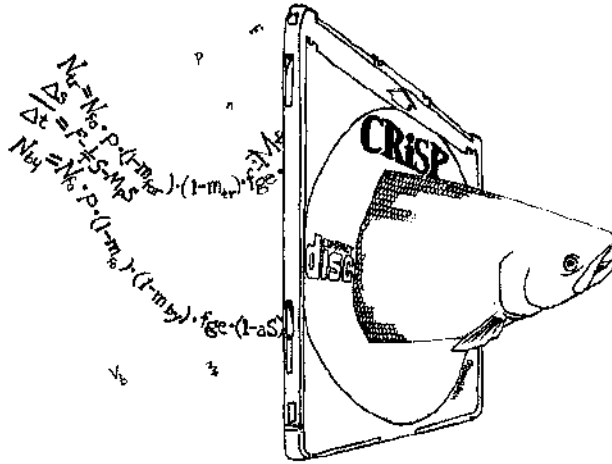


Columbia River Salmon Passage Model



CRiSP.1.6

Theory, Calibration and Validation

DRAFT

April 14, 2000

Developed by Columbia Basin Research

School of Fisheries

University of Washington

Contributors

The Columbia River Salmon Passage (CRiSP.1) model was developed as a team effort involving scientists, managers and computer programmers.

Authors

James Anderson - Principal Investigator, University of Washington
Nicolas W. Beer - Research Associate, University of Washington
Susannah Iltis - Public Information Specialist, University of Washington
David Salinger - Research Associate, University of Washington
Chris Van Holmes - Research Associate, University of Washington
Richard Zabel - Research Associate, University of Washington

with the assistance of:
Joshua Hayes and Pamela Shaw

Acknowledgments

We wish to thank the following people for their support and suggestions in the development of this model.

David Askren - Bonneville Power Administration
James Geiselman - Bonneville Power Administration
Albert E. Giorgi - Don Chapman and Associates

Funding

Model development was funded by the Bonneville Power Administration under contract:

Contract Number: DE-BI79-89BP02347

Project Number: 89-108

and U.S. Army Corps of Engineers under contract:

Contract Number: DACW68-96-C-0018

Table of Contents

I. Introduction	1
I.1 - General Description	1
I.1.1 - CRiSP.1 Submodels.....	3
II. Theory	5
II.1 - Model Computation Diagram.....	5
Reservoir Passage	6
Ecological Submodels	6
II.2 - Flows.....	7
II.2.1 - Overview of Flow Computation	7
II.2.2 - Monte Carlo Flow Calculation.....	7
Hydroregulation Models.....	8
Flow Modulation	8
Monte Carlo Flow Modulator Validation	13
Flow Loss	15
Headwater Computation.....	17
Downstream Propagation	19
II.2.3 - Scenario Mode Flow Generation	20
Headwater Modulation	21
Reservoir Volume and Flow	21
Theory for Parameter Estimation	23
Maximum Unregulated Flows.....	25
Storage Reservoirs Parameter Values.....	26
II.2.4 - Flow-Velocity-Elevation	28
Pool Volume	28
Water Velocity.....	32
Flow-Velocity Calibration	33
II.2.5 - Temperature	35
II.3 - Fish Migration	36
II.3.1 - Theoretical Framework.....	36
Probability Density Function	36
Passage Probability.....	37
II.3.2 - Migration Models	38
Implementing the Travel Time Algorithm	42
II.4 - Reservoir Survival.....	44
II.4.1 - Theoretical Framework.....	44
II.4.2 - Predation Mortality	47
General Model.....	47
Zone Specific Formulations of the Predation Model.....	48
Predator Abundance	49
Outline of Calculations for Predator Abundance	50
Predator removal adjustments	56
Predator Density /Reservoir Volume Interaction	57
II.4.3 - Supersaturation Mortality	58
Theory	58
Parameter Determination	63
II.5 - Total Dissolved Gas.....	71
II.5.1 - Introduction.....	71
II.5.2 - Gas Production Equations.....	71
Theory	71
II.5.3 - Tailrace Dynamics	74
Introduction.....	74

Separate Flows	74
Mixing	76
Entrainment	77
II.5.4 - Reservoir Dissolved Gas Distributions	83
Theory	83
Parameter Determination	85
II.5.5 - Other Gas Inputs.....	85
Total Dissolved Gas in the Tailrace.....	86
Total Dissolved Gas at a Confluence	86
Total Dissolved Gas Dissipation	86
II.6 - Dam Passage.....	89
II.6.1 - Forebay Delay	91
Dam Delay Model.....	92
II.6.2 - Spill.....	94
Flow Archive Spill	94
Spill from Spill Schedule Tool	95
Spill Caps	95
Spill Efficiency.....	95
II.6.3 - Fish Guidance Efficiency (FGE) Theory	97
Constant FGE	97
Age Dependent FGE	97
FGE Estimation	99
Multiple Powerhouses	100
Fish Passage Efficiency (FPE).....	102
Dam Passage Survival.....	103
II.6.4 - Transport Parameters.....	105
Transportation schedule	105
Transportation Separation.....	107
II.7 - Stochastic Processes.....	108
II.7.1 - Stochastic Parameter Probability Density	108
II.7.2 - Stochastic Parameters.....	109
II.7.3 - Scales of Stochastic Variability	110
III. Calibration.....	111
III.1 - Calibration Overview.....	111
III.1.1 - Parameter Determination and Calibration techniques....	111
III.1.2 - Parameter Determination and Calibration status.....	113
Parameter Determination and Calibration Status by	
Type.....	113
Parameter Determination and Calibration Status by Sub-	
model.....	114
III.2 - Total Dissolved Gas Calibration.....	116
WES linear and exponential curves	116
Exponential Empirical Equation	117
Hyperbolic Empirical Equation.....	118
GasSpill 1 and GasSpill 2 Mechanistic Equations.....	119
K Entrainment	121
III.3 - Predation Rate Parameter Calibration.....	123
Survival Calibration Process	123
Survival Data.....	124
III.3.1 - Parameter Determination and Calibration	124
Predator Densities	124
Predator Activity Coefficient Determination	124
Temperature Response	125

III.3.2 - Predator Density - Temperature Response Interaction ...	125
Density Data Revised	126
III.3.3 - Results	126
III.4 - Calibration of Fish Travel Time Algorithms.....	131
Travel Time Calibration Process	131
Estimating Vvar	131
Smolt Start/Stop Date.....	132
Travel Time Data	132
Variance in Migration Rate	132
III.4.1 - Results	132
IV. Testing the Model with Data.....	133
IV.1 - Overview	133
IV.2 - FGE Validation.....	133
IV.3 - Travel Time Validation.....	133
IV.4 - Survival Validations.....	133
V. Sensitivity Analysis.....	134
V.1 - Description.....	134
V.2 - Results	134
V.3 - Summary	134
VI. Parameter Definitions.....	135
VII. References	136

List of Figures

Fig. 1	Map of river with dams and fish hatcheries	2
Fig. 2	Dam showing fish passage routes. Fish collected in bypass systems are returned to the tailrace or, in some situations, transported downstream. ..	2
Fig. 3	Diagram of model elements	5
Fig. 4	Reservoir mortality processes	6
Fig. 5	Main objects for the Flow submodel	8
Fig. 6	Hydroregulation model simulated input - Wells, 1981	9
Fig. 7	Historic flows at Rocky Reach, 1981	9
Fig. 8	Spectrogram: eleven year time series	10
Fig. 9	Points of flow modulation in system.	11
Fig. 10	Weekly shape pattern	12
Fig. 11	O-U shape; $r = 0.5$, $\sigma = 13$	13
Fig. 12	Flows at John Day Dam, 1981	14
Fig. 13	January and July flows at John Day Dam, 1981	14
Fig. 14	Diagram of reach structure for loss calculation	16
Fig. 15	Inputs at Rocky Reach minus inputs at Wells, 1981	16
Fig. 16	Random factor modulation at Rocky Reach, 1981	17
Fig. 17	Region of regulated F_R and unregulated F_U rivers	18
Fig. 18	Pool geometry for volume calculations showing perspective of a pool and cross-sections. The pool bottom with remains constant while the surface widens in the downstream direction	30
Fig. 19	Reservoir with flowing and pool portions	32
Fig. 20	Pool elevation vs. volume for Lower Granite and Wanapum Pools	34
Fig. 21	Water particle travel time vs. flow for CRiSP.1 (points) and Army Corps calculations (lines) at two elevations full pool(0) and 38 ft below full pool for Lower Granite Dam.	35
Fig. 22	Movement along axis of segment vs. time. Shown are mean path, three paths, and 95% confidence intervals. For these simulations, r is set at 10, and σ set at 20.	36
Fig. 23	Plot of eq (47) for various values of t . Parameters r , σ and L are set at 5, 8, and 100 respectively.	37
Fig. 24	Fish distribution, $p(x, t)$, at t_j and t_{j-1} . Size of the shaded area represents probability of fish leaving the segment over the interval $t_j - t_{j-1}$	38
Fig. 25	Examples of the logistic equation (eq (52)) with various parameter values. In all four plots, the parameter values for the solid curves are: $\beta_0 = 1.0$, $\beta_1 = 2.0$, $\alpha = 0.2$, and $T_0 = 20$. In the upper left plot β_0 is varied, and β_1 is varied in the upper right. In the lower left plot, α is varied, and T_0 is varied in the lower right.	41
Fig. 26	Schematic diagram of a river system. Arrows represent the migration of release groups 1 and 2 through reaches. At the confluence, groups are combined for counting purposes only, i.e they still exhibit their unique migration characteristics.	42

Fig. 27	Plots of a single iteration of the travel time algorithm through a single reach. One thousand fish released at the upstream node are distributed through time at the next downstream node. Parameter: $r = 10$, $\sigma = 8$, $L = 100$.	43
Fig. 28	Elements in reservoir mortality algorithm. Elements used in all model conditions designated by (). Element selected by the user is designated by ()	44
Fig. 29	Equation 66 fit to data from Vigg and Burley (1991). Note that each point represents the mean from 11 to 22 replicates.	49
Fig. 30	Predator concentration function at dam	57
Fig. 31	Factors in gas bubble disease model. Elements used in all model conditions designated by (). Elements selected by the user are designated by ().	58
Fig. 32	The dissolved gas mortality equation is a function of three parameters.	59
Fig. 33	Vertical distribution of fish	60
Fig. 34	Juvenile steelhead cumulative mortality from gas bubble disease at different levels of tdg supersaturation. Data points from Dawley et al. (1976).	65
Fig. 35	Cumulative mortality vs. exposure time to tdg supersaturation for different fish length.	67
Fig. 36	Mortality rate of fish of different lengths.	68
Fig. 37	Fits of mortality rate parameters to mortality rate data corrected for depth and fish length. Data points from Dawley et al. (1976), curve from fit of eq (79). There are extreme points not shown on the steelhead graph.	69
Fig. 38	Representation of spillway and stilling basin.	72
Fig. 39	LGS production values with and without entrainment and observed data (points).	79
Fig. 40	LWG production values with and without entrainment and observed data (points).	80
Fig. 41	RIS production values with and without entrainment and observed data (points).	81
Fig. 42	WAN production values with and without entrainment and observed data (points).	82
Fig. 43	A Divided Reservoir	83
Fig. 44	Reservoir Gas Dynamics	83
Fig. 45	Dam processes showing passage routes and mortality. Forebay delay is further illuminated in Fig. 46.	90
Fig. 46	Transfer of fish from reservoir to forebay to dam. Diagram shows allocation of fish from a reservoir time slice of 12 hours to dam time slices of 6 hours each. Mortality is associated with dam and spill passage as well as forebay transit and delay.	91
Fig. 47	Variables for dam passage delay model	92
Fig. 48	Cumulative passage versus dam delay in days at Little Goose Dam	93
Fig. 49	Critical parameters in fish guidance are fish forebay depth z , screen depth D and elevation drop E . Only fish above z are bypassed. Bypass stops when the surface is below the bypass orifice depth.	97
Fig. 50	Fge and fish depth over fish age	99
Fig. 51	Multiple powerhouse configuration showing allocation of spill and powerhouse flows.	101

Fig. 52	Flow allocation through two powerhouse projects.	101
Fig. 53	Routing of fish for calculation of FPE	102
Fig. 54	Probability function (pdf) and cumulative function of the broken stick probability distribution	108
Fig. 55	Calibration process involves using passage and environmental data to es- timate the model ecological parameters	112
Fig. 56	Comparison of observed and modeled gas supersaturation for 1994 data. Lower Granite Pool Chi-square = 1.88, $p > 0.05$. Ice Harbor Pool Chi- square = 3.38, $p > 0.05$. Priest Rapids Pool Chi-square = 2.01, $p > 0.05$. Bon- neville Pool Chi-square = 1.08, $p > 0.05$	121
Fig. 57	Example of optimization of k_{entrain} values for 1998.	122
Fig. 58	Spring chinook, modeled vs. observed survivals. The LGR - MCN survivals for 1995 were singled out to highlight the poor behavior of (the late sea- son portion of) that data.	128
Fig. 59	Steelhead, modeled vs. observed survival.	129
Fig. 60	Fall chinook, modeled vs. observed survivals. The late season releases have been singled out as have the 1997 releases.	130

List of Tables

Table 1	Daily modulator parameters for river	13
Table 2	Variance about mean flow for observed and modulated flows at three dams in 1981	15
Table 3	Flow loss modulator parameter for eq (8)	17
Table 4	Flow minimum (kcfs) at dams.	20
Table 5	Unregulated headwater flow parameter estimates	24
Table 6	Regulated headwater flow parameter estimates	24
Table 7	Maximum unregulated flow (kcfs)	25
Table 8	Storage reservoirs. Shaded items are used in model.	26
Table 9	Storage reservoirs flood control elevation rule curves	27
Table 10	Geometric data on Columbia River system. Elev is normal full pool elevation, in feet above mean sea level. MOP is minimum operating pool elevation.	34
Table 11	Summary of the forms of the predation mortality rate equation	49
Table 12	Population abundance estimates for John Day Pool, 1984-1986 (Beamesderfer and Rieman 1991). 95% confidence intervals are in parentheses.	50
Table 13	Northern pikeminnow density and distribution in John Day Pool, based on 1990-1991 CPUE data, assuming total abundance the same as 1984-1986.	50
Table 14	Walleye density and distribution in John Day Pool, 1984-1986. Relative densities are mean for 1984-1986 from Beamesderfer and Rieman (1988).	51
Table 15	Smallmouth bass density and distribution in John Day Pool, 1984-1986. Relative densities are mean for 1984-1986 from Beamesderfer and Rieman (1988).	51
Table 16	Mean daily salmonid consumption estimates for the major predators (salmonids predator ⁻¹ day ⁻¹) from Vigg et al. (1991). Walleye and smallmouth bass estimates are for the reservoir only.	51
Table 17	Consumption rates for N. Pikeminnow, Walleye and Smallmouth Bass in John Day Pool, 1984-1986, from Vigg et al. (1991). Mean for April-June.	52
Table 18	Consumption rates for N. Pikeminnow, Walleye and Smallmouth Bass in John Day Pool, 1984-1986, from Vigg et al. (1991). Mean for July-August	52
Table 19	Pikeminnow density indices (CPUE) in all reaches, 1990-1991	52
Table 20	Relative CPUEs for smallmouth bass and walleye (standardized to John Day Pool) based on the abundances from Zimmerman and Parker (1995). Raw data from N. Bouwes, ODFW, pers. comm.	54
Table 21	River dimensions from Ward et al. (1995). Tailrace is assumed to be 0.6 km in length; forebay is assumed to be 6.0 km in length.	54
Table 22	1990 predator densities for Spring (SP) and Fall (FA) migrations, by project and zone, with pikeminnow percentage (% PM) given for each. ...	55
Table 23	Pikeminnow reduction program. Percent reduction in predation due to pikeminnow as a result of the pikeminnow reduction program at each project in each year (Peters et al. 1999, 113). Estimates of predation reduc-	

tion for 2001-2006 are included in Peters et al. (1999, 113).	56
Table 24 Survival data and mortality rates from Dawley et al. (1976)	63
Table 25 Depths of fish in the deep water tanks and Gc used to determine mortality rate coefficients	66
Table 26 Total dissolved gas mortality rates and fish length in shallow tank experiments (Dawley et al. 1976). Plotting symbols refer to Fig. 35.	67
Table 27 Tdg mortality coefficients based on Dawley.	68
Table 28 Fish depth information	69
Table 29 Spill_side tokens for each dam.	75
Table 30 Tailrace Mixing coefficients	76
Table 31 Estimations of K_entrain from CRiSP.1 runs using filtered DART data (observed and modeled TDG > 100%).	78
Table 32 Spill efficiency (% fish passed in spillway /% flow passed in spillway). 96	
Table 33 CRiSP.1 estimated FGE for steelhead.	99
Table 34 Bypass and forebay elevations of dams with bypass systems	100
Table 35 Transport operations for historical data files, 1975-1994.	105
Table 36 Separation efficiencies at transport projects.	107
Table 37 Model probability density functions	110
Table 38 Lower Snake and Lower Columbia Dams, gas production curves using linear or exponential models.	116
Table 39 Mid-Columbia Dams and Dworshak dam gas production curves using linear or exponential model	117
Table 40 Hells Canyon Dam gas production curves using exponential model	117
Table 41 Values for exponential empirical tdg model and last year of its use .	118
Table 42 Values for hyperbolic empirical tdg model	118
Table 43 Parameters for Gas spill model equations	120
Table 44 Variables for reservoir geometry, in feet. Dam abbreviations correspond to dams in Table 42.	120
Table 45 Spring chinook CRiSP.1 survivals and NMFS survivals for the research reach and down to Bonneville for each year.	127
Table 46 Steelhead CRiSP.1 survivals and NMFS survivals for the research reach and down to Bonneville for each year.	128
Table 47 Fall chinook CRiSP.1 survivals and NMFS survivals for the research reach and down to Bonneville for each year.	130

I. Introduction

This document describes the theory, calibration and validation of the Columbia River Salmon Passage model (CRiSP.1). The model tracks the downstream migration and survival of migratory fish through the tributaries and dams of the Columbia and Snake Rivers to the estuary.

CRiSP.1 describes in detail the movement and survival of individual stocks of natural and hatchery-spawned juvenile salmonids through hundreds of miles of river and up to nine dams. Constructed from basic principles of fish ecology and river operation, CRiSP.1 provides a synthesis of current knowledge on how the major hydroelectric system in the country interacts with one of its major fisheries. Biologists, managers and others interested in the river system can use this interactive tool to evaluate the effects of river operations on smolt survival.

There are two modes that CRiSP.1 can use: a Scenario Mode that illustrates the interactions of model variables, and a Monte Carlo Mode, which is stochastic, providing measures of variability and uncertainty in predicted passage survival. Between any two points in the river system, estimates of probability distributions for survival and travel time can be determined for any stock.

CRiSP.1 has advanced programming features including:

- *graphical interface* to access and change model variables and equations
- *flexible data structure* that allows expansion of the model while assuring backwards compatibility with earlier versions
- *configurability* to a different river without reprogramming
- *on-line help* tool.

The model runs on Windows95/NT operating systems and on Sun SPARCstations under the Solaris2 and X Windows graphical interfaces.

CRiSP.1 was developed at the University of Washington's School of Fisheries under a contract from the Bonneville Power Administration's (BPA) Fish and Wildlife Division.

I.1 - General Description

CRiSP.1 models passage and survival of multiple salmon substocks through the Snake and Columbia rivers and their tributaries and the Columbia River Estuary (Fig. 1). The model recognizes and accounts for the following aspects of the life-cycles of migratory fish and their interaction with the river system in which they live.

Fish survival through reservoirs depends on:

- predator density and activity
- total dissolved gas (tdg) supersaturation levels dependent on spill
- travel time through a reservoir.

Fish migration rate depends on:

- fish behavior and age

- water velocity which in turn depends on flow, cross-sectional area of a reach, and reservoir elevation.

Fish passage through dams (Fig. 2) depends on:

- water spilled over the lip of the dam
- turbine operations
- bypass screens at turbine entrances and fish guidance sluiceways
- fish diel behavior.

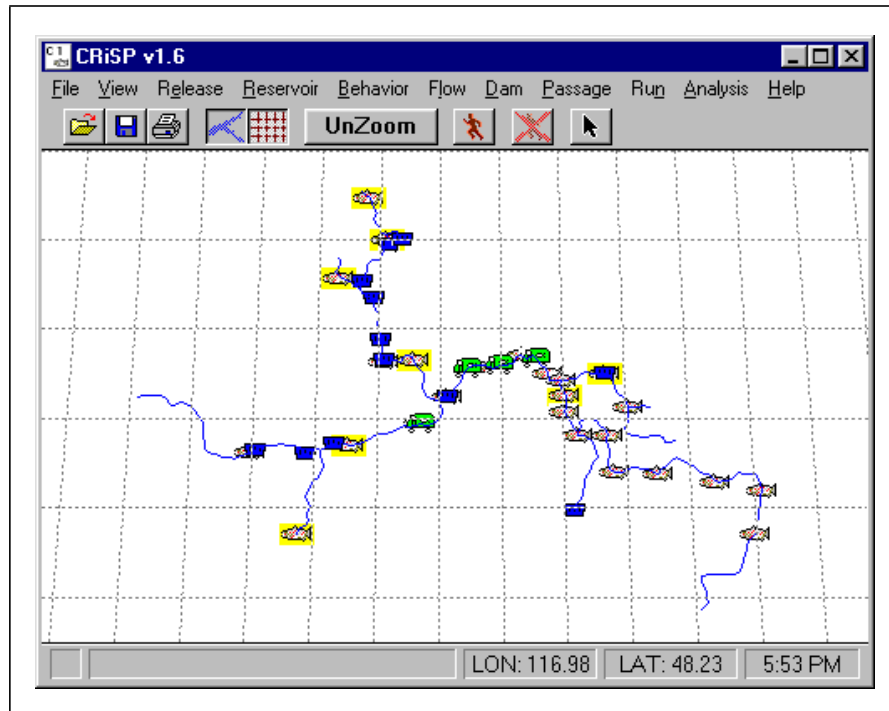


Fig. 1 Map of river with dams and fish hatcheries

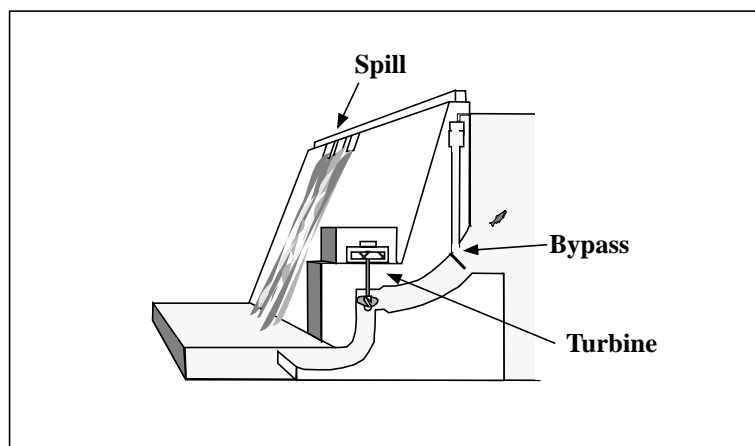


Fig. 2 Dam showing fish passage routes. Fish collected in bypass systems are returned to the tailrace or, in some situations, transported downstream.

I.1.1 -CRiSP.1 Submodels

CRiSP.1 integrates a number of submodels that describe interactions of isolated components. Together they represent the complete model. These elements include submodels for: fish travel time, reservoir mortality, dam passage, total dissolved gas supersaturation, and flow/velocity relationship. The structure of CRiSP.1 allows the user to select different formulations of these submodels at run time. In this sense, CRiSP.1 can be configured to simple interactions or it can be set up to consider many ecological interactions. CRiSP.1, as it is presently calibrated, has an intermediate level of complexity: age dependent travel time is implemented, but other age dependent factors are switched off. A brief description of submodels follows.

Travel Time

The smolt migration submodel, which moves and spreads releases of fish down river, incorporates flow, river geometry, fish age and date of release. The arrival of fish at a given point in the river is expressed through a probability distribution. All travel time factors can be applied or they can be switched off individually, resulting in a simplified migration model.

The underlying fish migration theory was developed from ecological principles. Each fish stock travels at an intrinsic velocity as well as a particular velocity relative to the water velocity. The velocities can be set to vary with fish age. In addition, within a single release, fish spread as they move down the river.

Predation Rate

The predation rate submodel distinguishes mortality in the reservoir, and the forebay and tailrace of dams. The rate of predation can depend on temperature, diel distribution of light, smolt age, predator density, and reservoir elevation.

Gas Bubble Disease

A separate component of mortality from gas bubble disease produced by total dissolved gas (tdg) supersaturation is incorporated into CRiSP.1. The mortality rate is species specific and is adjusted to reflect the effect of fish length and population depth distribution.

Dam Passage

Timing of fish passage at dams is developed in terms of a species dependent distribution factor and the distribution of fish in the forebay, which can change with daily and seasonal light levels. Fish guidance efficiency can be held constant over a season or it can vary with fish age and reservoir level.

Transportation Passage

Transportation of fish at collection dams is in accordance with the methods implemented by the U.S. Army Corps of Engineers. The start and termination of transportation and separation of fish according to species can be determined for any dam under the same rules used to manage the transportation program. Time in transportation and transportation mortality can also be set.

Total Dissolved Gas Supersaturation

Total dissolved gas (tdg) supersaturation, resulting from spill at dams, can be described with a mechanistic submodel that includes information of the geometry of the spill bay and physics of gas entrainment. Alternatively, supersaturation can be described by empirical models.

Flow

Flow is modeled in two ways: it can be specified at dams using results of system hydro-models or it can be described in terms of daily flows at system headwaters. When flow is described in headwater streams, the flow submodel generates a random set of seasonal flows that have statistical properties in accordance with the available water over a year. In this fashion, the model statistically reproduces flow for wet, average and dry years. The user controls the mainstem river flows by adjusting the outflow of the storage reservoirs within their volume constraints.

Water Velocity

Water velocity is used in CRiSP.1 as one of the elements defining fish migration. Velocity is determined from flow, reservoir geometry and reservoir elevation.

Reservoir Drawdown

Reservoir elevation is set on a daily basis from elevation information in the system hydro-models or from user specified files. As water levels drop, part of the reservoir may become a free-flowing stream.

Stochastic Processes

CRiSP.1 can be run in a Monte Carlo Mode in which flows and model parameters vary within prescribed limits. In this mode, survival to any point in the river can be determined as a probability distribution.

Geographical Extent

CRiSP.1 can describe a river to any desired level of detail by changing a single file containing the latitude and longitude of river segments, dams and release sites. In its present configuration, two river-description files are available. One file contains an abbreviated river map with the major tributaries. It contains three representative release sites, although more can be added easily. A second river descriptions file defines a more extensive river and tributary system and has upwards of 100 hatchery release sites.

II. Theory

II.1 - Model Computation Diagram

CRiSP.1 is a composite of individual integrated process submodels that jointly determine smolt migration and survival. The equations underlying some submodels are mechanistic and are derived from underlying theory. In these equations the parameters have ecological or physical meaning. The equation relating water flow to velocity, for example, is based on principles of hydrology. A second type of equation is empirical and has no underlying ecological or physical meaning. These are used because they fit the data and are amenable to statistical fitting techniques. The parameters of these types of equations seldom have ecological interpretations. For example, in the total dissolved gas (tdg) supersaturation submodel four alternative equations are available to relate tdg supersaturation to spill. Here, the parameters just determine the shape of the response. A third type of equation is a mixture of empirical and mechanistic. The predation rate equation (submodel) is an example of this mix with predation activity and density parameters multiplying the empirical predation temperature response.

The CRiSP.1 model calculates changes in fish population numbers as fish move through tributaries, reservoirs, and dams. Figure 3 is a diagram of the computational tree. Shaded boxes represent fish entering the system of dams and reservoirs on a daily basis. Unshaded square boxes represent calculations for travel time and survival of fish through the system. Rounded boxes represent input data to the calculation modules.

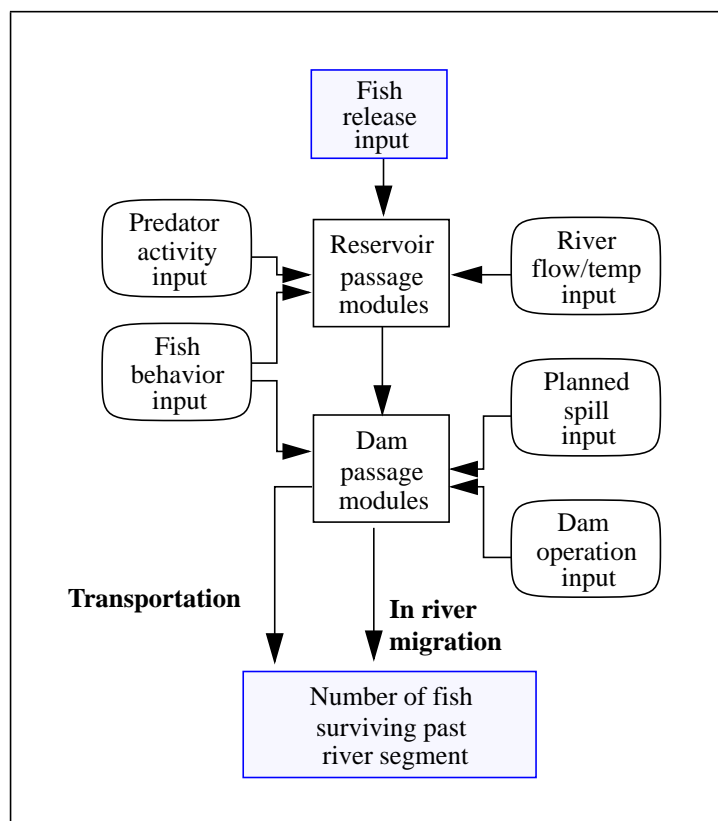


Fig. 3 Diagram of model elements

Reservoir Passage

In CRiSP.1, passage and survival of fish through a reservoir is expressed in terms of the fish travel time through the reservoir, the predation rate in the reservoir and a mortality rate resulting from fish exposure to total dissolved gas supersaturation, an effect called Gas Bubble Disease. CRiSP.1 combines these individual mortality factor models (Fig. 4).

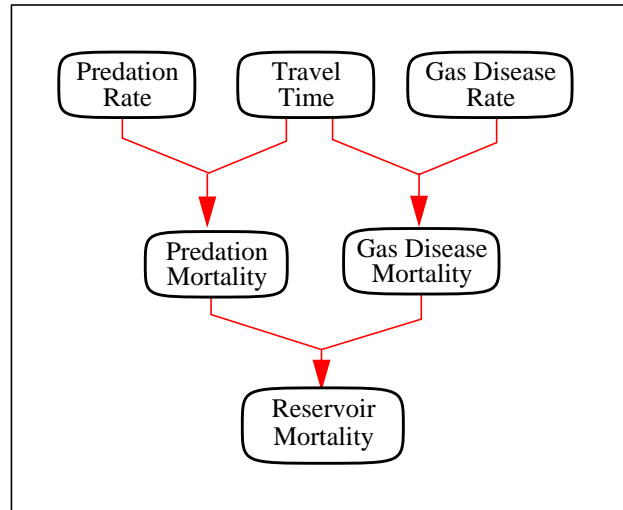


Fig. 4 Reservoir mortality processes

The modeling approach has been to develop alternative submodels of reservoir mortality factors so that various hypothesis can be compared.

Ecological Submodels

Ecological submodels were developed from first principles relating environmental variables with fish behavioral and physiological factors to determine fish passage. Environmental variables, including weather-related factors such as temperature, and system operating factors such as flow, spill and fish transportation, describe the observable state of the environment in which fish live and characterize the rates of fish passage and survival which, through the model equations, generate predicted passage. In the model these variables are contained under **Reservoir**, **Behavior**, **Flow**, and **Dam** menus.

The model can use both raw information and statistically analyzed data. The model runs on data expressed as initial release numbers and numbers of fish passing any point or bypass route in the river system. Release information is accessed through the **Release** menu. Passage information is accessed through the **Passage** menu of the model. This provides detailed information of passage at any level from passage of a specific dam route to passage through the entire system.

II.2 - Flows

II.2.1 - Overview of Flow Computation

This section defines the theory for calculation of flows in CRiSP.1. Flow information is treated differently for the Monte Carlo and Scenario Modes. In the Monte Carlo Mode, average flows over defined periods at the dams are read as input from flow archive files. The period average flows are then *modulated* to give simulated daily flows at the dams. Using this information, flows in the headwaters are calculated with an *upstream propagation* algorithm. Finally, flows through river segments are calculated from the headwaters with the *downstream propagation* algorithm. In the Scenario Mode, flows can be specified at headwaters using modulators based on historical flows or drawn in using the mouse. Outflows from storage reservoirs are specified according to the volume constraints of the reservoirs. Finally, river flows are produced using the *downstream propagation* algorithm which combines storage reservoir flows and unregulated headwater flows.

II.2.2 - Monte Carlo Flow Calculation

When running CRiSP.1 in the Monte Carlo Mode, flow information is specified at dams from flow archive files generated by one of several hydroregulation models. CRiSP.1 uses a step-wise process to calculate daily headwater flows. These steps are as follows:

1. Read period-averaged flows at dams from the flow archive file
2. Modulate period-averaged dam flows to give daily dam flows
3. Modulate losses in reservoirs
4. Propagate upstream flows to determine daily headwater flows as well as gains and losses from river segments
5. Propagate downstream flows through all river segments using the headwater flows and the segments' gains and losses.

Calculation of river flows in the Monte Carlo Mode begins with flows at the dams and distributes upstream flows to achieve a mass balance. The procedure uses water conservation equations for losses/gains in river segments and flows at unregulated streams and from storage reservoirs. Definitions for flow calculations (Fig. 5) are listed below.

- Regulated headwater segment has a dam, a storage reservoir, and a river source.
- Unregulated headwater segment has a confluence at its downstream end and a river source at its upstream end.
- Loss is a withdrawal (+) or deposit (-) of water to a river segment from an unspecified source. Losses are used to represent irrigation removals and ground water returns to river segments.
- Dams are points that regulate flow, but only dams specified in the flow archive file are considered to be regulation points.
- Confluences are points where two flows upstream of the confluence combine to create the flow downstream of the point.

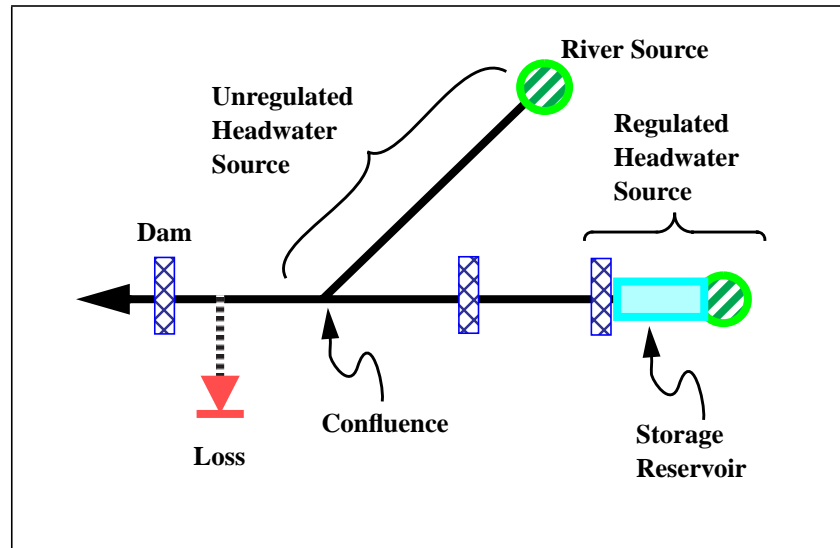


Fig. 5 Main objects for the Flow submodel

Hydroregulation Models

Flow files for the Monte Carlo runs are obtained from *Flow Archive* files that are generated from runs of hydroregulation models maintained by two agencies:

- HYDROSIM is run by the Bonneville Power Administration
- HYSSR is run by the U.S. Army Corps of Engineers

The models provide flow on a monthly or bimonthly basis over the entire Columbia Basin hydrosystem and are themselves complex models with many variables and special conditions. As a result, these models are not available to be run directly, although outputs of model runs are available for use in CRiSP.1.

The models use information on natural runoff, regional electrical demand and storage capacity of the reservoirs to model the stream flow on a period averaged basis. Models use historical flow records for natural runoff and generate river flows that meet power generation demand in monthly periods. The exceptions to the monthly periods are April and August which are each divided into two periods. In addition, the HYDROSIM model provides elevations of all reservoirs.

Flow Modulation

Flow inputs in the Monte Carlo Mode runs consist of predicted daily flow averaged over monthly or bimonthly intervals at each dam used in CRiSP.1. This input generated from HYDROSIM, or HYSSR flow archive files typically looks like Fig. 6 below. While this record retains most of the annual and seasonal flow variations, actual historic river flows (Fig. 7) exhibit considerable weekly and daily variations that are not replicated by the hydroregulation models used as flow data for CRiSP.1.

The purpose of the modulator is to more accurately simulate real flow patterns encountered by adding variations at finer time-scales consistent with historic flows. These variations include both random and deterministic components.

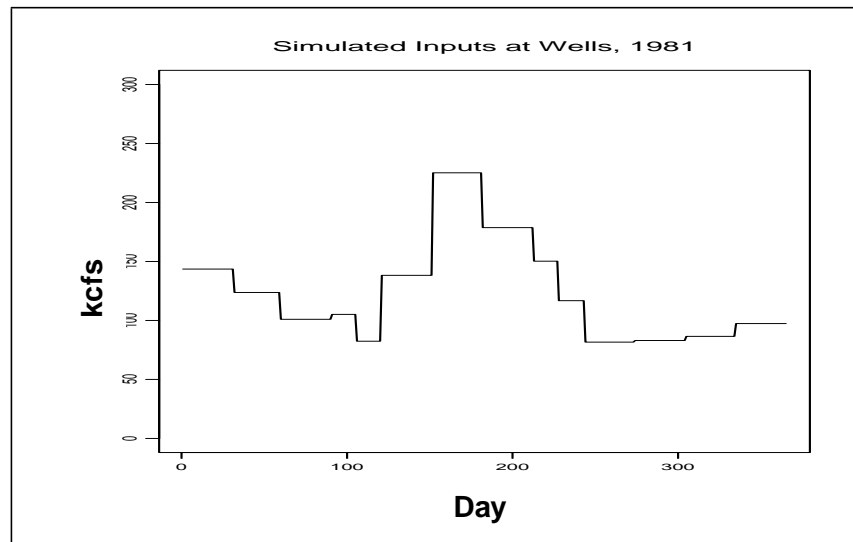


Fig. 6 Hydroregulation model simulated input - Wells, 1981

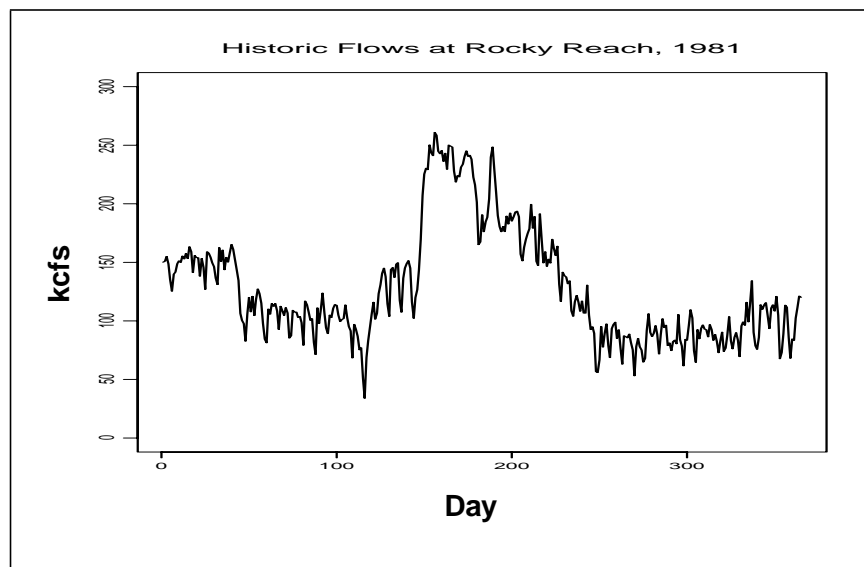


Fig. 7 Historic flows at Rocky Reach, 1981

Spectral Analysis of Flow

The CRiSP.1 modulators were developed from the following analysis of flows in the Columbia River system. The goal was to develop a modulator that represented daily and weekly variations in flow and had the same spectral qualities as the flows in the river system as it is now operated.

A spectral analysis of an eleven-year time series (1979-1989) of flows revealed the general trend is a decline in spectral power that is qualitatively similar to a pink noise spectrum¹. In addition, the spectrum has distinct peaks at frequencies of $1/7$, $2/7$, $3/7$ etc., indicating a seven day cycle (Fig. 8).

This spectrum suggest several distinct processes. The weekly component is the result of flow decreasing on weekends when electric power consumptions is less. The pink noise element of the spectrum is probably the result of seasonal and short term correlations in weather patterns that alter the power consumption and unregulated runoff directly.

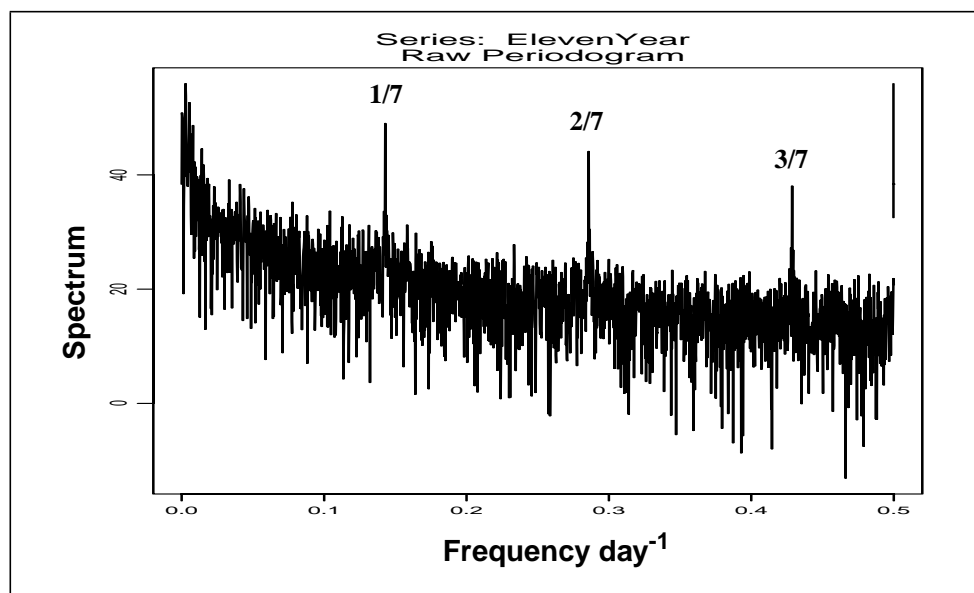


Fig. 8 Spectrogram: eleven year time series

Modulator Applications

The strategy for using period averaged archive flows to simulate flows with the spectral qualities of the actual ones involves adding flow variations at several points in the system (Fig. 5). These variations are produced by modulators. Since flows start in the headwaters and are summed downstream, flow variation can be added sequentially according to the manner by which they are produced. First, the archive flows are prescribed at all dams. Next, three modulations are applied. *Weekly* and *daily* modulations are added at the regulated headwaters to reproduce variations that occur between dams from additions and subtractions of water in the river segments and a *loss* modulation is added at downstream dams. After modulation, an upstream propagation process is applied to calculate the flows in unregulated headwaters. This forces the total modulation into the unregulated streams. In the case of the weekly modulation this is an artifact since it is induced by hydrosystem operation. The error is not significant though, since the weekly modulation is a small fraction of the total variation.

1. Pink noise is random pattern that exhibits some correlation for short time scales

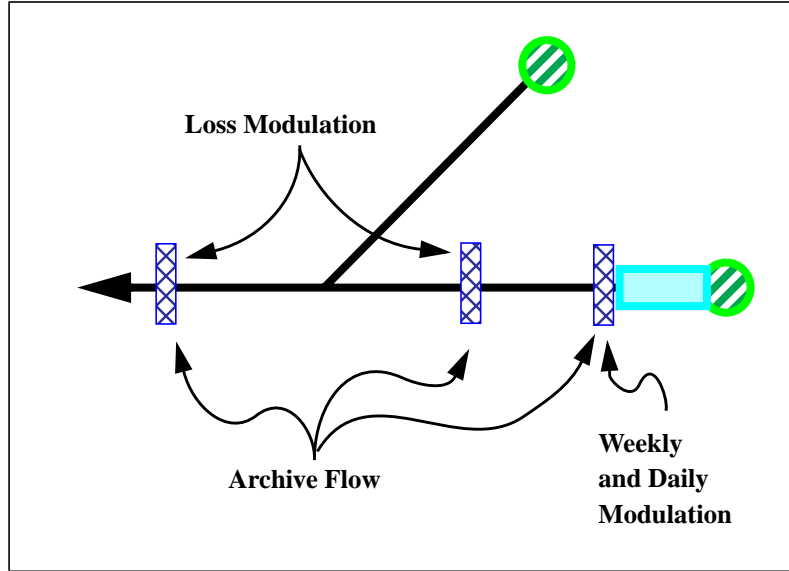


Fig. 9 Points of flow modulation in system.

Weekly Modulators

The weekly modulation, applied in the regulated headwaters, simulates hydrosystem power generations patterns in which electrical demand decreases on weekends. The modulators, producing lower flows on weekends and higher flows midweek (Fig. 10), are approximated with a three-term Fourier series with fixed amplitude. The equation is

$$F(t)_{\text{week}(j)} = -G \sum_{n=1}^3 a_n \cos(b_n(t + \delta)) \quad (1)$$

where

- $F(t)_{\text{week}(j)}$ = weekly variation in flow for headwater dam j
- G = flow scaling factor in kcfs

This is set to 12.0 to reproduce the observed weekly variation in flow at Wells Dam for the years 1979 to 1989 excluding 1983 for which flows are missing.

- a_n, b_n = Fourier coefficients
 $a_1 = 1, a_2 = 2/3, a_3 = 1/3$
 $b_1 = 6\pi/7, b_2 = 4\pi/7, b_3 = 2\pi/7$
- t = day of the year
- δ = offset for day of week alignment.

The offset is calculated so that for any year from 1900 to 2100 the minimum value of W occurs on Sunday.

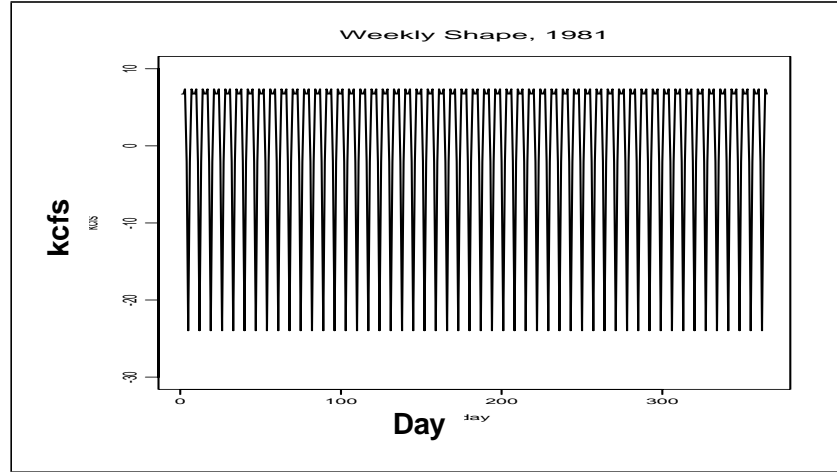


Fig. 10 Weekly shape pattern

Daily Modulators

Daily modulation simulates all variations not associated with the weekly and seasonal variations. A discrete realization of an Ornstein-Uhlenbeck (OU) process (Gardiner 1985) was used to generate the daily variation. The process has two important characteristics: variations are slightly correlated from one day to the next and variances stabilize over time. This is a correlated random walk in which autocorrelation decays in time. The stochastic differential equation for an O-U process is

$$\frac{dF_{\text{day}}}{dt} = -r \cdot F_{\text{day}} + \sigma \cdot w(t) \quad (2)$$

where

- F_{day} = daily variation in flow in kcfs at headwater dam
- r = deterministic rate of change of flow per unit of flow (the range is confined such that $0 < r < 1$)
- σ = intensity on the random variations in flow
- $w(t)$ = Gaussian white noise process describing the temporal aspects of the flow variation.

An O-U process has a conditional probability density function (Goel and Richter-Dyn 1974)

$$P(x|y, t) = \frac{\exp\left[-\frac{1}{2}\left(\frac{x - m(t)}{V(t)}\right)^2\right]}{\sqrt{2\pi V^2(t)}} \quad (3)$$

where the mean and variance of the process are defined

$$m(t) = y \cdot \exp(-rt) \quad (4)$$

$$V^2(t) = \frac{\sigma^2}{2r}(1 - e^{-2rt}) \quad (5)$$

When rt is large enough that $\exp(-2rt)$ is negligible, m and V^2 tend to be constant values and the time series is stationary.

Changing the continuous differential equation into a discrete one with $\Delta t = 1$ reservoir time step, and rearranging gives

$$F(t+1)_{\text{day}(j)} = (1 - r_j) \cdot F(t)_{\text{day}(j)} + \sigma_j \cdot w(t) \quad (6)$$

$r = 0$ gives an unbiased random walk, $r = 1$ gives a series of uncorrelated normal variates.

For the modulators, a system in stochastic equilibrium is sought such that $m = 0$. Taking $X_0 = y = 0$ gives $m = 0$, and discarding the first 35 iterations yields stable variance for any value of r useful in this context. Modulator parameters selected for the different portions of the system are given in Table 1 and are based on daily flow data for the years 1979 to 1989 at Wells and Lower Granite Dams.

Table 1 Daily modulator parameters for river

River	σ_j	r_j
Upper Columbia	13	0.5
Lower Columbia	13	0.5
Snake	7	0.5

Random daily variation is added by a numerical form of an Ornstein-Uhlenbeck (O-U) random process created for each run (Fig. 11).

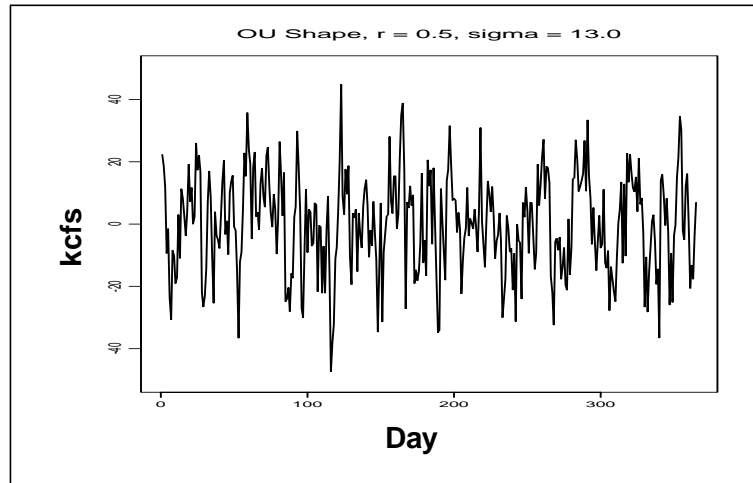


Fig. 11 O-U shape; $r = 0.5$, $\sigma = 13$

Monte Carlo Flow Modulator Validation

Using daily flow records for Ice Harbor, Priest Rapids and John Day dams during 1981, monthly and bimonthly (April and August) average daily flows were computed and appended to a CRiSP.1 flow archive from which CRiSP.1 generated modulated flows for these dams. Graphs of observed and model-produced flows for the first 300 days of the year at John Day Dam appear in Fig. 12. The model appears to produce realistic patterns of flow variation that mimic natural flows very well.

At a finer scale, however, note that CRiSP-modulated flows generally exhibit less variability than do observed flows, e.g. compare January and July (Fig. 13). In general, modulated flows are about as variable as observed flows in January, but clearly less variable than observed flows in July. This is also reflected in the variance around the mean flow, given in Table 2. This phenomenon is probably due at least partially to “step-like changes” of flows in July that do not occur in January. There is some variation around the mean due solely to that trend, and this will not be captured in a purely random modulation scheme.

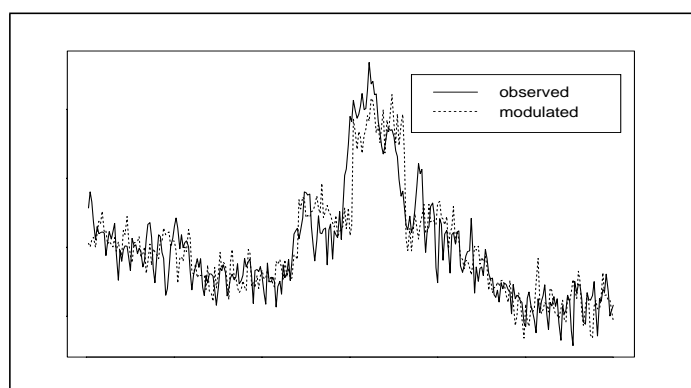


Fig. 12 Flows at John Day Dam, 1981

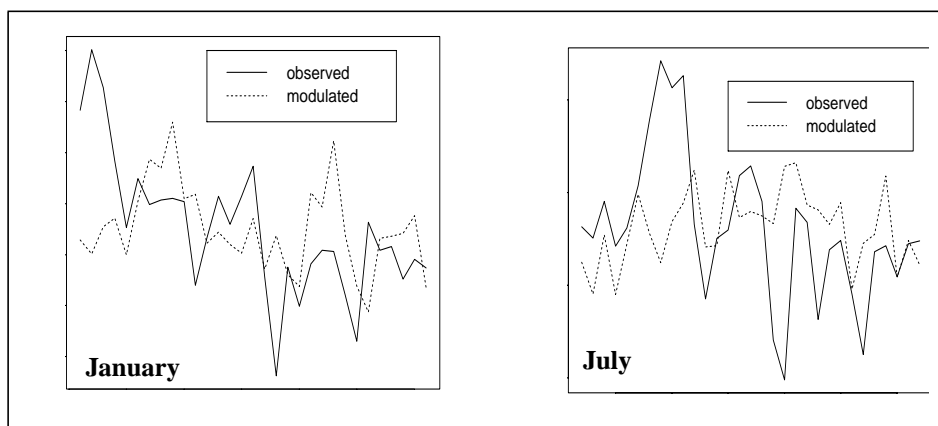


Fig. 13 January and July flows at John Day Dam, 1981

Table 2 Variance about mean flow for observed and modulated flows at three dams in 1981

Dam	Month	Variance about monthly mean flow	
		Observed	Modeled
John Day	January	728.38	287.54
	July	1620.08	401.74
Priest Rapids	January	67.34	160.29
	July	512.97	170.42
Ice Harbor	January	247.65	156.96
	July	149.83	61.83

Flow Loss

The term ‘loss’ represents withdrawals from the system, mainly for irrigation. These withdrawals are positive in CRiSP.1. Negative losses are return flows through ground water.

The loss data in a segment represents the change in flow that occurs between the flow input (calculated from the flow of upstream segments) and the flow output (stored as data in the segment). Where not specified, flow loss is set to zero.

During the upstream propagation operation, new flow loss values are computed for reaches that lie between two dams. A dam is said to have no component of unregulated flow if no unregulated headwater flows into the dam without first flowing through some regulation point.

For each reach r enclosed between a dam and upstream regulation points (Fig. 5), a new flow loss $F_{L(r)}$ is set by distributing any mass imbalance over all reaches between the dam and/or regulated inflow points in proportion to each reach’s maximum allowable flow:

$$F_{L(r)} = \left[\sum_{j=1}^n F_{R(j)} - F_{D(r)} \right] \frac{F_{M(r)}}{\sum_{i=1}^p F_{M(i)}} \quad (7)$$

where

- $F_{D(r)}$ = flow output at dam immediately below reach r
- $F_{L(r)}$ = new flow loss at reach r , as adjusted for mass imbalance
- $F_{M(r)}$ = flow maximum at reach r
- $F_{M(i)}$ = flow maximum at reach i
- $F_{R(j)}$ = flow at regulation point j
- n = number of upstream regulated points

- p = number of reaches between dam r and all regulation point.

Note: maximum allowable flows are set in the **columbia.desc** file using the keyword **flow_max**.

Flow loss is not modified by the upstream propagation in any reach not fully enclosed by regulated headwaters or dams. After appropriate loss values are set, flow loss in every segment is used as input data for unregulated headwater calculations.

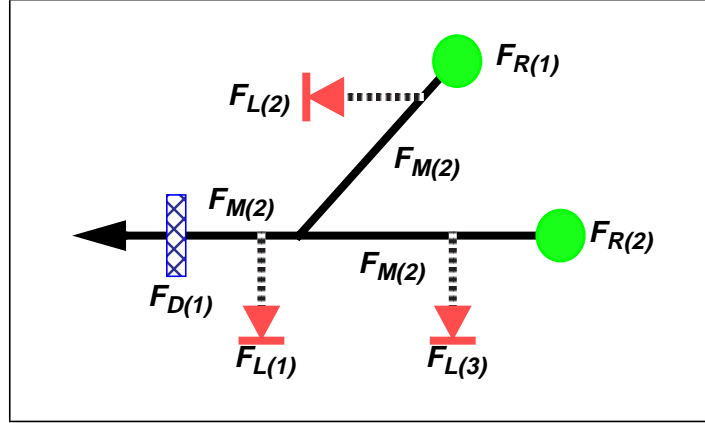


Fig. 14 Diagram of reach structure for loss calculation

Reservoir Loss Modulation

At downstream dams, variations in flow from losses due to irrigation and evaporation and additions from surface and subsurface groundwater flows are accounted for with *loss* modulators. The intensity of this variation is based on the differences in flows observed at adjacent dams as indicated in period averaged hydro-model flows (Fig. 15).

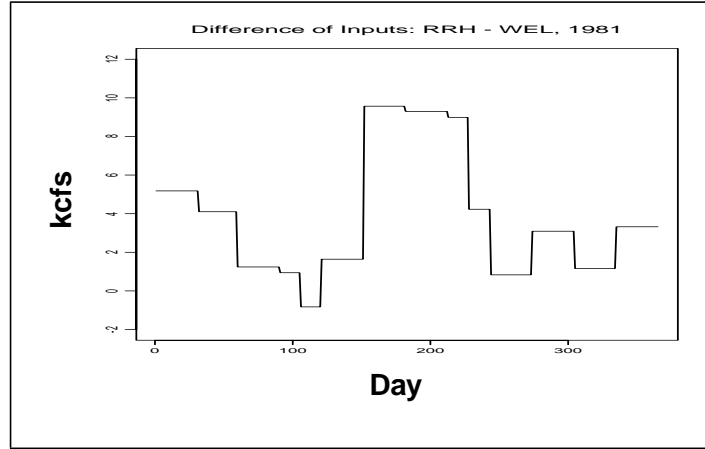


Fig. 15 Inputs at Rocky Reach minus inputs at Wells, 1981

The loss modulation is simulated with a white noise process (Fig. 16). A normal variate random factor is added to modulated flow of all run of the river dam. The equation is

$$F_{loss(i)} = \sigma_i \cdot \text{Norm}(0, 1) \quad (8)$$

where

- $F_{loss(i)}$ = modulated flow loss at downstream dam i

- σ_i = the standard deviation of the difference in flows (kcfs) at dam i and $i + 1$ as computed by daily observed flows at all dams over the years 1979-1981.

Table 3 Flow loss modulator parameter for eq (8)

Dam	σ_i (kcfs)	Dam	σ_i (kcfs)
Bonneville	11.0	Little Goose	5.4
The Dalles	4.1	Priest Rapids	4.0
John Day	17.0	Wanapum	5.0
McNary	12.75	Rock Island	2.65
Ice Harbor	2.75	Rocky Reach	3.0
Lower Monumental	2.4	Wells	6.5

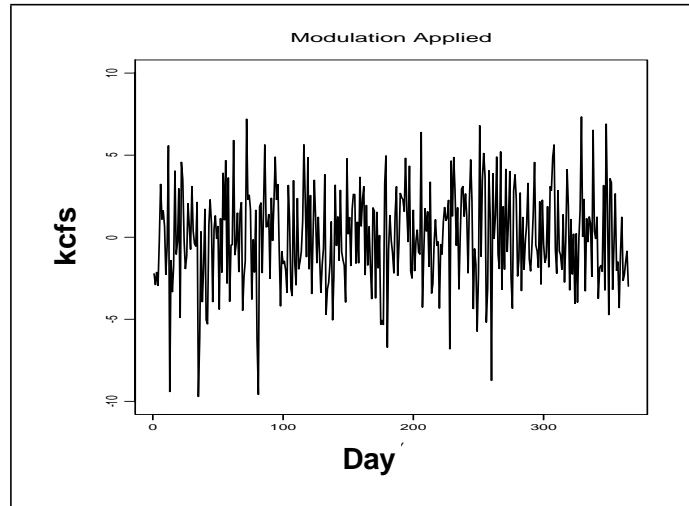


Fig. 16 Random factor modulation at Rocky Reach, 1981

Headwater Computation

Once flows are modulated at dams and the losses and gains are calculated, the headwater flows can be calculated with the algorithms described below.

Regulated Headwater

Regulated headwaters are storage reservoir outflows for the Monte Carlo Mode. No losses are considered for storage reservoir flows other than the dam outflow.

Unregulated Headwaters

Each unregulated headwater is examined. If the flow for a given headwater has not yet been computed, then flow for that and all adjacent unregulated headwaters is calculated.

The *region* of computation for a segment is defined as all segments within the river map subgraph with endpoints consisting of the nearest downstream dam, and the nearest regulation points or headwaters upstream from the dam. An example of a region with several unregulated headwaters is given in Fig. 17.

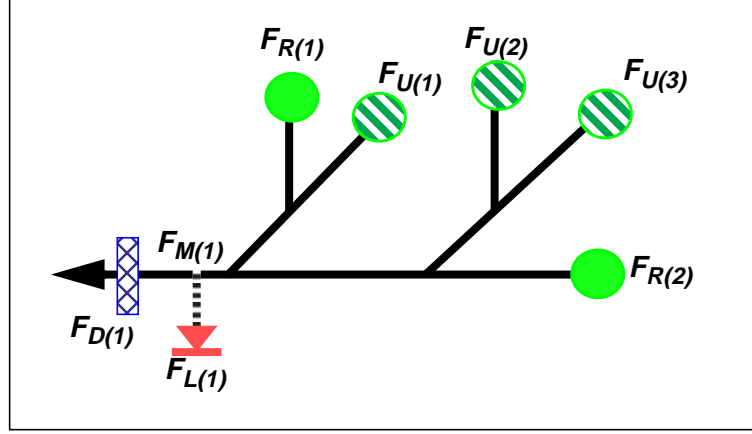


Fig. 17 Region of regulated F_R and unregulated F_U rivers

To calculate the unregulated headwater flows, first the total unregulated flow input to dam r ($D(1)$ in Fig. 17) is computed by subtracting the total regulated flow from flow at dam r . The equation is

$$F_{TU(r)} = F_{D(r)} - \sum_{j=1}^p F_{R(j)} \quad (9)$$

where

- $F_{TU(r)}$ = total unregulated flow input to dam r
- p = number of regulated flows in region
- $F_{D(r)}$ = flow output at dam r
- $F_{R(j)}$ = flow output at regulation point j .

The total unregulated flow is then distributed over all unregulated tributaries upstream of dam r in proportion to each tributary's maximum flow, as specified in **columbia.desc** by the keyword `flow_max`. The flow coefficient K at each unregulated headwater i is the percentage of total unregulated flow contributed by that headwater and is defined

$$K_i = F_{Umax(i)} / \left(\sum_{j=1}^q F_{Umax(j)} \right) \quad (10)$$

where

- K_i = flow coefficient at unregulated headwater i
- q = number of adjacent unregulated headwaters in region
- $F_{Umax(i)}$ = maximum flow at unregulated headwater i or j .

Finally, the flow at each unregulated headwater in the region of the dam, $F_{U(i)}$, is defined

$$F_{U(i)} = K_i \cdot F_{TU} \quad (11)$$

The logic for the unregulated flow calculation is complete except when flow at any unregulated headwater falls below the minimum set in **columbia.desc** for that headwater, which can be zero. In this case

$$\begin{aligned} &\text{if } F_{U(i)} < F_{U(i)min} \\ &\text{then } F_{U(i)} = F_{U(i)min} \end{aligned} \quad (12)$$

and then for each reach r enclosed by dams the new loss $F_{L(r)}$ is

$$F_{L(r)} = \left[\sum_{j=1}^n F_{R(j)} - F_{D(r)} + \sum_{i=1}^m F_{U(i)} \right] \frac{F_{M(r)}}{\sum_{i=1}^p F_{M(i)}} \quad (13)$$

where

- $F_{D(r)}$ = flow output at dam immediately below reach r
- $F_{L(r)}$ = new flow loss at reach r , as adjusted for mass imbalance
- $F_{M(r)}$ = flow maximum at reach r or i
- $F_{R(j)}$ = flow at regulation point j
- $F_{U(i)}$ = flow at unregulated headwater i
- m = number of unregulated headwaters above r ($m = 3$ in Fig. 17)
- n = number of regulated points adjacent to nearest upstream regulation point ($n = 2$ in Fig. 17)
- p = number of reaches between dam r and all upstream regulation points ($p = 9$ in Fig. 17).

Downstream Propagation

Downstream propagation of flow in the Monte Carlo Mode is computed after modulation, flow loss and unregulated headwater flows are computed. Starting at a headwater, flow is propagated by traversing the downstream segments, subtracting loss at each to determine new flow values, and adding flows together at confluences. Thus, flows are assigned at each segment in a downstream recursive descent traversal. The flow for each day is

$$F_i(t) = \sum_{i+1} F_i(t) - F_{L(i)} \quad (14)$$

where

- $F_i(t)$ = flow regulation point i at reservoir time increment t
- $F_{L(i)}$ = flow loss at reach i
- $F_j(t)$ = flow at regulation point j immediately upstream at reservoir time increment t .

Combined Modulated Flow

The modulators are combined with archive flows to give daily flows at the dams according to the equation

$$F(t)_i = F(t)_{\text{arch}(i)} + \sum_j^J \{F(t)_{\text{day}(j)} + F(t)_{\text{week}(j)}\} + \sum_i^I F_{\text{loss}(i)} \quad (15)$$

if $F(t)_i < F_{\text{min}(i)}$ then $F(t)_i = F_{\text{min}(i)}$

where

- $F(t)_i$ = modulated flow at dam i
- $F(t)_{\text{arch}(i)}$ = archive flow at dam i
- $F(t)_{\text{day}(i)}$ = daily modulated flow in regulated headwater j
- $F(t)_{\text{week}(i)}$ = weekly modulated flow in regulated headwater j
- $F_{\text{loss}(i)}$ = loss modulated flow in river segment upstream of dam i
- $F_{\text{min}(i)}$ = minimum allowable flow at dam i
- J = number of regulated headwaters upstream of dam i
- I = number of dams upstream of dam i , including dam i .

At each dam, flows are adjusted to conform to minimum values given in Project Data and Operating Limits (Report 49, Revised Book No. 1 and 2, U.S. Army Corps of Engineers, North Pacific Division, July 1989). If the flow drops below the minimum it is set to the minimum flow. Minima are in the **.dat** file under the keyword flow_min. Note: flow minima also exist in the **columbia.desc** file and are used to set minimum flows in river segments.

Table 4 Flow minimum (kcfs) at dams.

Dam	$F_{\text{min}(i)}$	Dam	$F_{\text{min}(i)}$
Bonneville	80	Dworshak	1
The Dalles	12.5	Hells Canyon	5
John Day	12.5	Priest Rapids	36
McNary	12.5	Wanapum	36
Ice Harbor	7.5	Rock Island	36
Lower Monumental	1	Rocky Reach	36
Little Goose	1	Wells	35
Lower Granite	1	Chief Joseph	35

II.2.3 - Scenario Mode Flow Generation

In the Scenario Mode, seasonal flows for unregulated, i.e. un-dammed, streams are identified on a daily basis. These can be set by the user simply by drawing headwater seasonal flows or they can be generated from modulators that distribute the total annual headwater runoff according to the historical seasonal patterns.

Unregulated headwater flows connect directly to the river mainstem or to storage reservoirs. For storage reservoirs, the user can set the schedule of outflow according to constraints of the volume of the reservoir and the inflow. System flows are determined by unregulated stream flows and regulated flows from storage reservoir dams.

Headwater Modulation

In the Scenario Mode, flow from unregulated headwaters are modeled by the following equation:

$$Y_t = mp \cdot (F_t + e_t) \quad (16)$$

where

- t = Julian day ($t = 1$ to 365)
- Y_t = estimated daily flow
- m = mean annual flow computed over a 10 year period
- p = fraction of mean annual for the scenario
- e_t = stochastic error term
- F_t = Fourier term

$$F_t = 1 + \sum_{k=1}^4 a_k \cdot \cos(k\omega t) + \sum_{k=1}^4 b_k \cdot \sin(k\omega t) \quad (17)$$

- a_k, b_k = Fourier coefficients estimated for each river
- $\omega = 2\pi/365$.

The equation given for F_t above is a smooth Fourier estimate for the annual stream flow for each river, in units of multiples of the mean. For each scenario, an error term is randomly generated to incorporate the expected fluctuations. There tend to be more pronounced deviations from the modeled curve in the wet season (spring), when the exact fluctuations are more difficult to predict. For this reason, the error component is generated from a low variance normal distribution in the dry season, and a higher variance normal distribution in the wet season. Also, since daily flows tend to be highly correlated, the generated (independent) error estimates (r_t) are artificially correlated according to the following equation:

$$e_t = 0.925 \cdot e_{t-1} + r_t \quad (18)$$

where

- r_t = randomly generated variable from a normal distribution centered on 0 with variance appropriate for dry and wet years as described above. The switch from dry year to wet year variance parameters occurs at $p = 0.4$.
- $e_0 = 0$.

The user chooses the type of year to be modeled relative to an average year, which is designated by $p = 1$. CRiSP.1 multiplies this proportion of the appropriate average flow parameter, m times $(F_t + e_t)$, which yields an estimate for daily flow for the Scenario Mode flow.

Reservoir Volume and Flow

The storage reservoirs receive flows from the headwaters which are set by the Scenario Flow Modulators or directly by the user. The flow out of the storage reservoirs can be set by the user under constraints established by the maximum and minimum volume of the storage reservoirs. The equation describing the reservoir usable volume is

$$\frac{dV}{dt} = F_U - F_R \quad (19)$$

where

- dV = change in reservoir volume in acre-ft
- dt = time increment, typically 1 day
- F_U = unregulated natural flow into the reservoir in kcfs
- F_R = regulated flow out of the reservoir, which is controlled by the user under volume constraints in kcfs.

The volume for each reservoir is determined a reservoir time step increment from a numerical form of the volume equation

$$V(i+1) = V(i) + c[F_U(i) - F_R(i)]\Delta t \quad (20)$$

where

- $V(i)$ = reservoir volume time step i with units of acre-ft
 - Δt = one day increment
 - F_U and F_R = unregulated and regulated flows in kcfs
 - $c = 1983.5$ is a conversion factor
- acre-ft = (86400 s/d) * (0.023 acre-ft/ k ft³) * (k ft³ / s) * (d)
- $V = (86400) * (0.023) * (F) * (\Delta t)$
- $V = 1983.5 * (F) * (\Delta t)$

The user requests reservoir output F_R with the following constraints: The user is allowed to draw any flow curve for reservoir withdrawal as long as the reservoir is between minimum and maximum operating volumes. If a request requires a volume exceeding the allowable range, CRiSP.1 alters the request to fit within the volume constraints. The algorithm is

$$V_{\text{request}}(i+1) = V(i) + c[F_U(i) - F_R(i)] \quad (21)$$

with constraints on reservoir outflow and volume defined by the algorithm¹

1.
 - if $V_{\text{request}}(i+1) > V_{\text{max}}$ then
 - $V_{\text{request}}(i+1) = V_{\text{max}}$
 - $F_R(i) = F_U(i) + [V(i) - V_{\text{max}}] / c$
 - else
 - if $V_{\text{request}}(i+1) < V_{\text{min}}$ then
 - $V_{\text{request}}(i+1) = V_{\text{min}}$
 - if $F_{\text{request}}(i) > F_U$ then
 - $F_R(i) = F_U(i)$
 - else
 - $F_R(i) = F_{\text{request}}(i)$
 - else
 - $F_R(i) = F_{\text{request}}(i)$

where

- F_R = outflow from reservoir according to the constraints
- F_U = unregulated inflow to reservoir
- V_{request} = requested outflow from reservoir
- F_{request} = requested outflow from reservoir
- $V(i)$ = reservoir volume in reservoir time step i
- V_{max} = maximum reservoir volume
- V_{min} = minimum reservoir volume.

Theory for Parameter Estimation

Average daily flow (designated flow_mean) was computed for all available years. Each daily flow was divided by that year's average. Elements of the resulting series were denoted by X_t , where t = day_of_year. Next, the first nine terms of a Fourier series were computed with a fast Fourier transform. Since the mean of each series was 1, corresponding to the normalized annual mean flow, it follows $a_0 = 1.0$. The remaining Fourier coefficients were estimated according to the equations

$$a_k = \frac{2}{365} \cdot \sum_{t=1}^{365} X_t \cos(k\omega t) \quad b_k = \frac{2}{365} \cdot \sum_{t=1}^{365} X_t \sin(k\omega t) \quad (22)$$

where

- $\omega = 2\pi/365$
- k = value between 1 and 4.

The residual time series, R_t were computed by the equation

$$R_t = X_t - 1 - \sum_{k=1}^4 [a_k \cdot \cos(k\omega t) + b_k \cdot \sin(k\omega t)] \quad (23)$$

The residuals were split into high-variance and low-variance parts, and sample standard deviations computed. mod_start_hi_sigma and mod_end_hi_sigma are the Julian day when high flow variance begins and ends. Period average high and low standard deviation are mod_hi_sigma and mod_lo_sigma, respectively.

Data

From *Hydrodata*, a CD-ROM database marketed by Hydrosphere, Inc., the daily flows were obtained for the following locations and dates:

- Clearwater River @ Orifino, Idaho: Oct. 1980 - Sept. 1989
- Salmon River @ Whitebird, Idaho: Oct. 1980 - Sept. 1989
- Grande Ronde River @ Troy, Oregon: Oct. 1980 - Sept. 1989
- Imnaha River @ Imnaha, Oregon: Oct. 1980 - Sept. 1989

Flow modulator parameter estimates derived from flow data listed above were compared to modulator parameters estimated from flows over the previous 10 years at the same location (Oct 1970-Sep 1980). The parameters were slightly different, but graphs of smooth flow curves were nearly identical for Clearwater, Salmon, and Imnaha rivers. The Grande Ronde had a different shape, so for this river the parameters were adjusted to include all data from 1970 to 1989 data.

Table 5 shows parameters estimated for the unregulated headwater modulators. Parameters mod_coeffs_a and mod_coeffs_b correspond to a_k and b_k respectively. Table 6 shows data for regulated headwaters, i.e., Columbia above Grand Coulee Dam, North Fork Clearwater above Dworshak Dam, and Snake River above Brownlee Dam. Daily mean flow observations for each year were obtained from the U.S. Army Corps of Engineers, North Pacific Division and processed as in Table 6. Data were obtained for the following locations and dates:

- North Fork Clearwater River: Oct. 1973 - Sept. 1991
- Grand Coulee Dam: Oct. 1971 - Sept. 1991
- Brownlee Dam: Oct. 1981 - Sept. 1991

Table 5 Unregulated headwater flow parameter estimates

	Clearwater	Salmon	G. Ronde	Imnaha
flow_mean (kcfs)	8.790	11.240	3.066	0.514
mod_coeffs_a = a_1	-0.76	-0.84	-0.34	-0.73
mod_coeffs_a = a_2	+0.09	+0.34	-0.18	+0.09
mod_coeffs_a = a_3	+0.10	-0.06	-0.03	+0.03
mod_coeffs_a = a_4	-0.14	-0.09	0.00	-0.04
mod_coeffs_b = b_1	+0.87	+0.50	+0.93	+0.74
mod_coeffs_b = b_2	-0.72	-0.64	-0.32	+0.56
mod_coeffs_b = b_3	-0.35	+0.44	+0.04	+0.20
mod_coeffs_b = b_4	-0.16	-0.25	-0.14	-0.12
mod_lo_sigma	0.06	0.04	0.05	0.06
mod_hi_sigma	0.29	0.20	0.28	0.25
mod_start_hi_sigma	46	86	7	46
mod_end_hi_sigma	196	196	175	196

Table 6 Regulated headwater flow parameter estimates

	Columbia	Snake	Clearwater
flow_mean (kcfs)	110.0	21.50	5.50
mod_coeffs_a = a_1	- 0.238	0.029	- 0.508
mod_coeffs_a = a_2	0.198	0.132	- 0.038
mod_coeffs_a = a_3	0.005	0.008	0.159
mod_coeffs_a = a_4	0.041	0.002	- 0.152
mod_coeffs_b = b_1	0.128	0.348	0.881
mod_coeffs_b = b_2	0.102	0.156	- 0.624
mod_coeffs_b = b_3	0.100	0.045	0.159

Table 6 Regulated headwater flow parameter estimates

	Columbia	Snake	Clearwater
mod_coeffs_b = b_4	0.024	0.061	- 0.082
mod_lo_sigma	0.062	0.05	0.230
mod_hi_sigma	0.084	0.10	0.305
mod_start_hi_sigma	96	96	96
mod_end_hi_sigma	196	196	196

Maximum Unregulated Flows

Observed maximum flows in the tributaries were obtained from the peak flow data in *Hydrodata*, a CD-ROM database marketed by Hydrosphere, Inc. The data record length was variable (Table 7).

Table 7 Maximum unregulated flow (kcfs)

Unregulated River	Maximum Flow
Wind	30
Hood	30
West Fork Hood	15
East Fork Hood	15
Klickitat	39
Warm Springs	8
Umatilla	18
Walla Walla	21
Tucannon	5
Clearwater	166
Middle Fork Clearwater	78
Red	10
Salmon	129
Little Salmon	10
Rapid River	10
South Fork Salmon	19
Pahsimeroi	1
East Fork Salmon	4
Redfish	1
Yakima	64

Table 7 Maximum unregulated flow (kcfs)

Unregulated River	Maximum Flow
Wenatchee	31
Entiat	6
Methow	33
Grande Ronde	36
Imnaha	6

Storage Reservoirs Parameter Values

Storage reservoirs volumes are obtained from *Project Data and Operating Limits* (1989 a, b) and are given in Table 8.

Table 8 Storage reservoirs. Shaded items are used in model.

Reservoir	Max Pool ft	Min Pool ft	Usable Storage in acre-ft	Powerhouse Hydraulic Capacity (kcfs)
Grand Coulee	1290	1208	5,185,500	280
Libby Dam	2459	2287	4,979,599	24.1
Hungry Horse	3565	3336	3,161,000	8.9
Duncan	1897	1794	1,398,600	20
Mica	2478	2320	7,770,000 ^a	41.6
Coulee total ^b			22,494,699	
Dworshak	1605	1445	2,015,800	10.5
Brownlee	2080	1976	975,318	34.5

a. estimated

b. In the model all storage reservoirs above Grand Coulee are summed to represent the combined storage capacity of the upper Columbia system.

Desired reservoir elevation levels for flood control, obtained from *Project Data and Operating Limits* (1989 a, b), are presented in Table 9. This is not used by CRiSP.1 at the present time.

Table 9 Storage reservoirs flood control elevation rule curves

Reservoir	Date (Elevation in ft.)			
	Nov 1	Dec 1	Jan 1	-
Libby Dam	2459	2448	2411	-
Dworshak	Sept. 1	Oct 1	Nov 15	Dec 15
	1600	1586	1579	1558

II.2.4 -Flow-Velocity-Elevation

The river velocity used in fish migration calculations is related to river flow and pool geometry and varies with pool drawdown as a function of the volume. The pool is represented as an idealized channel having sloping sides and longitudinal sloping bottom. As a pool is drawn down, part of it may return to a free flowing stream that merges with a smaller pool at the downstream end of the reservoir. The submodel is illustrated in Fig. 18 and Fig. 19. Important parameters are as follows:

- H_u = full pool depth at the upstream end of the segment
- H_d = full pool depth at the downstream end of the segment
- L = pool length at full pool
- x = pool length at lowered pool
- E = pool elevation drop below full pool elevation
- W = pool width averaged over reach length at full pool
- θ = average slope of the pool side
- F = flow through the pool in kcfs
- U_{free} = velocity of free flowing river.

Other parameters illustrated in Fig. 18 are used to develop the relationships between the parameters listed above and water velocity and pool volume. They are not named explicitly.

Pool Volume

Reservoir volume depends on elevation. Elevation is measured in terms of E , the elevation drop below the full pool level. The volume calculation is based on the assumptions that the width of the pool at the bottom and the pool side slopes are constant over pool length. As a consequence of these two assumptions, the pool width at the surface increases going downstream in proportion to the increasing depth of the pool downstream. When $E > H_u$, the drawn down elevation is below the level of the upstream end and the upper end of the segment becomes a free flowing river section that connects to a pool downstream in the segment. When $E < H_u$, the reservoir extends to the upper end of the segment and for mathematical convenience CRiSP.1 calculates a larger volume and subtracts off the excess. The volume relationship (as a function of elevation drop for E positive measured downward) is developed below.

The total volume is defined

$$\begin{aligned} V(E) &= V_1(E) & E \geq H_u \\ V(E) &= V_1(E) - V_2(E) & E < H_u \end{aligned} \quad (24)$$

First the equation for V_1 is developed. Note that when $E \geq H_u$ the volume V_1 divides into two parts

$$V_1 = 2V' + V'' \quad (25)$$

where V' is a side volume and V'' is the thalweg¹ volume. They are defined

1. A thalweg is the longitudinal profile of a canyon.

$$V' = \frac{zxy'}{6} \quad V'' = \frac{zxy''}{2} \quad (26)$$

where

$$x = L \frac{H_d - E}{H_d - H_u} \quad (27)$$

$$z = H_d - E \quad (28)$$

$$y' = z \tan \theta \quad y'' = W - (H_d + H_u) \tan \theta. \quad (29)$$

Combining these terms, when $E \geq H_u$ it follows pool volume is

$$V_1 = \frac{zxy'}{3} + \frac{zxy''}{2} \quad (30)$$

In terms of the fundamental variables in equations (25) to (30) this is

$$V_1(E) = L \left[\frac{(H_d - E)^2}{H_d - H_u} \right] \left[\frac{W}{2} - \left(\frac{H_d}{6} + \frac{H_u}{2} + \frac{E}{3} \right) \tan \theta \right] \quad (31)$$

for $E \geq H_u$ and $x \leq L$.

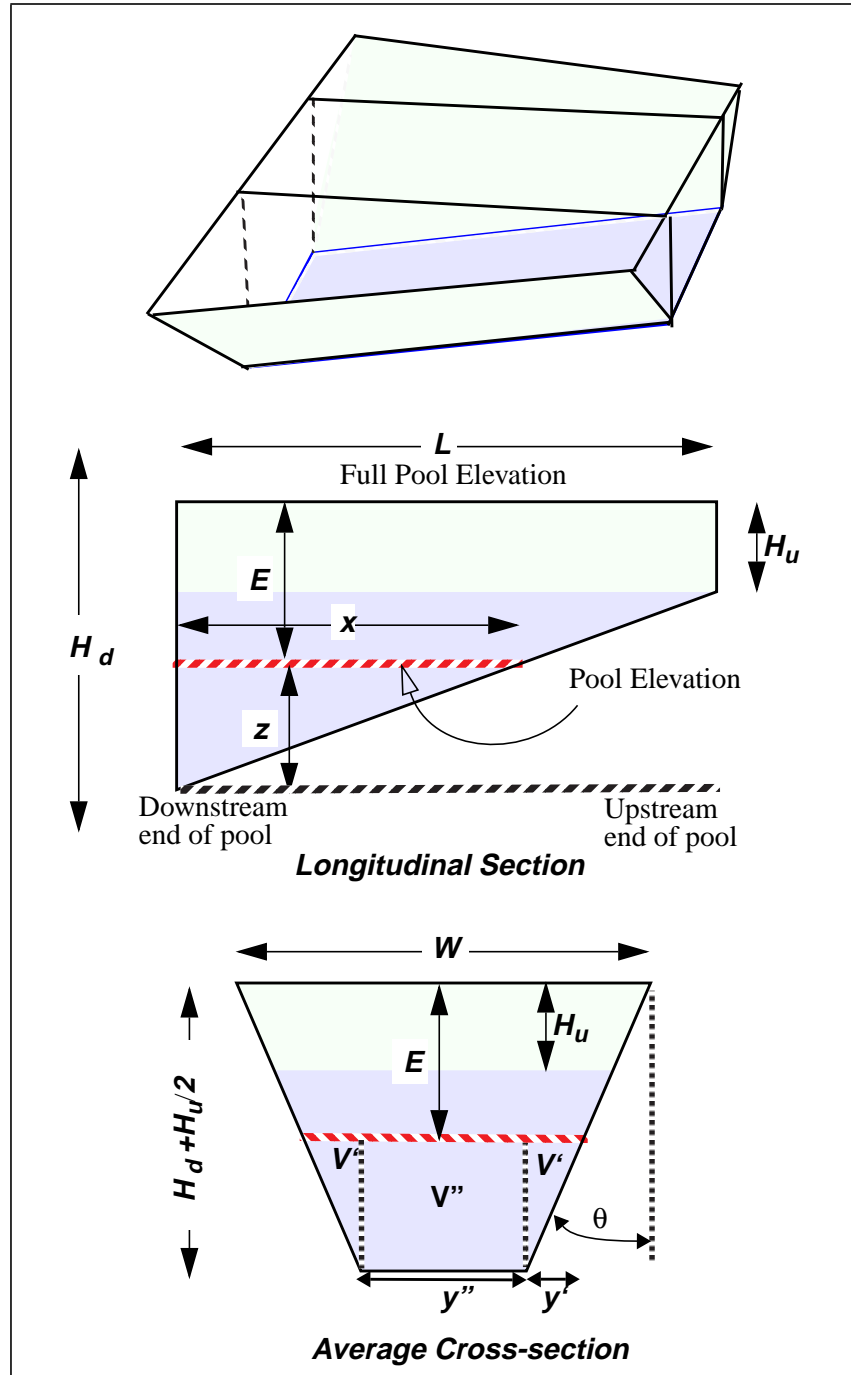


Fig. 18 Pool geometry for volume calculations showing perspective of a pool and cross-sections. The pool bottom remains constant while the surface widens in the downstream direction

When the pool elevation drop is less than the upper depth (so $E < H_u$ and $x = L$) pool volume is $V(E)$ where

$$V(E) = V_1(E) - V_2(E) \quad (32)$$

The term $V_1(E)$ is the volume of the pool extended longitudinally above the dam, where the depth is H_u , so as to form the same triangular longitudinal cross-section as before. This is done so that the volume can still be expressed by eq (31). The term $V_2(E)$ is the excess volume of the portion of the pool above the dam and can be expressed

$$V_2(E) = L \left[\frac{(H_u - E)^2}{H_d - H_u} \right] \left[\frac{W}{2} - \left(\frac{H_d}{2} + \frac{H_u}{6} + \frac{E}{3} \right) \tan \theta \right] \quad (33)$$

Summarizing, the volume relationship as a function of elevation drop, for E positive measured downward, is

$$\begin{aligned} V(E) &= V_1(E) & E \geq H_u \\ V(E) &= V_1(E) - V_2(E) & E < H_u \end{aligned} \quad (34)$$

where

$$\begin{aligned} V_1(E) &= L \left[\frac{(H_d - E)^2}{H_d - H_u} \right] \left[\frac{W}{2} - \left(\frac{H_d}{6} + \frac{H_u}{2} + \frac{E}{3} \right) \tan \theta \right] \\ V_2(E) &= L \left[\frac{(H_u - E)^2}{H_d - H_u} \right] \left[\frac{W}{2} - \left(\frac{H_d}{2} + \frac{H_u}{6} + \frac{E}{3} \right) \tan \theta \right] \end{aligned} \quad (35)$$

The equation for full pool volume can be expressed

$$V(0) = L \left[W \frac{H_d + H_u}{2} - \frac{\tan \theta}{3} \left(\frac{(H_d + H_u)^2}{2} + H_d H_u \right) \right] \quad (36)$$

When the bottom width is zero the full pool volume becomes

$$V(0) = \frac{LW}{3} \left[\frac{H_d^3 - H_u^3}{H_d^2 - H_u^2} \right] \quad (37)$$

Water Velocity

Water velocity through a reservoir is described in terms of the residence time T and the length of the segment L . The residence time in a segment depends on the amount of the reservoir that is pooled and free flowing (Fig. 19).

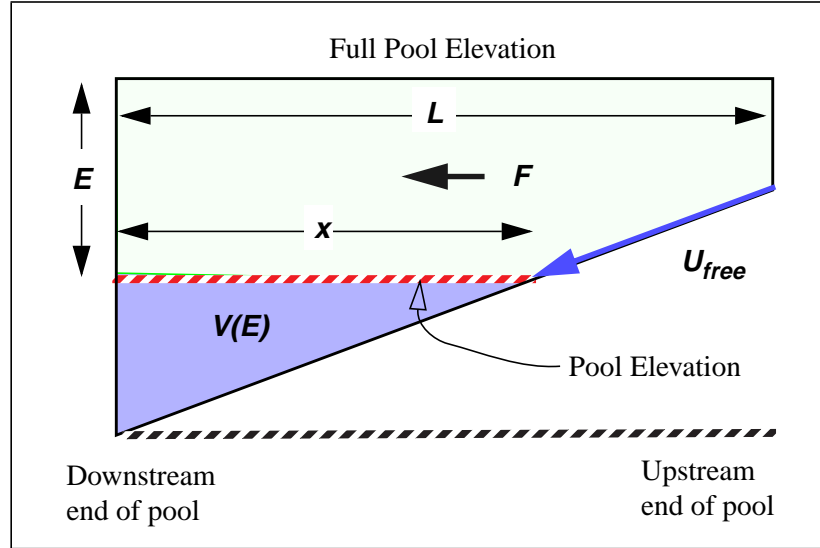


Fig. 19 Reservoir with flowing and pool portions

The equations for residence time are

$$T = \frac{V(E)}{F} + \frac{L-x}{U_{free}} \quad E \geq H_u$$

$$T = \frac{V(E)}{F} \quad E < H_u$$
(38)

where

- $V(E)$ = pool volume (ft³) as a function of elevation drop E in feet
- F = flow in 1000 cubic feet per second or kcfs
- L = segment length in feet
- x = pool length defined by eq (27) and with units of feet
- U_{free} = velocity of water in the free stream (kfs) (using the John Day River, the default value is 4.5 ft/s which is 4.5×10^{-3} kfs)
- T = residence time in this calculation is in kilo seconds or ks.

The velocity in the segment is

$$U = \frac{L}{T}$$
(39)

The velocity with the above units is in thousands of feet per second. Combining equations eq (35), eq (38) and eq (39) the segment velocities are:

for $E \geq H_u$

$$U = \frac{L}{\frac{V_1(E)}{F} + \frac{L-x}{U_{free}}} \quad (40)$$

and for $E < H_u$

$$U = \frac{LF}{V_1(H_u) + V_2(E)} \quad (41)$$

where

- U = average river velocity in ft/s
- U_{free} = the velocity of a free flowing stream in ft/s
- F = flow in kcfs
- E = elevation drop (positive downward) in ft
- H_u = depth of the upper end of the segment in ft
- V_1 and V_2 = volume elements defined by eq (35).

Flow-Velocity Calibration

The calibration of the volume equation requires determining the average pool slope from the pool volume. The equation is the smaller angle of the two forms

$$\theta = \operatorname{atan}\left(\frac{3W(H_d + H_u) - 6\frac{V(0)}{L}}{(H_d + H_u)^2 + 2H_dH_u}\right) \quad (42)$$

or

$$\theta = \operatorname{atan}\left(\frac{W}{H_d + H_u}\right)$$

where

- $V(0)$ = pool volume at full pool.

This scheme using eq (42) reflects the volume versus pool elevation relationship developed for each reservoir by the U.S. Army Corps of Engineers. Capacity versus elevation curves were obtained from several dams to check the accuracy of our volume model. The figures below show data points from these curves versus CRiSP.1's volume curve for two dams. Fig. 20 illustrates Lower Granite pool, with model coefficients of $H_u = 40$ ft., $H_d = 118$ ft, $\theta = 80.7^\circ$, $L = 53$ miles, $W = 2000$ ft, and Wanapum pool, with model coefficients $H_u = 42$ ft., $H_d = 116$ ft, $\theta = 87.0^\circ$, $L = 38$ miles, $W = 2996.1$ ft.

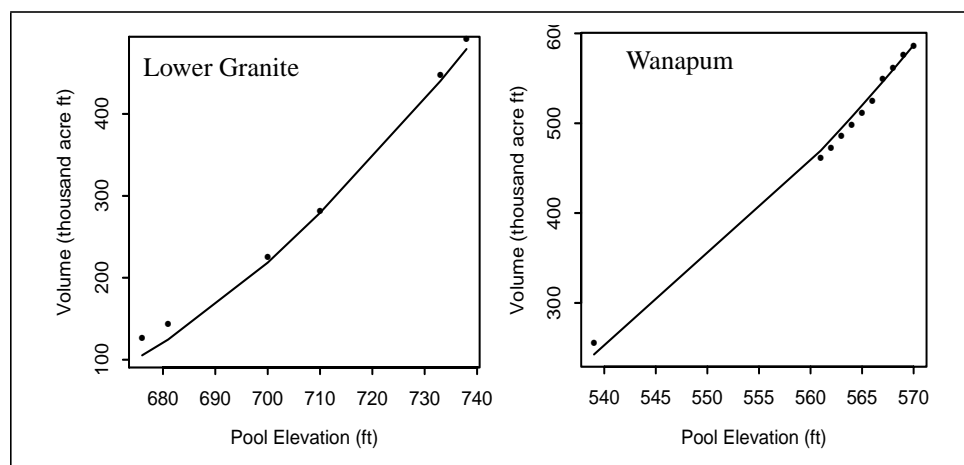


Fig. 20 Pool elevation vs. volume for Lower Granite and Wanapum Pools

Table 10 Geometric data on Columbia River system. Elev is normal full pool elevation, in feet above mean sea level. MOP is minimum operating pool elevation.

Segment	L	Elev	MOP	V	A	W	H _u	H _d	θ
Units	miles	ft MSL	ft MSL	kaf	k ft ²	feet	feet	feet	° of arc
Bonneville	46.2	77.0	70.0	565	101.8	3643	22	93	88
The Dalles	23.9	160.0	155.0	332	114.6	3624	60	105	87
John Day	76.4	268.0	257.0	2,370	255.9	5399	34	149	86.9
McNary	61	340.0	335.0	1,350	182.6	5153	40	105	88
Hanford Reach	44	---	---	131	24.6	3213	29	29	---
Priest Rapids	18	488.0	465.0	199	91.2	3208	32	101	87
Wanapum	38	572.0	539.0	587	127.4	2996	42	116	87.0
Rock Island	21	613.0	609.0	113	44.4	982	15	44	64.4
Rocky Reach	41.8	707.0	703.0	430	84.8	1815	37	108	84.5
Wells	29.2	781.0	767.0	300	84.8	3023	91	111	86
Chief Joseph	52	956.0	930.0	516	81.9				
Ice Harbor	31.9	440.0	437.0	407	105.2	2154	18	110	83.3
L. Monumental	28.7	540.0	537.0	377	108.4	1937	42	118	81.3
Little Goose	37.2	638.0	633.0	365	80.9	2200	40	140	78.2
Lower Granite	53	738.0	733.0	484	75.3	2000	48	140	80.7

The water particle residence time in a segment is given in eq (38). The pool volume velocity/travel time equation was tested against particle travel calculations for Lower Granite

Pool as reported by the U.S. Army Corps of Engineers in the Lower Granite Drawdown studies report (1993) (Fig. 21).

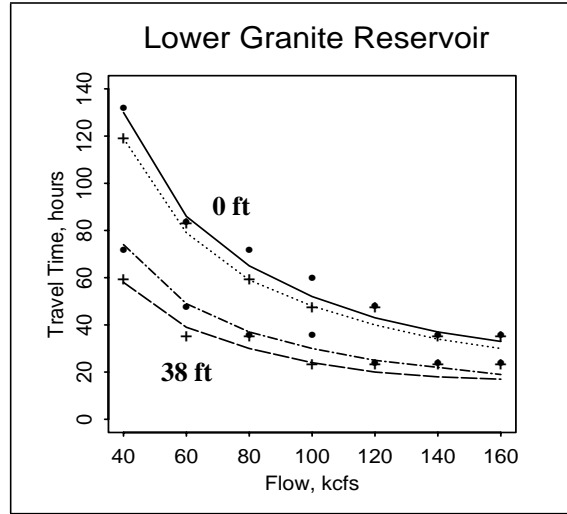


Fig. 21 Water particle travel time vs. flow for CRiSP.1 (points) and Army Corps calculations (lines) at two elevations full pool(0) and 38 ft below full pool for Lower Granite Dam.

II.2.5 -Temperature

River temperature is computed in two stages. First, hydrosystem temperature inputs are calculated from mixing headwater temperatures according to the equation

$$\theta(t) = \frac{\sum_i \theta_i(t) F_i(t)}{\sum_i F_i(t)} \quad (43)$$

where

- $F_i(t)$ = flow from headwater i through the river segment in question on day t
- $\theta_i(t)$ = temperature from headwater i on day t
- $\theta(t)$ = temperature for selected river segment on day t .

Headwater temperatures are identified for the Snake River using measured temperatures from Lower Granite Dam as available in the U.S. Army Corps of Engineers CROHMS database. Head water temperatures for the Mid-Columbia are identified from CROHMS and supplemented using data collected by the U.S. Geological Survey (USGS).

Second, changes to the temperatures within the hydrosystem are made by adding $\Delta\theta(s,t)$ for each day t at site s where the true $\theta(t)$ for the site is known.

II.3 - Fish Migration

II.3.1 -Theoretical Framework

The movement of fish through river segments is described in terms of an average migration velocity and a stochastic velocity that varies from moment to moment. The migration velocity equation for a group of fish is defined by the Wiener stochastic differential equation

$$\frac{dX}{dt} = r + \sigma W(t) \quad (44)$$

where

- X = position of a fish down the axis of the river
- dX/dt = velocity of fish in migration
- r = average velocity of fish in the segment

This is a combination of water movement and fish behavior.

- σ = spread parameter setting variability in the fish velocity
- $W(t)$ = Gaussian white noise process to represent variation in velocity.

Numerical simulation of time vs. distance traveled according to eq (44) is illustrated in Fig. 22.

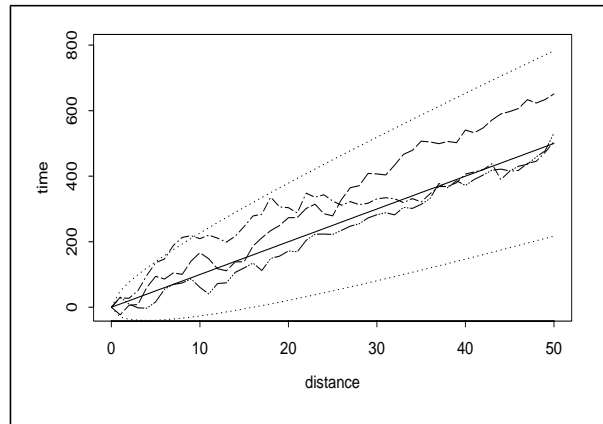


Fig. 22 Movement along axis of segment vs. time. Shown are mean path, three paths, and 95% confidence intervals. For these simulations, r is set at 10, and σ set at 20.

Probability Density Function

The stochastic equation describing fish positions is random so we must define the probability distribution of fish position over time instead of the actual position, which changes from one fish to another. The probability density function (pdf) of the stochastic differential equation (44) can be defined with a Fokker-Planck (Gardiner 1985) equation

$$\frac{\partial p}{\partial t} = -r \frac{\partial p}{\partial x} + \frac{\sigma^2}{2} \frac{\partial^2 p}{\partial x^2} \quad (45)$$

where $p = p(x, t)$ is the pdf describing the probability density of the fish being at position x at

time t given it was at position $x = 0$ at time $t = 0$.

Boundary Conditions

To solve the pdf from eq (45), boundary conditions must be identified. We assume that upon release into a segment a fish can move upstream or downstream in the segment but once it has reached the downstream end of the segment, at $x = L$, it will move into the next segment. The next downstream segment may be a confluence or the forebay of a dam. The boundary conditions are

$$\begin{aligned} p(L, t) &= 0 \\ p(-\infty, t) &= 0 \end{aligned} \quad (46)$$

Solution

The solution to the partial differential equation (45) describing the probability distribution of fish in a river segment is a probability density function for the fish. This is

$$p(x, t) = \frac{1}{\sqrt{2\pi\sigma^2 t}} \left[\exp\left(-\frac{(x - rt)^2}{2\sigma^2 t}\right) - \exp\left(\frac{2Lr}{\sigma^2} - \frac{(x - 2L - rt)^2}{2\sigma^2 t}\right) \right] \quad (47)$$

An example of the distribution of p with respect to x for different times is illustrated in Fig. 23. The pdf in the figure can be interpreted as probability where a fish is in the river at any time. It can also be interpreted as the distribution of a group of fish in a river segment if they have experienced no predation. Notice that the group moves down the segment and spreads over time. At the absorbing boundary representing a dam, the fish enter the boundary regions and pass through to the next segment. Note that the equation cannot define the deterministic path of fish with time.

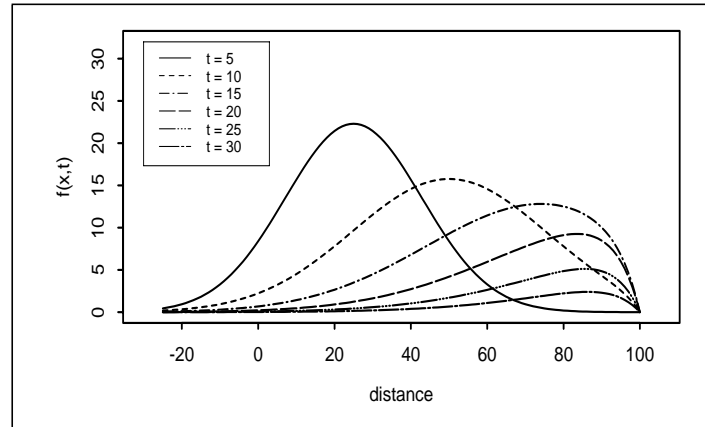


Fig. 23 Plot of eq (47) for various values of t . Parameters r , σ and L are set at 5, 8, and 100 respectively.

Passage Probability

The probability that a fish that entered the river segment at time t_i is still in the river segment at time t_j is obtained by integrating eq (47) over reservoir length. This is expressed

$$\begin{aligned}
P(t_j|t_i) &= \int_{-\infty}^L p(x, t_j - t_i) dx = \\
&= \Phi\left(\frac{L - r \cdot (t_j - t_i)}{\sigma \sqrt{t_j - t_i}}\right) - \exp\left(\frac{2Lr}{\sigma^2}\right) \Phi\left(\frac{-L - r \cdot (t_j - t_i)}{\sigma \sqrt{t_j - t_i}}\right)
\end{aligned} \tag{48}$$

where

- Φ = cumulative distribution of the standard normal distribution
- L = segment length
- r = average migration velocity through the segment (developed in the Migration Models section).

The probability of a fish leaving a segment between time t and $t + \Delta t$ is

$$\Delta P(t_j|t_i) = P(t_j|t_i) - P(t_{j-1}|t_i) \tag{49}$$

This is the arrival time distribution at the point L , which is generally a dam or river confluence. The number of fish exiting each river segment is defined by eq (49).

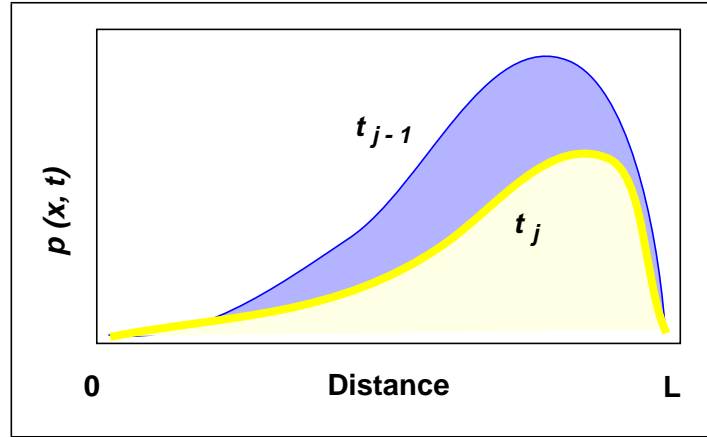


Fig. 24 Fish distribution, $p(x, t)$, at t_j and t_{j-1} . Size of the shaded area represents probability of fish leaving the segment over the interval $t_j - t_{j-1}$

II.3.2 -Migration Models

Active Migration equation

The goal of the active migration equation is to be flexible enough to capture a variety of migratory behaviors without requiring an excessive number of parameters to fit. The equation has a term that relates migration rate to river velocity and a term that is independent of river velocity. Both terms have temporal components, with migration rate increasing with time of year.

The flow independent migration rate is driven by two parameters, β_{\min} and β_{\max} . β_{\min} is the flow independent migration rate at the time of release (T_{RLS}), and β_{\max} is the maximum flow

independent migration rate. In eq (50) below, it is easier to express the equation in terms of β_0 and β_1 , with the following relations:

$$\begin{aligned}\beta_{\min} &= \beta_0 + \frac{\beta_1}{2} \\ \beta_{\max} &= \beta_0 + \beta_1\end{aligned}\tag{50}$$

With $\beta_{\max} > \beta_{\min}$, the fish have a tendency to migrate faster the longer they have been in the river. This tendency can be “turned off” by setting $\beta_{\max} = \beta_{\min}$ (that is, $\beta_1 = 0$). Also, flow independent migration can be turned off entirely by setting $\beta_{\max} = \beta_{\min} = 0$ (that is, $\beta_0 = \beta_1 = 0$).

The magnitude of the flow dependent term is determined by β_{flow} . This term determines the percentage of the average river velocity that is used by the fish in downstream migration. This term has a seasonal component determined by the T_{SEASN} term, which is expressed in terms of Julian date. This has the effect of the fish using less of the flow early in the season and more of the flow later in the season. Values of T_{SEASN} that are relatively early in the season mean that the fish mature relatively early. The α parameter determines how quickly the fish mature from early season behavior to later season behavior. Setting α_2 equal to 0 has the effect of “turning off” the flow/season interaction, resulting in a linear relationship between migration rate and river flow.

The full migration rate model (Zabel, Anderson and Shaw, 1998) is:

$$\begin{aligned}r(t) &= \beta_0 + \beta_1 \left[\frac{1}{1 + \exp(-\alpha_1(t - T_{\text{RLS}}))} \right] \\ \beta_{\text{FLOW}} \bar{V}_t &\left[\frac{1}{1 + \exp(-\alpha_2(t - T_{\text{SEASN}}))} \right]\end{aligned}\tag{51}$$

where

- $r(t)$ = migration rate (miles/day)
- t = Julian date
- β 's = regression coefficients, described above
- \bar{V}_t = average river velocity during the average migration period
- α_1, α_2 = slope parameters
- T_{SEASN} = seasonal inflection point (in Julian Days)
- T_{RLS} = release date (in Julian Days).

Both the flow dependent and flow independent components of eq (51) use the logistic equation (term in brackets). The logistic equation is expressed in general as

$$y = \beta_0 + \beta_1 \left[\frac{1}{1 + \exp(-\alpha(t - T_0))} \right]\tag{52}$$

This equation has a minimum value of β_0 and a maximum value of $\beta_0 + \beta_1$. T_0 determines the inflection point, and α determines the slope. Fig. 25 contains example plots of the equation and demonstrates how varying the parameter affects the shape of the curve.

The logistic equation is used instead of a linear equation because upper and lower bounds can be set. This eliminates the problem of unrealistically high or low migration rates that can occur outside observed ranges with linear equations. Also, for suitable parameter values, the logistic equation effectively mimics a linear relationship.

Other Model Options

As mentioned above, simpler models are nested within the full migration model. For example, setting $\beta_1 = 0$ removes the flow-independent experience term. The resulting model

$$r(t) = \beta_0 + \beta_{FLOW} \bar{V}_t \left[\frac{I}{I + \exp(-\alpha_2(t - T_{SEASN}))} \right] \quad (53)$$

has only the flow-dependent experience factor, which assumes that fish migrate more rapidly later in the season by migrating in high flow regions of the river and/or by spending a greater portion of the day in the river rather than holding up along the shore.

By also setting $\alpha_2 = 0$, all experience related migration rate increases are removed. The resulting model

$$r(t) = \beta_0 + (\beta_{FLOW} \bar{V}_t)/2 \quad (54)$$

assumes a linear relation between migration rate and river velocity. Other combinations of assumptions are also available in CRiSP.1.

Velocity Variance

The spread parameter σ sets the variability in the migration velocity. This term represents variability from all causes including water velocity and fish behavior. In CRiSP.1, $\sigma^2 = V_{var}$ which is the variance in the velocity. This can vary on a daily basis.

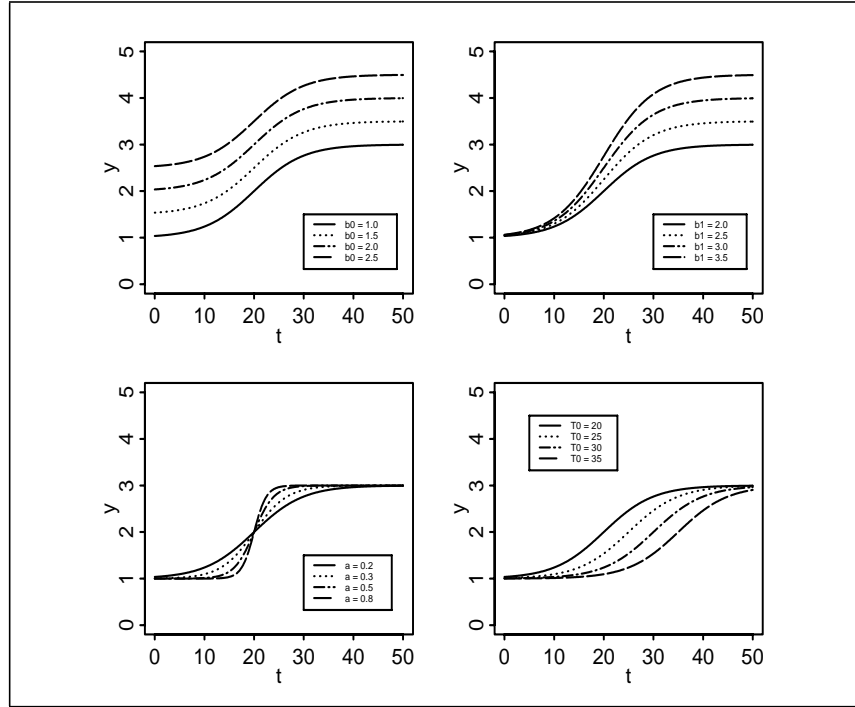


Fig. 25 Examples of the logistic equation (eq (52)) with various parameter values. In all four plots, the parameter values for the solid curves are: $\beta_0 = 1.0$, $\beta_1 = 2.0$, $\alpha = 0.2$, and $T_0 = 20$. In the upper left plot β_0 is varied, and β_1 is varied in the upper right. In the lower left plot, α is varied, and T_0 is varied in the lower right.

Variance in Migration Rate

Variance in the migration rate is applied for each release, thus randomly representing differences in the migration characteristics of each release. Although studies suggest differences in migration can partly be attributed to differences in fish condition and perhaps stock to stock variations, these factors have not been sufficiently identified so their contribution to differences in travel time is randomized. The equation is

$$r_i(t) = r(t) \cdot V(i) \quad (55)$$

where

- $r(t)$ = determined from eq (51)
- $V(i)$ = variance factor that varies *between* releases only.

$V(i)$ is drawn from the broken-stick distribution. The mean value is set at 100%, representing $r(t)$, and the upper and lower values are set with sliders under the migration rate variance item in the **Behavior** menu.

Pre-smolt behavior

In some cases, fish are released into the river before they are ready to initiate migration. This may be the case with hatchery releases or fish that are sampled and released in their rearing grounds. The probability of moving from the release site is determined by two dates, $smolt_{start}$ and $smolt_{stop}$:

$$p = \begin{cases} 0 & \text{for } (t < smolt_{start}) \\ \frac{(t - smolt_{start})}{(smolt_{stop} - smolt_{start})} & \text{for } (t < smolt_{start} < smolt_{stop}) \\ 1 & \text{for } (t > smolt_{stop}) \end{cases} \quad (56)$$

In other words, the probability of initiating migration is 0 before $smolt_{start}$, 1 after $smolt_{stop}$, and linearly increasing with time between the two values. Fish are subjected to predation prior to the onset of smoltification. The predation activity coefficient for pre-smolt mortality uses the activity coefficient for the first day of smoltification $t = 1$.

Implementing the Travel Time Algorithm

The basic unit of the travel time algorithm is a reach of river between two nodes, where a node is a dam, confluence of two rivers, or a release point (Fig. 26). The travel time algorithm passes a group of fish from node to node and determines the distribution of travel times from an upstream node to the next downstream node.

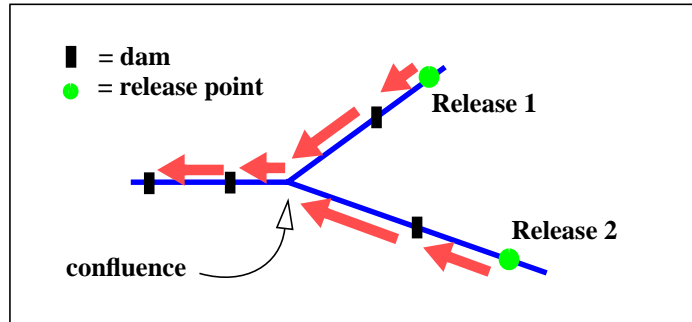


Fig. 26 Schematic diagram of a river system. Arrows represent the migration of release groups 1 and 2 through reaches. At the confluence, groups are combined for counting purposes only, i.e they still exhibit their unique migration characteristics.

CRiSP.1 groups fish according to user preference. The user defines *species* (and *stocks*, if desired) in the **columbia.desc** file and associates behavioral characteristics with each species through the user interface or the yearly input data file¹. For instance, the user may decide that all chinook 1's should be treated identically or that wild and hatchery stocks be treated separately. All releases that are treated similarly are referred to as a release group, except for the random selection of a migration rate variance.

During one iteration of the travel time submodel, fish from a release group pass through a reach. The input to CRiSP.1 is the number of fish from the release group that are ready to depart a node during the time interval. This input group is passed to the next node downstream with the travel time distributions determined by eq (48) and eq (49). Fig. 27 demonstrates a single iteration of the travel time algorithm.

1. As configured, the **columbia.desc** defines three species: chinook 1 = spring chinook, chinook 0 = autumn chinook, and steelhead.

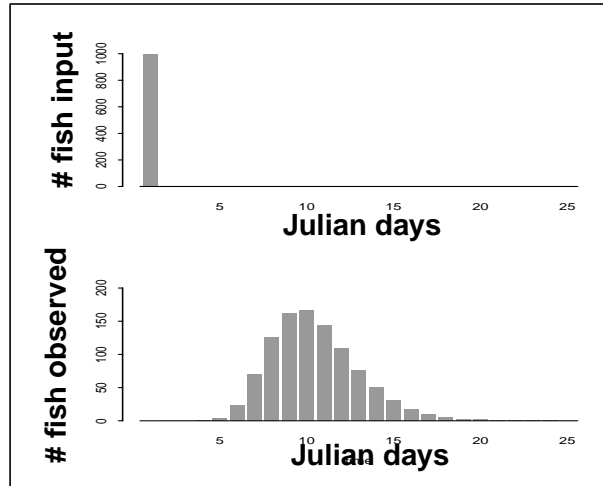


Fig. 27 Plots of a single iteration of the travel time algorithm through a single reach. One thousand fish released at the upstream node are distributed through time at the next downstream node. Parameter: $r = 10$, $\sigma = 8$, $L = 100$.

II.4 - Reservoir Survival

The main component of fish mortality in the reservoirs is the predation rate. The predation rate is dependent on factors such as the number and behavior of predators, size of prey, genetic disposition of prey, disease, stress from dam passage, and degree of smoltification. The theory presented below approximates the mortality processes in the reservoirs. The CRiSP.1 model incorporates some of the details of the interactions of the various factors in mortality in further modeling the predation rate. The included factors are pictured in (Fig. 28). In the model, we further partition the reservoir into forebay, tailrace and reach (also called reservoir) segments for the purpose of travel time and mortality modeling.

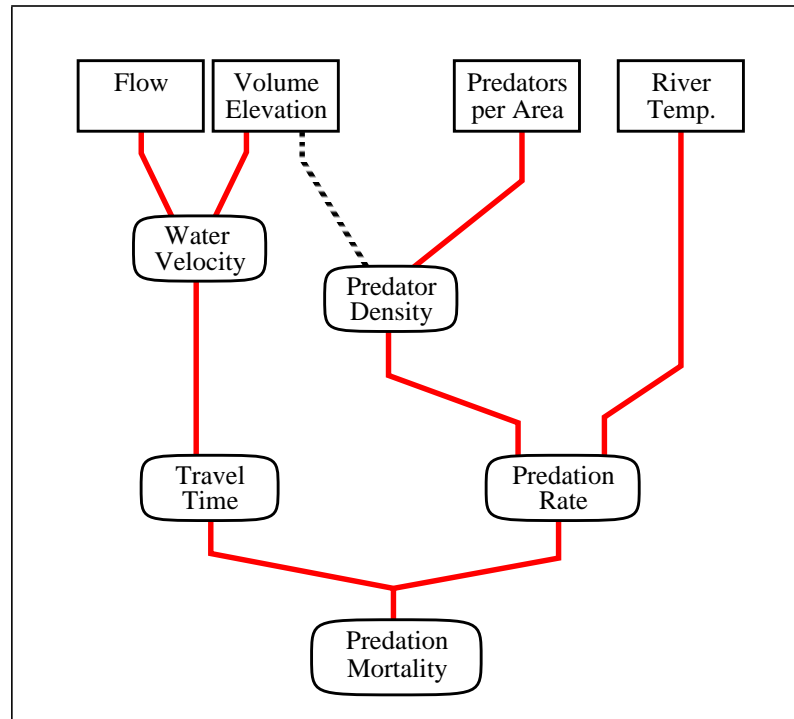


Fig. 28 Elements in reservoir mortality algorithm. Elements used in all model conditions designated by (—). Element selected by the user is designated by (---).

II.4.1 -Theoretical Framework

The theoretical framework for describing reservoir mortality in the current model uses the time fish spend in a river segment and the segment rate of mortality. The basic equation describing the rate of mortality as a function of time is

$$\frac{dS}{dt} = -\phi S \quad (57)$$

where

- S = measure of smolt density in the river segment and can be taken as the total number in the segment
- ϕ = mortality rate from all causes.

In the present model, two causes of mortality are identified: predation and gas bubble disease. CRiSP.1 assumes the rates of each are independent and this is expressed by the equation

$$\frac{dS}{dt} = -\phi S = -(M_p + M_n)S \quad (58)$$

where

- M_p = mortality rate from predation with units of time⁻¹
- M_n = mortality rate from total dissolved gas supersaturation with units of time⁻¹
- S = number of smolts leaving reservoir per day (smolts reservoir⁻¹)
- ϕ = combined mortality rate as used in eq (62).

Fish enter and leave river segments every day and spend differing amounts of time in a segment as described by the migration equations. Thus, on a given day the group of fish leaving a segment may have entered on different days and thus have different residence time in the segment. To describe the number of fish that survive a river segment on a daily basis CRiSP.1 solves eq (57) for each group, identified by when they entered the segment and when they exited. The solution is

$$S(t_j | t_i) = S_0(t_j | t_i) \cdot \exp \left(- \int_{t_i}^{t_j} \phi(t) dt \right) \quad (59)$$

where

- $S_0(t_j | t_i)$ = potential number of fish that enter the segment on day t_i and survive to leave the segment on day t_j
- $S(t_j | t_i)$ = actual number of fish that enter the segment on day t_i and leave on day t_j .

Applying an elementary property of integrals the integral is expressed

$$\int_{t_i}^{t_j} \phi(t) dt = \int_0^{t_j} \phi(t) dt - \int_0^{t_i} \phi(t) dt \quad (60)$$

In general, the numerical form of the integral is

$$\int_0^{t_j} \phi(t) dt = \sum_{k=0}^j \phi(t_k) \Delta t \quad (61)$$

where

- Δt = reservoir computational time increment.

The resulting equation for the number of fish passing through each river segment as a function of when it entered the segment is expressed

$$S(t_j | t_i) = S_0(t_j | t_i) \cdot \exp \left(- \sum_{k=0}^j \phi(t_k) \Delta t + \sum_{k=0}^i \phi(t_k) \Delta t \right) \quad (62)$$

The input term $S_0(t_j | t_i)$ expressing the potential number that exit on day t_j given then entered the segment on day t_i can be expressed

$$S_0(t_j|t_i) = N(t_i) \cdot \Delta P(t_j|t_i) \quad (63)$$

where

- $N(t_i)$ = number of fish that enter the river segment on day t_i
- $\Delta P(t_j | t_i)$ = probability that a fish entering on day t_i survives to exit on day t_j .

This probability is defined by eq (49) on page 38.

II.4.2 - Predation Mortality

Predation mortality rate in CRiSP.1 is dependent on predator abundance (density), predator temperature response, and a predator activity coefficient. These factors combine to determine a predation rate (r) which is applied to the smolt population in each time step to determine predation mortality.

Predation occurs in three zones: forebay and tailrace and main reservoir or river reach. Each zone has its own predator abundances (which vary from project to project) and predator activity coefficients (set system-wide via the calibration process). The predation mortality is then a function of exposure time.

Predator abundances may vary yearly and are based on predator index studies (Beamesderfer and Rieman 1988; Rieman et al. 1991; Ward et al. 1995). The major predator is the northern pikeminnow (*Ptychocheilus oregonensis*, formerly called northern squawfish) which accounts for approximately 78 percent of the predation mortality (Rieman et al. 1991). The other major predators (walleye, and smallmouth bass) are converted into northern pikeminnow equivalents via their consumption rates. The effects of the predator removal program on pikeminnow populations have been accounted for from 1991 on.

The *predator temperature response function* determines maximum consumption rates as a function of temperature and is based on laboratory experiments by Vigg and Burley (1991). Several forms of the function are available in CRiSP.1. The parameters in the temperature response function are set during the calibration process (calibration of the model to NMFS survival estimates). Thus, the predator temperature response may account also for response of the prey species in the model to variation in temperature.

The *predator activity coefficient* scales the maximal consumption rate to represent *in situ* conditions where predator-prey encounters may be less frequent, alternative prey may exist, and predators may not be feeding to satiation. As stated above, this coefficient varies by reservoir zone to account for the differences in predator-prey behavior in each zone.

General Model

The *predation rate* is assumed to be proportional to predator abundance and consumption rate. Consumption rate is scaled by the temperature response function, with consumption increasing with higher water temperature. The general form of the predation rate in the i th zone (forebay, tailrace, or reservoir) for the j th project is:

$$r_{ij}(T) = \alpha_i \cdot P_{ij} \cdot f(T) \quad (64)$$

where

- T is temperature ($^{\circ}\text{C}$),
- P_{ij} is the predator density in the i th zone (forebay, tailrace, or reservoir) for the j th project.
- α_i is the predator activity coefficient in the i th river zone, and
- $f(T)$ is the temperature response equation.

The predation survival is determined from the predation rate in each time step as follows:

$$S_{ij} = e^{-r_{ij}t}. \quad (65)$$

where t is time (in days).

For the temperature response function, the sigmoidal form (reparameterized) from Vigg and Burley (1991) is employed

$$f(T) = C_{MAX} / (1 + \exp(-\alpha_T(T - T_{INF}))) \quad (66)$$

where

- C_{MAX} = the maximum consumption rate
- α_T = a slope parameter
- T_{INF} = the inflection point of the curve.

With this equation, predation rate approaches its maximal rate at higher temperatures. An example of equation (66) fit to data from Vigg and Burley (1991) is shown in Fig. 29. The parameter values for this plot are $C_{MAX} = 8.0$, $\alpha_T = 0.40$, and $T_{INF} = 16.7$.

The old (exponential) form of the temperature response function is also available but is no longer supported in the calibration. The exponential form is

$$f(T) = ae^{bT} \quad (67)$$

This form may be reasonable for the spring migration period where higher temperatures are not encountered.

As formulated in equation (64), predation rate is dependent on predator abundance but not on smolt abundance. Thus with a given predator density and temperature, mean predator consumption rate is linearly related to smolt abundance. This is consistent with data provided by Vigg (1988) except at extremely high smolt abundances (which represent only a few points out of hundreds). Also, the Vigg (1988) study was conducted in the tailrace.

Note also that the CRiSP.1 predation algorithm is very similar to the RESPRED model as described by Beamesderfer et al. (1990). The differences are that RESPRED has a type III functional response of predators on prey; i.e., consumption rate tails off at high prey abundances. Also, RESPRED uses a gamma distribution for the temperature response function instead of the sigmoidal one utilized by CRiSP.1.

Zone Specific Formulations of the Predation Model

As noted above, the predation equation (64) varies according to reservoir zone (forebay, tailrace or reach). The forebay and reservoir predation models are based on exposure time as calculated from the migration submodel. Tailrace residence times tend to be very short, so we have assumed one time step residence and have calibrated the model with that in mind.

Another type of model would incorporate exposure (travel) distance as well as exposure time. The tailrace predation model can be thought of as a travel distance based predation model.

Table 11 Summary of the forms of the predation mortality rate equation

Reservoir zone	α	applied
forebay, reservoir	α_f, α_r	per time step
tailrace	α_t	per tailrace

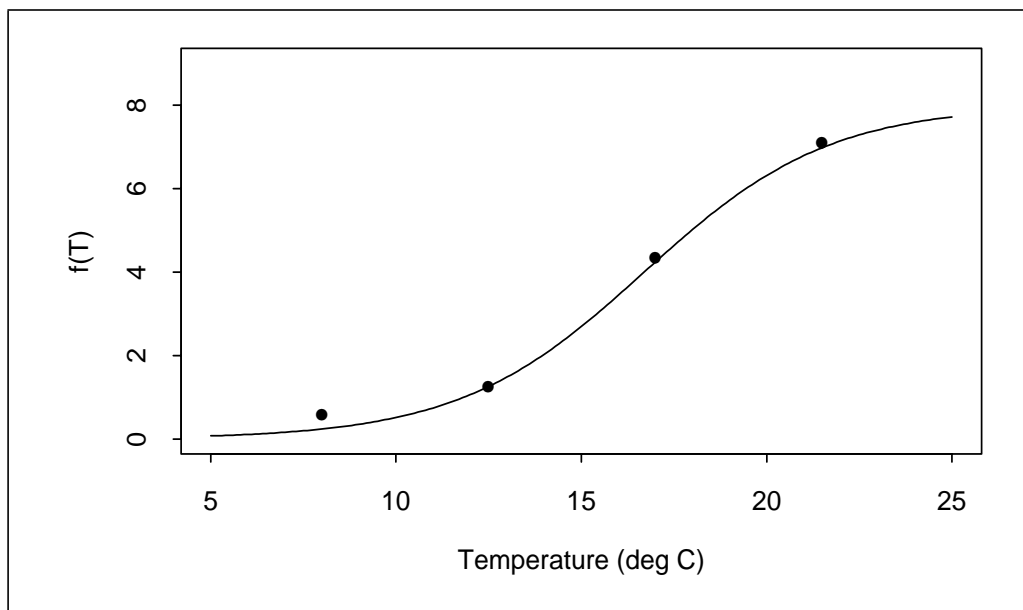


Fig. 29 Equation 66 fit to data from Vigg and Burley (1991). Note that each point represents the mean from 11 to 22 replicates.

Predator Abundance

Predator abundances (as relative predator densities) are needed for each zone of each reservoir. These abundances are based on the predator index studies performed by U.S. FWS, ODFW and WDFW (Ward et al. 1995; Zimmerman and Parker 1995). The major predators are northern pikeminnow, walleye and smallmouth bass. Abundances for these predators were based on mark-recapture studies in John Day Pool from 1983-1986 (Beamesderfer and Rieman 1991). For pikeminnow, predator index data from 1990-1991 was used as base abundances because the predator removal program had little or no effect in those years. Bass and walleye abundances were converted to *pikeminnow equivalents* based on their consumption rates relative to pikeminnow consumption rates (see Table 16) (Vigg et al. 1991).

Because abundances based on the mark-recapture studies have very broad confidence intervals (Beamesderfer and Rieman 1991), and because the predator index are not intended to provide *absolute* abundances (Ward et al. 1995; Zimmerman and Parker 1995), the abundance data should be considered in a *relative* sense. The purpose of the predator index studies was to gauge relative differences in predator abundances among reservoirs and within reservoir zones. This is how this information is utilized in CRiSP.1.

The C_{MAX} parameter (in the temperature response function) in CRiSP.1 has the effect of scaling predation rate up or down such that model-predicted survivals are consistent with observed survivals. (This will be explained more fully in section III.3.1 - Parameter

Determination and Calibration on page 124.) This can be thought of as a scaling of the relative predator abundances to reflect the actual predator abundances.

Outline of Calculations for Predator Abundance

The major piscivorous predators on juvenile salmonids are northern pikeminnow (*Ptychocheilus oregonensis*), formerly known as northern squawfish, smallmouth bass (*Micropterus dolomieu*), and walleye (*Stizostedion vitreum*).

Outline of steps:

1. Compute densities in John Day Pool based on 1984-1986 Mark-Recapture data and relative abundances in different reservoir zones (for each species).
2. Calculate CPUE -> density conversion factors.
3. Estimate densities in other reservoirs/zones based on CPUE data. For some zones, Pike-minnow abundance indices must be converted to CPUE based on linear regression of CPUE vs. indices in cases where both are available.
4. Convert SMB and walleye to "Pikeminnow equivalents" based on relative consumption rates. These densities are different for Spring and Fall due to seasonal differences in consumption rates by the predators. The CPUE is then multiplied by 1080 to convert to density (based on John Day population estimates).

Mean population abundances (1984-1986) in John Day Pool for these three species are provided in Table 12. Information and interim calculations are provided in Tables 13 - 21. Table 22 gives the resulting densities for Spring and Fall. It also gives the pikeminnow percentage, which is needed when accounting for results of the pikeminnow removal program.

Table 12 Population abundance estimates for John Day Pool, 1984-1986 (Beamesderfer and Rieman 1991). 95% confidence intervals are in parentheses.

N. Pikeminnow (>250 mm)	Smallmouth Bass (>200 mm)	Walleye (>250 mm)
85,316 (65,693-106,645)	34,954 (35,166-44,741)	15,168 (6,067-32,914)

Table 13 . Northern pikeminnow density and distribution in John Day Pool, based on 1990-1991 CPUE data, assuming total abundance the same as 1984-1986.^a

zone	John Day Forebay	mid- reservoir	McNary tailrace	McNary tailrace BRZ	total
CPUE	0.69	0.25	0.76	16.33	
Area	10.74	186.7	9.7	1.07	208.2
rel. abundance	0.094	0.592	0.093	0.221	1.0
abundance	8019.7	50507.1	7934.4	18854.8	85316
density	746.7	270.5	818.0	17621.3	
comb. density	746.7	297.6		17621.3	

a. CPUE mult factor = density/CPUE = 1080.

Table 14 Walleye density and distribution in John Day Pool, 1984-1986. Relative densities are mean for 1984-1986 from Beamesderfer and Rieman (1988).

zone	John Day Forebay	Arlington	Irrigon	McNary tailrace	McNary tailrace BRZ	total
relative density	0.002	0.114	0.305	0.58	0.000	1.0
Area	10.74	117.1	69.6	9.7	1.07	208.2
abundance						15,168
comb. density	0.	77.2				

Table 15 Smallmouth bass density and distribution in John Day Pool, 1984-1986. Relative densities are mean for 1984-1986 from Beamesderfer and Rieman (1988).^a

zone	John Day Forebay	Arlington	Irrigon	McNary tailrace	McNary tailrace BRZ	total
relative density	0.374	0.289	0.277	0.060	0.0	1.0
Area	10.74	117.1	69.6	9.7	1.07	208.2
rel. abund.	0.070	0.586	0.334	0.010		1.0
abundance	2446.8	20483.1	11674.6	349.5	0.0	34,954
comb. density	227.8	165.5				

a. For final calculation, forebay and mid-reservoir were averaged (weighted by area) to give a density of 168.8.

Table 16 Mean daily salmonid consumption estimates for the major predators (salmonids predator⁻¹ day⁻¹) from Vigg et al. (1991). Walleye and smallmouth bass estimates are for the reservoir only.

Month	Pikeminnow			Walleye	Bass
	Tailrace	Reservoir	Forebay		
April	0.123	0.043	0.053	0.021	0.003
May	0.416	0.251	0.280	0.113	0.009
June	0.318	0.086	0.136	0.118	0.019
July	1.950	0.154	0.270	0.447	0.118
August	0.350	0.094	0.130	0.232	0.070

Table 17 Consumption rates for N. Pikeminnow, Walleye and Smallmouth Bass in John Day Pool, 1984-1986, from Vigg et al. (1991). Mean for April-June.

Species	Reservoir Zone		
	Forebay	Mid-Reservoir	Tailrace BRZ
N. Pikeminnow	0.156 ^a	0.127	0.330
Walleye	–	0.08	–
Smallmouth Bass	0.010 ^b	0.010	–

a. Mean from Table 16 for April - June.

b. Assumed to be same as reservoir consumption rate.

Table 18 Consumption rates for N. Pikeminnow, Walleye and Smallmouth Bass in John Day Pool, 1984-1986, from Vigg et al. (1991). Mean for July-August

Species	Reservoir Zone		
	Forebay	Mid-Reservoir	Tailrace BRZ
N. Pikeminnow	0.20 ^a	0.124	1.21
Walleye	–	0.34	–
Smallmouth Bass	0.094 ^b	0.094	–

a. Mean from Table 16 for July - August.

b. Assumed to be same as reservoir consumption rate.

Table 19 Pikeminnow density indices (CPUE) in all reaches, 1990-1991

Reach		CPUE	ref
Bonneville	tailrace	6.30	c
	tailrace BRZ	16.35	c
	forebay	5.71	a
	mid-reservoir	2.102	a
The Dalles	tailrace	0.512	a
	tailrace BRZ	5.47	a
	forebay	1.104	a
	mid-reservoir	1.61	d
John Day	tailrace	2.75	a
	tailrace BRZ	21.54	a
	forebay	0.69	c
	mid-reservoir	0.25	c

Table 19 Pikeminnow density indices (CPUE) in all reaches, 1990-1991

Reach		CPUE	ref
McNary	tailrace	0.76	c
	tailrace BRZ	16.33	c
	forebay	0.17	c
	mid-reservoir	0.51	d
	upper reservoir	0.89	d
Ice Harbor	tailrace	0.45	d
	tailrace BRZ	8.42	d
	forebay	0.08	e
	mid-reservoir	0.30	e
Lower Monumental	tailrace	0.76	e
	tailrace BRZ	1.30	e
	forebay	0.67	e
	mid-reservoir	0.83	e
Little Goose	tailrace	1.52	b
	tailrace BRZ	16.31	b
	forebay	0.64	e
	mid-reservoir	0.39	e
Lower Granite	tailrace	1.63	b
	tailrace BRZ	28.29	b
	forebay	0.48	e
	mid-reservoir	0.17	e
	upper reservoir	1.86	b

a = 1990 CPUE data (from Zimmerman et al. 1997)

b = 1991 CPUE data (from Zimmerman et al. 1997)

c = mean 1990 and 1991 CPUE data (from Zimmerman et al. 1997)

d = CPUE estimated from 1990 density index (data from Ward et al. 1993)

e = CPUE estimated from 1991 density index (data from Ward et al. 1993)

Linear regressions for estimating CPUE's from density index based on reciprocal square root zero catch-
es: $R^2 = 0.818$ (intercept = -3.11, slope = 3.13, $p < 0.001$) for index < 1.6; $R^2 = 0.711$ (intercept =
-7.64, slope = 7.44, $p < 0.01$) for index > 1.6.

Table 20 Relative CPUEs for smallmouth bass and walleye (standardized to John Day Pool) based on the abundances from Zimmerman and Parker (1995). Raw data from N. Bouwes, ODFW, pers. comm.

Reservoir	Smallmouth	Walleye
Bonneville	0.69	6.39
The Dalles	0.83	2.88
John Day	1.00	1.00
McNary	0.89	1.11
Ice Harbor	3.93	0.00
L. Monumental	3.87	0.00
Little Goose	4.92	0.00
Lower Granite	11.72	0.00

Table 21 River dimensions from Ward et al. (1995). Tailrace is assumed to be 0.6 km in length; forebay is assumed to be 6.0 km in length.

	length (km)	ave. width (km)	total S.A. (km ²)	S.A. tailrace (km ²)	S.A. forebay (km ²)	S.A. reservoir
Bonneville	74.3	1.37	101.79	0.82	8.22	92.75
The Dalles	38.5	1.42	54.67	0.85	8.52	45.30
John Day	122.9	1.79	219.99	1.07	10.74	208.18
McNary	52.0	1.58	82.16	0.95	9.48	71.73
Snake R. below Ice Harbor	16.0	0.61	9.76	0.37		9.76
Ice Harbor	51.3	0.61	31.29	0.37	3.66	27.26
L. Monumental	46.2	0.58	26.80	0.35	3.48	22.97
Little Goose	59.9	0.51	30.55	0.31	3.06	27.18
Lower Granite	85.3	0.64	54.59	–	3.84	50.37

The predator abundance calculations above arrive at the predator densities shown in Table 22. As stated earlier, the densities are considered to be *relative*, that is they provide a relationship between densities from one reach or zone to the next. They are not intended to be absolute predator densities.

The difference between Spring and Fall densities stems from the differences in per predator consumption rates in those periods (see Tables 17 and 18). These densities are the *base* densities for 1990 and prior years. For subsequent years, adjustments are made as a result of the pikeminnow removal program.

Table 22 1990 predator densities for Spring (SP) and Fall (FA) migrations, by project and zone, with pikeminnow percentage (% PM) given for each.

Project	Zone	Density (SP)	% PM (SP)	Density (FA)	% PM (FA)
Estuary	reservoir	2137.73	0.853	3314.1	0.551
Jones Beach	reservoir	2008.13	0.844	3184.5	0.532
Columbia Gorge	reservoir	1835.33	0.829	3011.7	0.506
Bonneville Tail	reservoir	7123.91	0.955	8244.91	0.825
Bonneville Dam	tailrace	17658.0	1.0	17658.0	1
Bonneville Dam	forebay	6173.27	0.998	6221.54	0.991
Bonneville Pool	reservoir	2458.31	0.869	3579.31	0.597
The Dalles Dam	tailrace	5907.6	1.0	5907.6	1
The Dalles Dam	forebay	1195.78	0.993	1253.84	0.947
The Dalles Pool	reservoir	2105.88	0.928	2670.63	0.731
Deschutes Confl.	reservoir	2105.88	0.928	2670.63	0.731
John Day Dam	tailrace	23263.2	1.0	23263.2	1
John Day Dam	forebay	754.57	0.987	824.53	0.903
John Day Pool	reservoir	353.52	0.824	631.23	0.461
McNary Dam	tailrace	17636.4	1.0	17636.4	1
McNary Dam	forebay	191.94	0.956	254.20	0.722
McNary Pool	reservoir	616.60	0.893	899.64	0.612
Lower Snake R	reservoir	894.63	0.941	1345.28	0.626
Ice Harbor Dam	tailrace	9093.6	1.0	9093.6	1
Ice Harbor Dam	forebay	123.25	0.701	398.19	0.216
Ice Harbor Pool	reservoir	430.23	0.878	880.88	0.429
Lower Monumental Dam	tailrace	1404.0	1.0	1404.0	1
Lower Monumental Dam	forebay	759.89	0.952	1030.63	0.702
Lower Monumental Pool	reservoir	1034.23	0.950	1478.01	0.664
Little Goose Dam	tailrace	17614.8	1.0	17614.8	1
Little Goose Dam	forebay	737.33	0.937	1081.53	0.639
Little Goose Pool	reservoir	605.39	0.891	1169.56	0.461
Lower Granite Dam	tailrace	30553.2	1.0	30553.2	1
Lower Granite Dam	forebay	628.30	0.825	1448.21	0.357
Lower Granite Pool	reservoir	1246.57	0.875	2590.50	0.421

Predator removal adjustments

The predator density estimates in Table 22 are for the years up to and including 1990. For subsequent years, the densities must be adjusted for the predator (pikeminnow) reduction program. Table 23 shows the percent reduction in predation due to pikeminnow at each project in each year. Note, this does not directly give the reduction in predator numbers.

To calculate the change in predator numbers due to the estimated change in predation, we use the fact that $e^{-x} \approx 1 - x$ when $x \ll 1$. Recall from equation (65) that survival in a specific river zone is given by

$$S = e^{-rt}$$

and that predator density P is a factor in r . Also, predation $\text{Pred} = I - S$. Since rt is on the order of 0.05, percent change in predation is approximately equal to percent change in predator density.

So, to calculate adjusted predator densities, reduce the pikeminnow portion of the predator density (from Table 22) by the amount of predation reduction shown in Table 23.

Table 23 Pikeminnow reduction program. Percent reduction in predation due to pikeminnow as a result of the pikeminnow reduction program at each project in each year (Peters et al. 1999, 113). Estimates of predation reduction for 2001-2006 are included in Peters et al. (1999, 113).

	1991	1992	1993	1994	1995	1996	1997	1998	1999	2000
Estuary	0.000	0.029	0.076	0.078	0.120	0.155	0.160	0.141	0.129	0.136
Jones Beach	0.000	0.029	0.076	0.078	0.120	0.155	0.160	0.141	0.129	0.136
Columbia Gorge	0.000	0.029	0.076	0.078	0.120	0.155	0.160	0.141	0.129	0.136
Bonneville Tailrace	0.006	0.029	0.076	0.078	0.120	0.155	0.160	0.141	0.129	0.136
Bonneville Pool	0.006	0.100	0.271	0.185	0.173	0.154	0.148	0.149	0.152	0.151
The Dalles Pool	0.065	0.272	0.274	0.274	0.283	0.309	0.329	0.298	0.305	0.306
Deschutes Conf.	0.065	0.272	0.274	0.274	0.283	0.309	0.329	0.298	0.305	0.306
John Day Pool	0.009	0.125	0.181	0.198	0.186	0.140	0.136	0.099	0.068	0.074
McNary Pool	0.000	0.020	0.016	0.013	0.009	0.007	0.004	0.003	0.001	0.001
Lower Snake	0.000	0.020	0.016	0.013	0.009	0.007	0.004	0.003	0.001	0.001
Ice Harbor Pool	0.000	0.137	0.107	0.080	0.058	0.041	0.027	0.017	0.009	0.004
Lower Mon. Pool	0.000	0.083	0.105	0.099	0.084	0.078	0.054	0.036	0.023	0.031
Little Goose Pool	0.000	0.057	0.129	0.122	0.128	0.115	0.124	0.088	0.061	0.064

Table 23 Pikeminnow reduction program. Percent reduction in predation due to pikeminnow as a result of the pikeminnow reduction program at each project in each year (Peters et al. 1999, 113). Estimates of predation reduction for 2001-2006 are included in Peters et al. (1999, 113).

	1991	1992	1993	1994	1995	1996	1997	1998	1999	2000
Lower Granite Pool	0.000	0.000	0.000	0.000	0.000	0.000	0.000	0.000	0.000	0.000

Predator Density /Reservoir Volume Interaction

Predators may be concentrated in the forebay or tailrace when the depth of the regions is decreased by lowering the reservoirs. It is possible that concentrating predators increases the encounter rate between predators and prey and thus effectively increases the mortality rate in the forebay and tailrace.

This mortality increase can be included in CRiSP.1 runs by choosing the appropriate check box in the **Runtime Settings** window opened from the **RUN** menu. If the **predator density/volume interaction** is selected, predator density is a function of pool elevation for reservoir, forebay and tailrace regions. Predator density adjustments to the forebay and tailrace (Fig. 30) are given by¹

$$\begin{aligned}
 P(h) &= P \frac{H}{h} & \text{if } \frac{h}{H} > 0.05 \\
 P(h) &= 20P & \text{if } \frac{h}{H} \leq 0.05
 \end{aligned}
 \tag{68}$$

where

- H = forebay (tailrace) depth at full pool
- h = forebay (tailrace) depth at a lowered pool
- P = predator density at full pool for the forebay (tailrace).

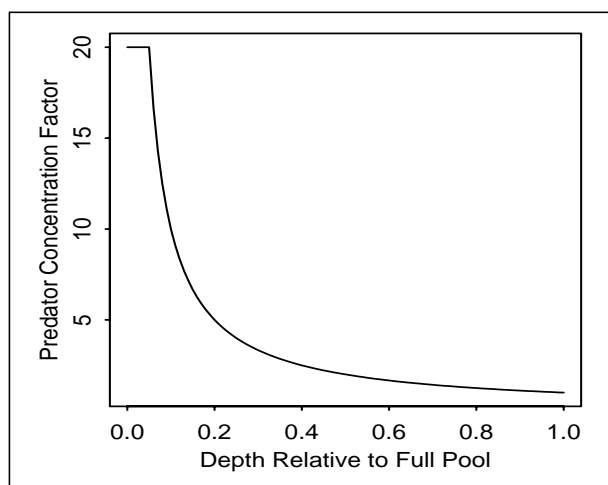


Fig. 30 Predator concentration function at dam

1. The limit $h/H < 0.05$ is arbitrary and required to prevent divide by zero errors. The limit equates to a river depth just over the head of most managers.

II.4.3 -Supersaturation Mortality

High levels of total dissolved gas in the river lead to the development of gas bubble disease (GBD) in smolts, as well as other aquatic life. This condition involves the formation of bubbles in the fish's organs, tissues, and vascular system. GBD is also suspected of compromising the fish's vitality by increasing its susceptibility to predators, bacteria and disease (Dissolved Gas Abatement Interim Letter Report, 1994). Because of the varied symptoms and effects of total dissolved gas, GBD will be considered an independent force of mortality.

There is uncertainty as to the significance of GBD-induced mortality at low levels of supersaturation (<110%) but it is clear in all studies that as the amount of supersaturation increases (> 110%) the rate of mortality increases significantly. The transition between low levels of generally sublethal effects to the higher level lethal condition involves a shift in the bubble-related mechanisms that lead to death. Specifically, at levels of supersaturation below the threshold fish are more susceptible to death related to infection and stress while above the threshold fish experience death from large intravascular bubbles (White et al. 1991).

Theory

In CRiSP.1, the level of total dissolved gas (tdg) is represented by percent of total dissolved gas saturated in the water above equilibrium. Tdg is generated by spill at the dams and then dissipated as the water moves downstream. In the model, the effects of both lethal and sublethal levels of tdg are considered as well as the changes in the effective tdg concentration resulting from depth and distance downstream.

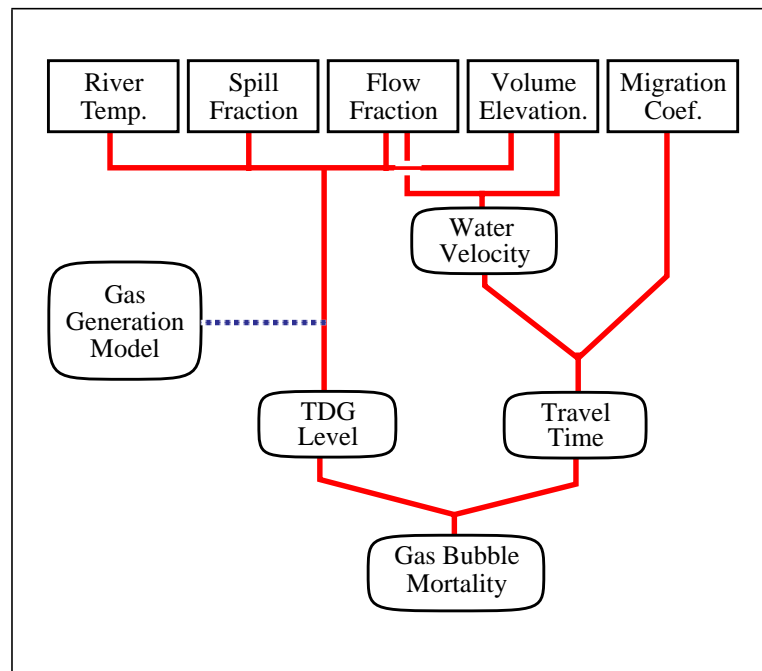


Fig. 31 Factors in gas bubble disease model. Elements used in all model conditions designated by (——). Elements selected by the user are designated by (.....).

The relationship between migration factors and gas bubble disease is illustrated in Fig. 31. Tdg supersaturation can be defined with any of submodels selected from the TDG Saturation Equations windows opened from the **Dam** menu.

Mortality Rate Equation

To incorporate both the lethal and sublethal effects of gas bubble disease, the model uses a piecewise-linear function that expresses the rate of mortality M_{tdg} as a function of G_s , the level of total dissolved gas above equilibrium (see figure below). This piecewise-linear characteristic is accomplished by using the Heaviside function $H()$ which switches from 0 to 1 as its argument changes from negative to positive. This allows the model to assume a moderate linear increase in mortality (slope a) at low levels of dissolved gas supersaturation. When the lethal threshold of saturation G_c is reached, the Heaviside function turns on and the mortality curve increases linearly but now at a higher rate (slope $a + b$). Using the work of Dawley et al. (1976) the empirical mortality rate equation is

$$M_{tdg} = a \cdot G_s + b(G_s - G_c) \cdot H(G_s - G_c) \quad (69)$$

where

- G_s = percent tdg above 100% as measured at the surface.
- G_c = threshold above 100% at which the gas bubble disease mortality rate is observed to change more rapidly towards more lethal levels.
- a = species-specific gas mortality rate coefficient with units of $G^{-1} \text{ day}^{-1}$ determining the initial rate of increase of mortality per %-increase in tdg.
- b = species-specific gas mortality rate coefficient with units of $G^{-1} \text{ day}^{-1}$, determining the change in mortality rate at G_c .
- $H()$ = Heaviside function, also known as the unit step function; equal to zero when its argument is negative, and equal to one when its argument is positive.

Eq(69) is illustrated in Fig. 32.

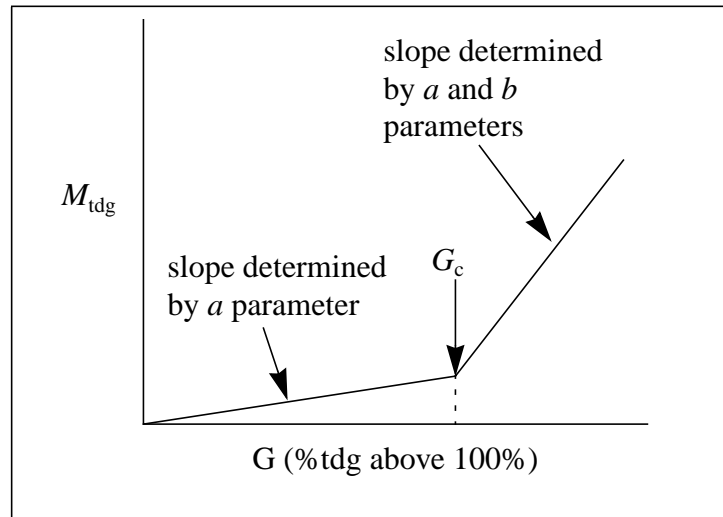


Fig. 32 The dissolved gas mortality equation is a function of three parameters.

Mortality Rates

Using the tdg mortality equation is given by eq (58) on page 45 and setting the predator mortality to zero, the resulting survival equation is

$$\log S = -M_{tdg}t \quad (70)$$

where

- S = cumulative survival
- M_{tdg} = tdg mortality rate at a specific level of supersaturation
- t = exposure time.

The survival curves provided by Dawley yielded pairs of (t, S) for varying levels of dissolved gas. The mortality rate is therefore

$$M_{tdg} = -\frac{\log S}{t} \quad (71)$$

Pairs of (G, M_{tdg}) were obtained using each of the data points determined from the graphs in Dawley et al. (1976). (This data and the calculated M_{tdg} are shown in Table 24 in the calibration section.)

Vertical Distribution

A population of fish from a given species will spread out vertically. A number of distribution functions have been hypothesized (Zabel 1994). For simplicity, CRiSP.1 uses an isosceles triangular distribution given by

$$Dist(z) = H(z_D - z)[m_0 z \cdot H(z) + (m_1 - m_0)(z - z_m)H(z - z_m) - m_1(z - z_b)H(z - z_b)] \quad (72)$$

where

- z_D = depth of the reservoir
- z_b = maximum depth of fish distribution
- z_m = mode of fish distribution
- m_0 = slope of distribution function above mode
- m_1 = slope of distribution function below mode.

The fish depth distribution is illustrated in Fig. 33.

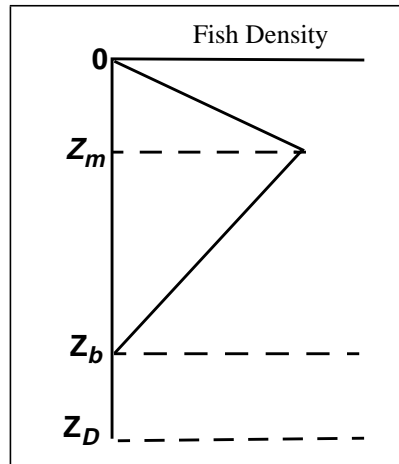


Fig. 33 Vertical distribution of fish

The work of Zabel (1994) shows that fish of a given species tend to seek specific depths that are correlated to level of illumination.

Size-mortality Relationship

Although no mechanism has been developed justifying a linear relationship, qualitatively the ability of a fish to establish gas equilibrium with its environment should be related to its volume to surface area ratio, which is proportional to fish length. Thus on physical principles of gas exchange a length relationship should be involved with tdg supersaturation mortality. For a first order estimate of the length relationship to mortality, the regression (shown in Fig. 36) is forced through the intercept:

$$M_n(L) = aL \quad (73)$$

where

- $M_n(L)$ = tdg mortality rate as a function of fish length
- L = fish length in mm
- $a = 0.000472 \text{ mm}^{-1}$, length coefficient for tdg mortality rate.

From eq (73), the tdg mortality rate can be corrected for fish length using

$$M_n(L) = M_n(L_e) \frac{L}{L_e} \quad (74)$$

where

- L = length of fish in environment
- L_e = length of fish in tdg mortality experiments.

Downstream dissipation

As fish move downstream in a reservoir their mortality rate due to TDG supersaturation generally decreases because dissolved gas levels are highest at the upstream end and dissipate as the water moves downstream. Using the reservoir gas distribution model (see Total Dissolved Gas section on page 71), the saturation level is expressed differently for each side of the river:

$$G_{right} = \left[G_{mix} - E + G_{dif} \cdot (1 - S_{fr}) \cdot e^{-\theta x} \right] \cdot e^{-k \cdot \frac{x}{v}} + E \quad (75)$$

$$G_{left} = \left[G_{mix} - E - G_{dif} \cdot S_{fr} \cdot e^{-\theta x} \right] \cdot e^{-k \cdot \frac{x}{v}} + E \quad (76)$$

The dissipation parameter k is defined with respect to time. To express this time-dependent process in spatial coordinates the time coordinate was transformed to distance downstream using the average velocity in the pool:

$$t = \frac{x}{v} \quad (77)$$

where

- v = average water velocity through the river segment
- x = distance downstream
- t = average water travel-time.

Transforming time to downstream distance using eq (77) defines a new dissipation parameter:

$$l = k/v \quad (78)$$

The surface supersaturation for each side of the river takes on the general form:

$$G_s(x) = [c_1 + c_2 \cdot e^{-\theta x}] \cdot e^{-lx} + E \quad (79)$$

which leads to

$$G_s(x) = c_1 \cdot e^{-lx} + c_2 \cdot e^{-(\theta+l)x} + E \quad (80)$$

where

- x = distance downstream and $0 \leq x \leq L$, where L is the pool length (miles)
- $c_1 = G_{\text{mix}} - E$
- $c_2 = G_{\text{dif}} \cdot (1 - S_{\text{fr}})$, for the right-bank flow and
 $- G_{\text{dif}} \cdot S_{\text{fr}}$, for the left-bank flow (see eq (96) and eq (97) on page 84)
- θ = reservoir mixing coefficient in (miles)⁻¹
- E = equilibrium value (0% supersaturation).

Then the rate of mortality as a function of fish depth and distance downstream can be expressed as:

$$M_{n,i} = a \cdot G_{s,i}(x) + b \cdot (G_{s,i}(x) - m_c z - n_c) \cdot H(G_{s,i}(x) - m_c z - n_c) \quad (81)$$

Where n indexes the julian day and i indexes the side of the river. There is thus a different mortality rate on each side of the river.

Integrate for Average Rate through Pool

For each side of the river the mortality rate is first averaged over the depth and length of the pool, and then an average mortality rate per day for the pool is created by calculating the flow weighted average over the two sides of the river. Thus the average mortality rate for a fish while it is in a pool is given by the equation:

$$\bar{M} = S_{fr} \cdot \bar{M}_1 + (1 - S_{fr}) \cdot \bar{M}_2 \quad (82)$$

where

$$\bar{M}_i = \frac{1}{L} \int_0^L \int_0^D Dist(z) \cdot (aG_{s,i}(x) + b[G_{s,i}(x) - m_c z - g_c] \cdot H[G_{s,i}(x) - m_c z - g_c]) dx dz \quad (83)$$

and

- \bar{M}_i = the mortality rate due to gas bubble disease averaged throughout the length and depth of the pool on side i .
- i = indexes the side of the river and hence the level of TDG on that side of the river, 1 - indexing the right-bank and 2 --indexing the left-bank.

Parameter Determination

Mortality Rates

There are three crucial parameters for the mortality rate equation:

- g_c = threshold above 100% at which the gas bubble disease mortality rate is observed to change more rapidly towards more lethal levels
- a = species-specific gas mortality rate coefficient with units of $G^{-1} \text{ day}^{-1}$ determining the initial rate of increase of mortality per %-increase in tdg
- b = species-specific gas mortality rate coefficient with units of $G^{-1} \text{ day}^{-1}$, determining the change in mortality rate above G_c .

Determination of the mortality equation parameters begins with determining the Depth dependent critical values (g_c) and the mortality rates observed in fish exposed to various TDG levels. These are shown in Table 24 along with the mortality rates calculated with eq (71). When these are known the a and b parameters follow from simple linear regressions of the mortality rate on the dissolved gas level, allowing for different slopes between the a and b values.

Table 24 Survival data and mortality rates from Dawley et al. (1976)

TDG	Days	Survival	Mortality rate	Days	Survival	Mortality rate
Chinook 0.25 meters				Steelhead 0.25 meters		
105	20	0.99	0.0005	1	1	0
	40	0.98	0.00051	2	1	0
	60	0.97	0.00051	5	0.96	0.0082
	80	0.9	0.0013	7	0.95	0.0073
	100	0.88	0.0013			
	120	0.87	0.0012			
110	20	0.97	0.0015	1	1	0
	40	0.95	0.0013	2	1	0
	60	0.84	0.0029	7	0.97	0.0044
	80	0.63	0.0058			
	100	0.52	0.0065			

Table 24 Survival data and mortality rates from Dawley et al. (1976)

TDG	Days	Survival	Mortality rate	Days	Survival	Mortality rate
115	10	0.95	0.0051	1	1	0
	20	0.84	0.0087	2	0.95	0.026
	30	0.72	0.011	3	0.7	0.12
	40	0.62	0.012	4	0.58	0.14
	50	0.49	0.014	5	0.48	0.15
	60	0.22	0.025	6	0.41	0.15
	70	0.12	0.03	7	0.37	0.14
	80	0.08	0.032			
	100	0.05	0.03			
120	10	0.77	0.026	0.8	0.76	0.34
	20	0.57	0.028	1	0.67	0.4
	30	0.32	0.038	1.2	0.42	0.72
	40	0.22	0.038	1.9	0.060	1.5
	50	0.1	0.046			
	60	0.03	0.058			
	70	0.02	0.056			
	80	0.01	0.058			
Chinook 2.5 meters				Steelhead 2.5 meters		
105	20	1	0	1	1	0
	40	1	0	2	1	0
	60	0.99	0.00017	3	1	0
	80	0.97	0.00038	4	1	0
	100	0.97	0.0003	5	1	0
	120	0.96	0.00034	6	1	0
110	20	1	0	1	1	0
	40	1	0	2	1	0
	60	0.99	0.00017	7	0.99	0.0014
	80	0.97	0.00038			
	100	0.95	0.00051			
	120	0.9	0.00088			
115	20	1	0	1	1	0
	40	1	0	3	1	0
	60	0.97	0.00051	7	0.97	0.0044
	80	0.88	0.0016			
	100	0.83	0.0019			
	120	0.78	0.0021			
120	20	1	0	2	0.99	0.005
	40	1	0	3	0.96	0.014
	60	0.95	0.00085	7	0.94	0.0088
	80	0.71	0.0043			
	100	0.64	0.0045			
	120	0.58	0.0045			
127	10	0.97	0.003	2	0.92	0.042
	20	0.88	0.0064	3	0.87	0.046
	30	0.7	0.012	4	0.82	0.05
	40	0.52	0.016	5	0.8	0.045
	60	0.38	0.016	6	0.77	0.044
	80	0.1	0.029	7	0.75	0.041
	100	0.07	0.027			

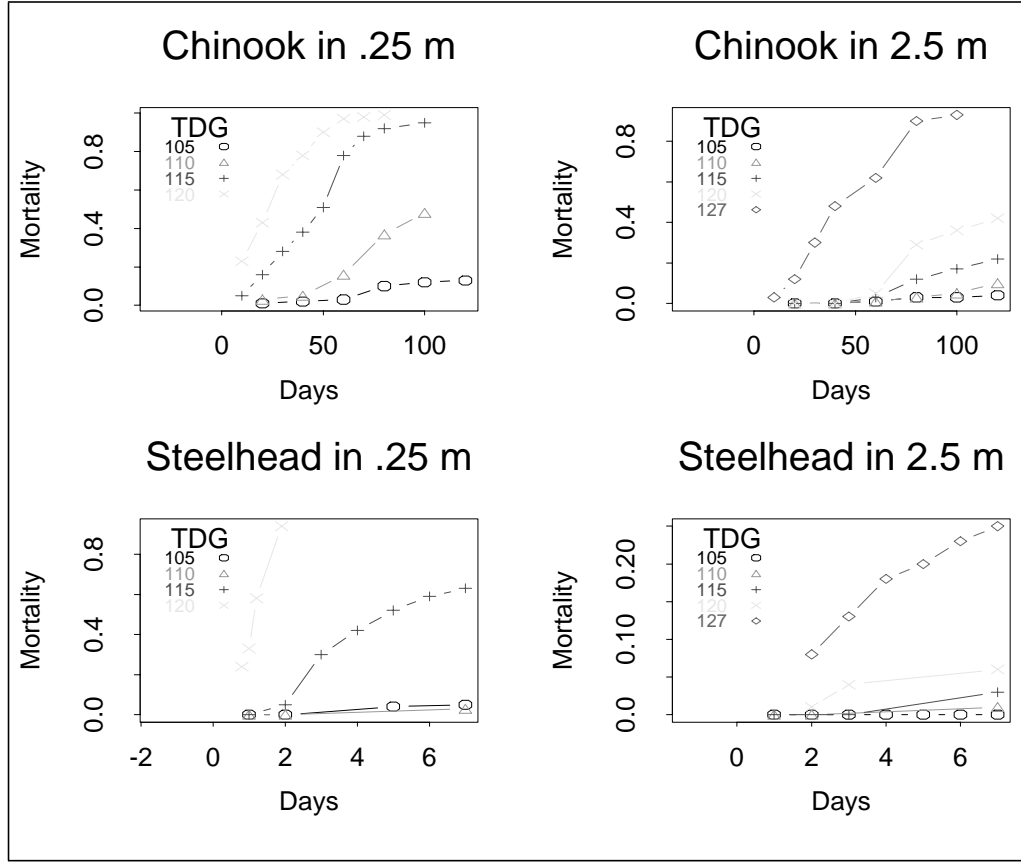


Fig. 34 Juvenile steelhead cumulative mortality from gas bubble disease at different levels of tdg supersaturation. Data points from Dawley et al. (1976).

Depth Dependent Critical Values

Fidler and Miller (1994) and Dawley et al. (1976) demonstrated that the critical supersaturation concentration (G_c) is depth dependent, with G_c increasing as depth increases. In other words, fish at lower depths are less susceptible to dissolved gas supersaturation. Based on the mechanisms controlling partial pressures of gas bubbles, the partial pressure increases ~10% per meter below the surface (Richards 1965) and Fidler and Miller noticed a linear change in the threshold depth for gas bubble trauma symptoms. The slope of this linear relationship is $73.89 \text{ mmHg m}^{-1}$, and given the relationship of TDG to pressure (.1316 %/mmHg), this equivalent to 9.72 m^{-1} or 2.96 ft^{-1} .

Based on this work, CRiSP.1 utilizes a linear relationship to relate G_{eff} (the effective gas concentration) to fish depth:

$$G_{\text{eff}} = g_{\text{surface}} - g_{\text{correction}} \quad (84)$$

$$g_{\text{correction}} = m \cdot z \quad (85)$$

where

- z is fish depth
- m is a slope parameter

- g_{surface} is the TDG at the surface
- $g_{\text{correction}}$ is the TDG experienced by the fish.

When the model is run, to obtain an G_{eff} for a stock, eq (84) is multiplied by fish density as a function of depth, and then this term is integrated over the reservoir depth. Calibration for juvenile salmon converted into the model units of percent tdg above 100%, where $m = 2.96$, the rate of increase of G_c (critical TDG level) with units of percent tdg above 100%.

Effective gas pressures used for the regressions to determine a and b were therefore corrected for the depth of the fish in the experimental tanks.

Table 25 Depths of fish in the deep water tanks and G_c used to determine mortality rate coefficients

species	Depth	$g_{\text{correction}}$
chinook	1.0 m	9.7
steelhead	1.5m	14.6

Size-mortality Relationship

Dawley et al. (1976) demonstrated that large fish have higher levels of mortality. In a shallow tank using fall chinook of different sizes exposed to 112% supersaturation they determined cumulative mortality curves were significantly different (Dawley et al. 1976, Fig. 10). These data can be used to infer the effect of fish length on tdg mortality in reservoirs since the study also demonstrated that shallow tank mortality curves had the same pattern as deep tank mortalities with higher tdg supersaturation levels. The studies indicated that mortality curves in shallow tanks at 112% saturation were equivalent to mortality curves in a deep tank with 122% supersaturation.

The resulting mortality-length relationship can be used to extrapolate experimental results to field conditions where the fish are larger. The first step is to determine an empirical relationship relating tdg supersaturation mortality to fish length. This is done by regressing the mortality rates against fish length for the fish in the 112% tdg experiments. With this relationship the results of fall chinook studies in the Dawley experiments are extrapolated to fall and spring chinook in the Lower Granite reservoir using different average fish lengths for each stock. The steelhead in the Lower Granite reservoir are treated similarly.

To determine the relationship between fish size and tdg supersaturation mortality the mortality rate is first estimated by fitting eq (73) to cumulative mortality vs. exposure time for different sized fall chinook and steelhead (Fig. 35). The estimated rates are given in Table 26.

Table 26 Total dissolved gas mortality rates and fish length in shallow tank experiments (Dawley et al. 1976). Plotting symbols refer to Fig. 35.

Species	Plotting Symbols	Length (mm)	Average Mortality rate
fall chinook	◦	40	0.00364
	+	53	0.0327
	Δ	67	0.0374

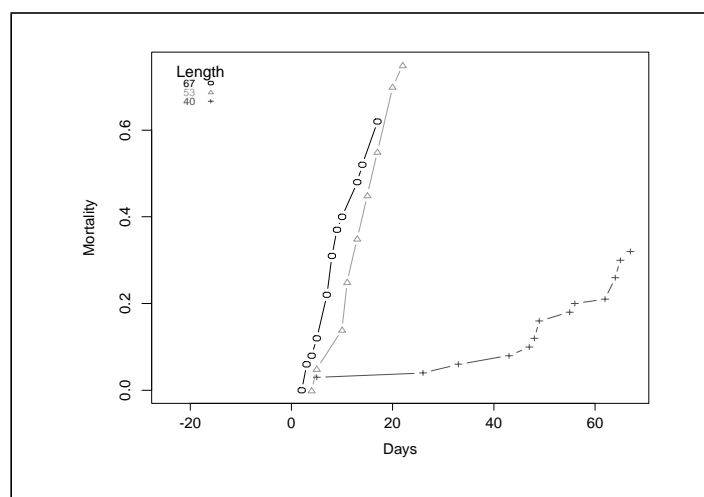


Fig. 35 Cumulative mortality vs. exposure time to tdg supersaturation for different fish length.

The resulting mortality rates plotted against fish length are illustrated in (Fig. 36). The graph combines fall chinook ranging from 40 to 67 mm. The line in the figure is a linear fit with a least squares regression constrained to pass through zero. The slope of the line relating mortality rate to length is 0.00126. The regression was not confined to go through zero because Dawley and Jensen both report that there is a sensitivity threshold for size therefore we do not constrain the line.

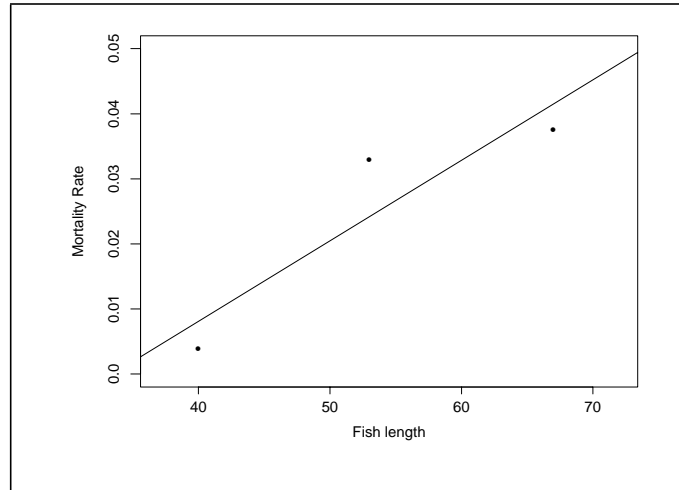


Fig. 36 Mortality rate of fish of different lengths.

Exposure Time Limits

In addition to a threshold for depth, there appears to be a threshold for time as well. This suggests that compensatory mechanisms are functional for a period of time and after that begin to break down. As a result, fish exposed to high levels of dissolved gas (for up to 2 months or more as in the Dawley experiments) are susceptible to mortality at a higher rate than fish exposed for a short period of time. We restrict the mortality rate data to fish exposed for 40 days or less, on the order of time that the fish are exposed in the river system. This subset of the mortality data is used to determine the TDG mortality coefficients.

Determination of Gas Mortality Parameters

Using eq (79), G_s , and the Dawley survival data for fish exposed under 40 days, the parameters a and b were fit using linear regression. Regression results are summarized in Table 27 and shown in Fig. 37.

Table 27 Tdg mortality coefficients based on Dawley.

Parameter	Fall Chinook	Spring Chinook	Steelhead
a	0.0001197	0.0001595	0.0006186
b	0.005071	0.006762	0.04762
g_c	10.9	10.9	10.9

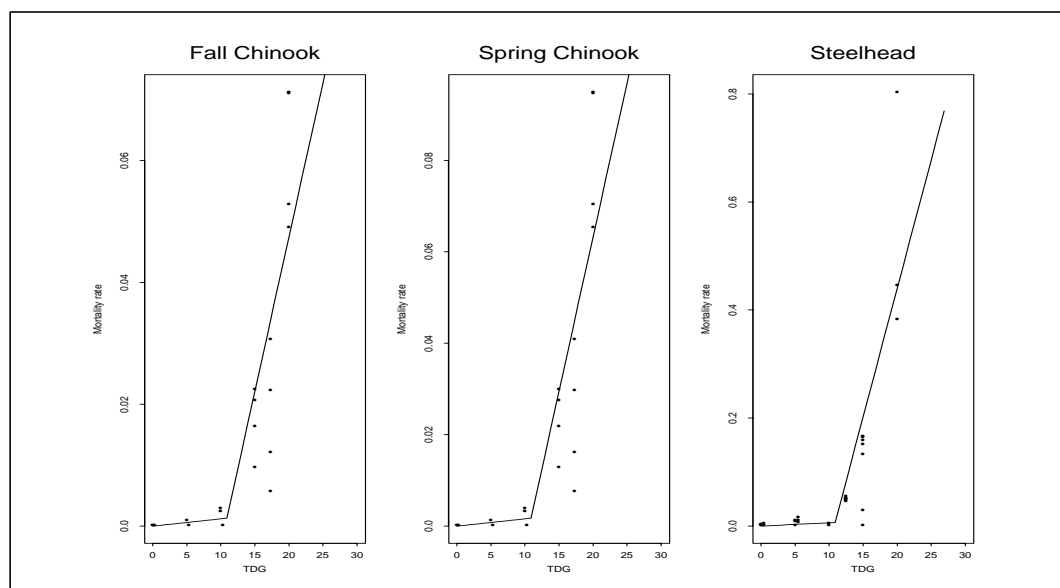


Fig. 37 Fits of mortality rate parameters to mortality rate data corrected for depth and fish length. Data points from Dawley et al. (1976), curve from fit of eq (79). There are extreme points not shown on the steelhead graph.

Vertical Distribution

The gas bubble disease rate depends on fish depth which is characterized by a mode depth and bottom depth. Fish depths vary continuously over day and night, fish age, and position in the river. For the current model a representative depth is required for each species. These were selected after reviewing the data on fish vertical distributions. The literature and essential elements are given in Table 28.

Table 28 Fish depth information

Species	Location	Time	Mode depth	Reference	CRiSP.1 values
spring chinook	Forebay	Day	39 ft 5 ft	Johnson et al. 1985 Ebel 1973	mode=12 maximum = 36
	Reservoir	Day	12-24 ft 27-36 ft	Smith 1974 Dauble et al. 1989	
		Night	0-12 ft 27-36 ft	Smith 1974 Dauble et al. 1989	
fall chinook	Forebay	Day	-	-	mode=12 maximum = 36
	Reservoir	Day	12-20 ft	Dauble et al. 1989	
		Night	12-20 ft	Dauble et al. 1989	

Table 28 Fish depth information

Species	Location	Time	Mode depth	Reference	CRiSP.1 values
steelhead	Forebay	Day	13 ft 4 ft	Johnson et al. 1985 Ebel 1973	mode=12 maximum = 36
		Night	-	-	
	Reservoir	Day	0-12 ft	Smith 1974	
		Night	12-24 ft	Smith 1974	

II.5 - Total Dissolved Gas

II.5.1 -Introduction

In a riverine environment total dissolved gas at equilibrium should be in relative balance with the atmospheric pressure. Natural sources, such as waterfalls or organic inputs, can cause the level of gas to rise above the equilibrium level, however the primary source of dissolved gas supersaturation in the Columbia and Snake Rivers is spill from hydroelectric dams. As water flows over the spillway air becomes entrained by the spill flow and is as a result the river becomes supersaturated in total dissolved gas. Though there are river systems that have problems with a lack of total dissolved gas, sinks of dissolved gas are relatively insignificant for the Snake and Columbia rivers and hence in CRiSP.1 the river never falls below the equilibrium level.

In CRiSP.1 dissolved gas can enter the system in two ways, either: 1) at a headwater, representing the amount of gas coming from upstream sources or 2) at a dam, resulting from spill. Headwater input is read in through the data files, whereas dissolved gas production at a dam is calculated by the model based on the level of spill. Dissolved gas is then propagated downstream with the water according to a system of reach dynamics outlined below.

II.5.2 -Gas Production Equations

Theory

For CRiSP.1.6, new equations have been implemented for gas production from spill. As a part of the U.S. Army Corps' Gas Abatement study, Waterways Experiment Station (WES) developed these new equations as an improvement over GASPILL, which had previously been the predominant model for gas production.

The new equations are an empirical fit of spill data and monitoring data collected by the Corps. The percent of total dissolved gas (tdg) exiting the tailrace of a dam is predicted as a function of the amount of discharge in kcfs. This level of tdg is not necessarily the highest level of gas reached, but rather the level of gas in the spill water after some of the more turbulent processes have stabilized. The calibration for each dam was fit to the nearest downstream monitor, which is typically about a mile downstream of the dam.

For the 8 lower Snake and lower Columbia dams that were studied by WES, the gas production equation may take one of three forms: linear function of total spill, a bounded exponential function of total spill, or a bounded exponential function of the spill on a per spillbay basis. These equations were adopted for all dams in CRiSP.1. See the calibration section below for more details.

Equations for tdg supersaturation are of two types. One type constitutes empirical equations with no underlying theory but which provide a general fit to observed supersaturation data as a function of spill. The other type constitutes mechanistic equations which define tdg levels in terms of physical processes producing spill. CRiSP.1 contains two empirical models and two mechanistic models. CRiSP.1 is calibrated to all submodels. In general, we recommend using the model called Gas Spill 2. Relevant parameters in the submodels are illustrated in Fig. 38.

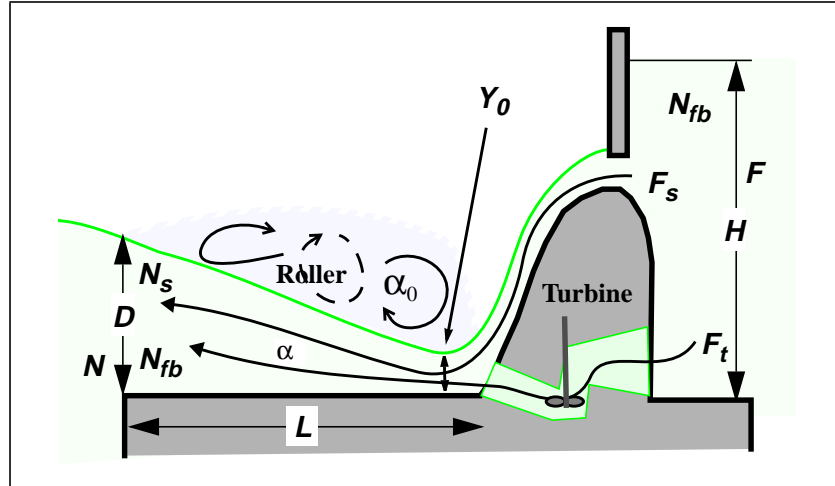


Fig. 38 Representation of spillway and stilling basin.

WES Linear Equation

$$\%TDG = m \cdot Q_s + b \quad (86)$$

where

- %TDG = the % total dissolved gas saturation, where 100% is equilibrium
- Q_s = the total amount of spill in *kcf/s*
- m, b = the empirically fit slope and intercept parameters.

WES Exponential Equations

$$\%TDG = a + b \cdot \exp(c \cdot Q_s) \text{ or} \quad (87)$$

$$\%TDG = a + b \cdot \exp(c \cdot q_s) \quad (88)$$

where

- %TDG = the % total dissolved gas saturation, where 100% is equilibrium
- Q_s = the total amount of spill in *kcf/s*
- q_s = the amount of spill through an individual spillbay
- a, b, c = the empirically fit model parameters.

CRiSP.1 is currently configured so that a separate spill pattern, and thus a separate gas production function, for night and for day can be set for each dam. (A spill pattern specifies which spill bays are used to discharge flow both in number and position.) Once the number of spill gates, n , for a particular pattern is set, Equation 3 is then converted into Equation 2 by the relation $q_s = Q_s/n$. This conversion formula assumes that the amount of spill is uniformly distributed among the open spill gates. The model parameters for the day and night gas production thus can be different for a given dam, reflecting a change in the position or number of gates and hence in the dynamics of gas production.

Empirical Exponential Equation

An empirical tdg supersaturation equation based on an exponential relationship between spill flow and supersaturation in the spilled water can be expressed

$$N_s = bF_s + a(1 - \exp(-kF_s)) \quad (89)$$

where

- N_s = percent supersaturation above 100%
- F_s = spillway flow volume in kcfs
- a , b and k = coefficients specific to each dam derived from tdg rating curves provided by the Bolyvong Tanovan of the Army Corps of Engineers.

The alternative exponential equation was developed first and was used in CRiSP.1 version 3. It was retained in version 4 for backward compatibility of models and is currently used as the backup model when spill exceeds a certain value for certain dams in certain years.

Empirical Hyperbolic Equation

The tdg supersaturation equation data can also be fit with a hyperbolic relationship between spill flow and supersaturation. The relationship is

$$N_s = bF_s + \frac{aF_s}{h + F_s} \quad (90)$$

where

- N_s = percent supersaturation above 100%
- F_s = spillway flow volume in kcfs
- a , b and h = coefficients specific to each dam and can be derived from tdg rating curves available from the Corps of Engineers.

Although this submodel can produce a degree of supersaturation at zero spill flow (when $h = 0$), this does not contribute to supersaturation in the tailrace water since the contribution of spill water to the tailrace is zero with zero spill as is defined in eq (102). This model is the preferred empirical model and should be used in place of the exponential model if an empirical model is selected.

Gas Spill 1

Gas Spill 1 is a three-parameter *multiplicative* model, used by the Army Corps of Engineers at Bonneville Dam only. The equation is

$$K_{20} = 10^a \cdot E^b \cdot P^c \quad (91)$$

Gas Spill 2

Gas Spill 2 is a three-parameter *additive* model used at all other dams. It is defined

$$K_{20} = a + b \cdot E + c \cdot P \quad (92)$$

where

- E = energy loss rate expressed as total headloss divided by residence time of water in the stilling basin

$$E = \frac{F_s}{LWD}(H - D) - \left(\frac{F_s}{D}\right)^3 \frac{1}{2gL} \quad (93)$$

- P = forebay percent saturation
- a , b , and c = dam dependent empirical coefficients.

II.5.3 -Tailrace Dynamics

Introduction

Extensive field studies led by the Army Corps of Engineers have provided a number of insights to how dissolved gas exits the dams and it is transported downstream. CRiSP.1 now allows for different scenarios on how the spill and powerhouse flows exit the dam.

Flow enters a dam containing a certain amount of dissolved gas. This flow is routed in part through the powerhouse and the rest through the spillway. Spill produces gas in the tailrace flow that generally exceeds incoming levels, whereas the flow exiting through the powerhouse retains the forebay gas level. The interaction between these two flows in the tailrace is dynamic. Currents can dilute the supersaturated spill by inducing mixing with the less-gassed powerhouse flow or the powerhouse flow can be *entrained* into the spill flow and also become gassed as a result. Varying flow and spill conditions can change the level of entrainment and mixing, as well as the amount of dissolved gas being produced.

In CRiSP.1, both tailrace mixing and entrainment can be specified at a dam. Because most of the data used to calibrate the gas production equations came from the water quality monitors downstream of the spillway, it is most likely that at last some dilution is represented by these coefficients. And because there is very little data from the powerhouse flow after it exits the dam it is also difficult to measure entrainment directly. To avoid over-determination due to too many parameters and too little data to separate out the mixing and entrainment dynamics, this calibration was thus kept simple by using an all or nothing approach to mixing in the tailrace based on observations from field studies rather than a statistical fit of the tailrace mixing parameter.

The final measure of CRiSP.1's calibration is the accuracy of the modeled forebay levels. If the amount of gas in the downstream forebay was underestimated then the entrainment function was used to adequately adjust the total amount of gas being added to the system. This was done using the procedure described in Entrainment section below.

Separate Flows

For the majority of dams on the Columbia and Snake the flows exit as “separate” flows. The spill flow will exit the dam with a dissolved gas value produced from spill and the powerhouse flow will often contain a lower gas level, typically closer to the level of gas in the forebay. This motivated a two-flow model for the river. The two flows are denoted (looking downstream) as “left flow” and “right flow.” Currently only the amount of flow and the dissolved gas level vary between the left and right flows in a reach or at a dam.

For each dam a spill_side is denoted in the **columbia.desc** file. For example looking downstream at Ice Harbor Dam, the spillway is on the right side of the dam, so the spill_side token, and consequently the spill flow is the right flow and the powerhouse flow is the left flow. For some projects this is a simplified view, in these cases if a bias in the spill flow exists as it exits the dam then that side was chosen as the spill_side. If the spill_side is not chosen, then the model has the right bank flow as the default for the spill side of a dam. Below is the table of spill_side values used by the model.

It should be noted that for some of these dams, there is essentially complete mixing in the tailrace of the two flows and hence both flows will exit the dam with the same dissolved gas level. The spill_side in this case will have no real impact. In the next section mixing is discussed in more detail.

Table 29 Spill_side tokens for each dam.

DAM	spill_side
CHJ	right
WEL	left
RRH	left
RIS	right
WAN	right
PRD	right
MCN	right
JDA	right
TDA	right
BON	right
DWR	left
HCY	right
LWG	right
LGS	right
LMN	left
IHR	right

The spill fraction determines the amount of flow which is attributed to the spill_side flow of the river. The amount of dissolved gas in each of the flows depends on four factors: the amount of gas in the forebay of the dam, the amount of gas produced by the spill flow, as explained in the previous section, and the amount of mixing and/or entrainment in the tailrace. The two latter dynamics, mixing and entrainment are both adjustable by dam and are explained in the following sections. Once mixing and entrainment are applied, a dissolved gas value is determined for each flow and passed in as input gas values to the next reach.

Mixing

Theory

In CRiSP.1, for dams where there is a significant amount of mixing in the tailrace, the flows from spill and the powerhouse are averaged according to their flow fractions. The mixed TDG value is contained in both flows upon exiting the tailrace. This has the effect of diluting the spill flow and raising the level of dissolved gas in the powerhouse flow.

To allow for all possibilities between the extremes of separate flows and full mixing, CRiSP.1 has a mixing coefficient for the dam which determines the amount of mixing happening between the powerhouse and spill flows before exiting the dam.

Mixing in the tailrace can be expressed by a decay process which decreases the difference between the two gas levels as a function of the mixing parameter set for each dam. At the dam the spill flow gets gas level N_{spill} and the powerhouse has the gas level of the forebay. Before exiting the dam, the difference in N between the two flows is decayed as shown in the following equation.

$$(N_{spill} - N_{turbine}) \cdot \exp(-\theta) \quad (94)$$

Letting $N_{dif} = N_{spill} - N_{turbine}$ and $N_{mix} = sfr \cdot N_{spill} + (1 - sfr) \cdot N_{turbine}$

after applying the mixing in the tailrace, we have as exiting gas levels:

$$N_{spill} = N_{mix} + (1.0 - sfr) \cdot N_{dif} \cdot \exp(-\theta) \quad \text{and}$$

$$N_{turbine} = N_{mix} - sfr \cdot N_{dif} \cdot \exp(-\theta).$$

Given this expression for mixing, a value of $\theta = 0$ leads to no mixing and the spill flow exits with the gas value generated by the gas production equations and the powerhouse retains the forebay value. For a value of $\theta = 10$, complete mixing is attained and both flows leave the dam with N_{mix} , the flow weighted average of the two gas levels.

Parameter Determination

For most of the fifteen Columbia and Snake dams modeled in CRiSP.1, spill and powerhouse flows exit the dams separately. This is represented by a zero mixing coefficient, $\theta = 0$ at the dam. Dworshak, The Dalles and Bonneville dams had complete mixing in the tailrace.

Table 30 Tailrace Mixing coefficients

DAM	θ
CHJ	0
WEL	0
RRH	0
RIS	0
WAN	0
PRD	0

Table 30 Tailrace Mixing coefficients

DAM	θ
MCN	0
JDA	0
TDA	10
BON	10
DWR	10
LWG	0
LGS	0
LMN	0
IHR	0

In the gas production field studies led by the Army Corps of Engineers, Waterways Experiment Station, a significant amount of mixing was observed in the tailraces of The Dalles Dam and Bonneville Dam. For these dams the gas production equations represent well-mixed powerhouse and spillway flows in the tailrace (*Evaluation and Analysis of Historical Dissolved Gas Data from the Snake and Columbia Rivers*, 1996), thus complete mixing was assumed in CRiSP.1 with $\theta = 10$. For the remaining mainstem dams WES's work supported separate spill and powerhouse flows, and for these dams their gas production equations represent the amount of gas in the spill flow.

On the mid-Columbia according to a field study for Chief Joseph prepared by the Army Corps of Engineers, Seattle District, the spill and powerhouse flows exit Chief Joseph Dam as separate flows (*Total Dissolved Gas Abatement at Chief Joseph Dam*, 1998). For the remaining dams separate flows were assumed.

Complete mixing at Dworshak was also assumed based on the steep structure of the dam and narrow tailrace at this dam.

Entrainment

Theory

Entrainment refers to the phenomena that the powerhouse flow actually becomes entrained by the spill flow and is gassed as a result. In this scenario, the spill TDG levels are not diluted but rather more TDG is added to the system via the powerhouse flow. The entrainment function is an empirical relationship between the total amount of gas added to the powerhouse flow and the amount of flow going over the spillway. The higher the spill the more gas that is added to the powerhouse, with the level of TDG in the exiting powerhouse flow ranging from the forebay TDG level to the TDG level in the spill flow. This relationship was motivated by the heuristic that the larger the amount of spill, the greater the "plunging" force and hence the greater amount of energy in the spill flow.

$$N_{phouse} = N_{forebay} + (N_{spill} - N_{forebay}) \cdot \exp(-k_{entrain} \cdot Q_{spill}) \quad (95)$$

Modeled forebay levels at Little Goose, Lower Monumental, Wanapum and Priest Rapids dams

with and without the entrainment coefficient at the previous dam are shown versus the observed forebay values in Fig. 39-Fig. 42 below.

These values are calibrated annually and represent annual averages. They can be expected to vary from year to year as details of the annual spill patterns and other conditions vary.

Table 31 Estimations of K_{entrain} from CRiSP.1 runs using filtered DART data (observed and modeled TDG > 100%).

Location	1994	1995	1996	1997	1998	1999
CHJ						0.05
WEL		.143	0.00	.94	1	0.175
RRH		.001	.005	0.00	.002	0.00
RIS		.014	.004	.018	.014	0.00
WAN	.052	.029	0.00	.054	.013	0.00
PRD		0.04	0.10	0.00	0.00	0.00
LWG		.009	.009	.012	.017	0.025
LGS		.868	.96	.555	.802	0.45
LMN		0.00	0.00	0.00	0.00	0.05
IHR		0.00	0.00	0.00	0.25	0.1
MCN		0.00	0.00	0.00	0.00	0.00
JDA		0.00	0.00	0.00	0.00	0.00
TDA	0.00	0.00	0.00	0.00	0.00	0.00

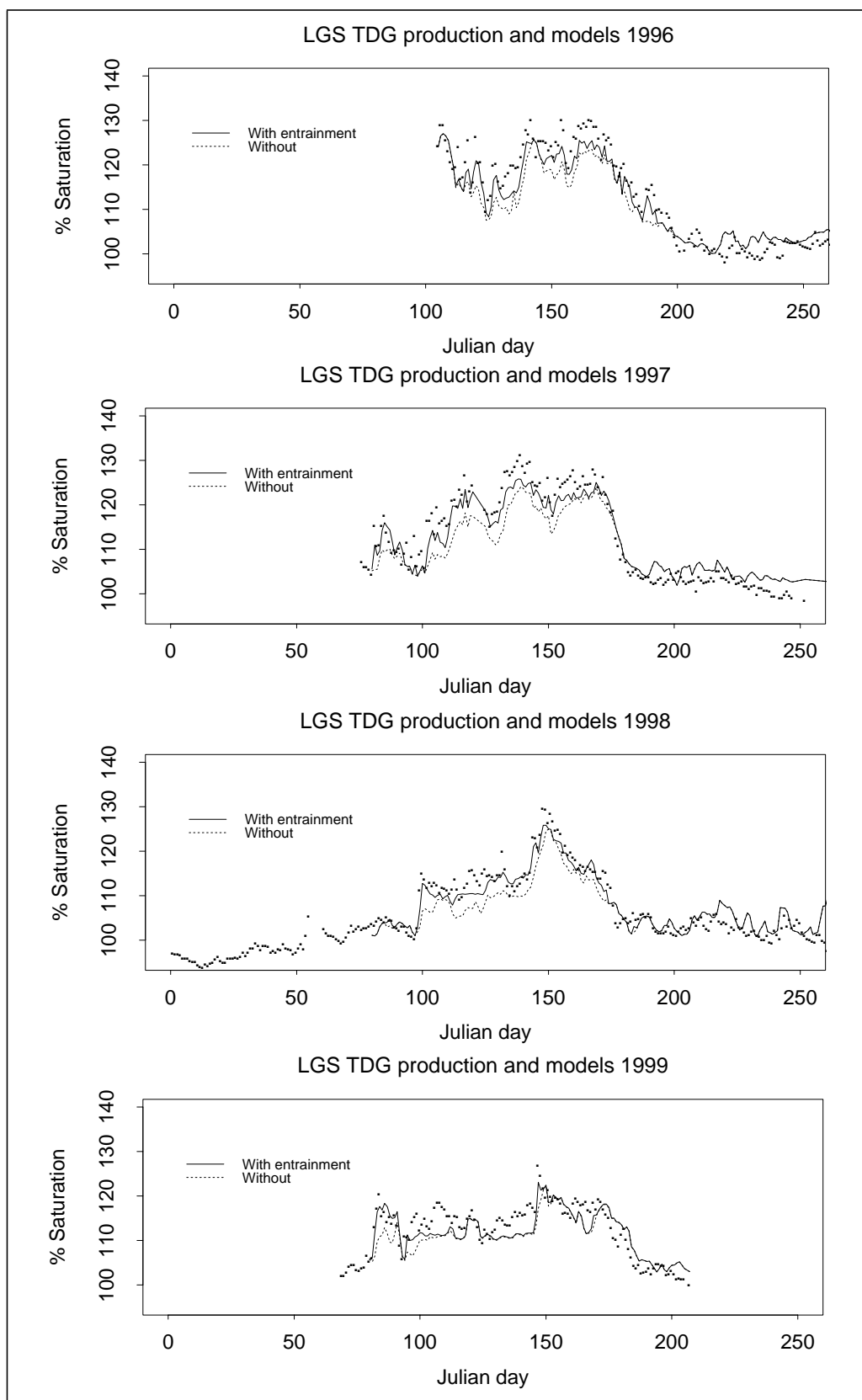


Fig. 39 LGS production values with and without entrainment and observed data (points).

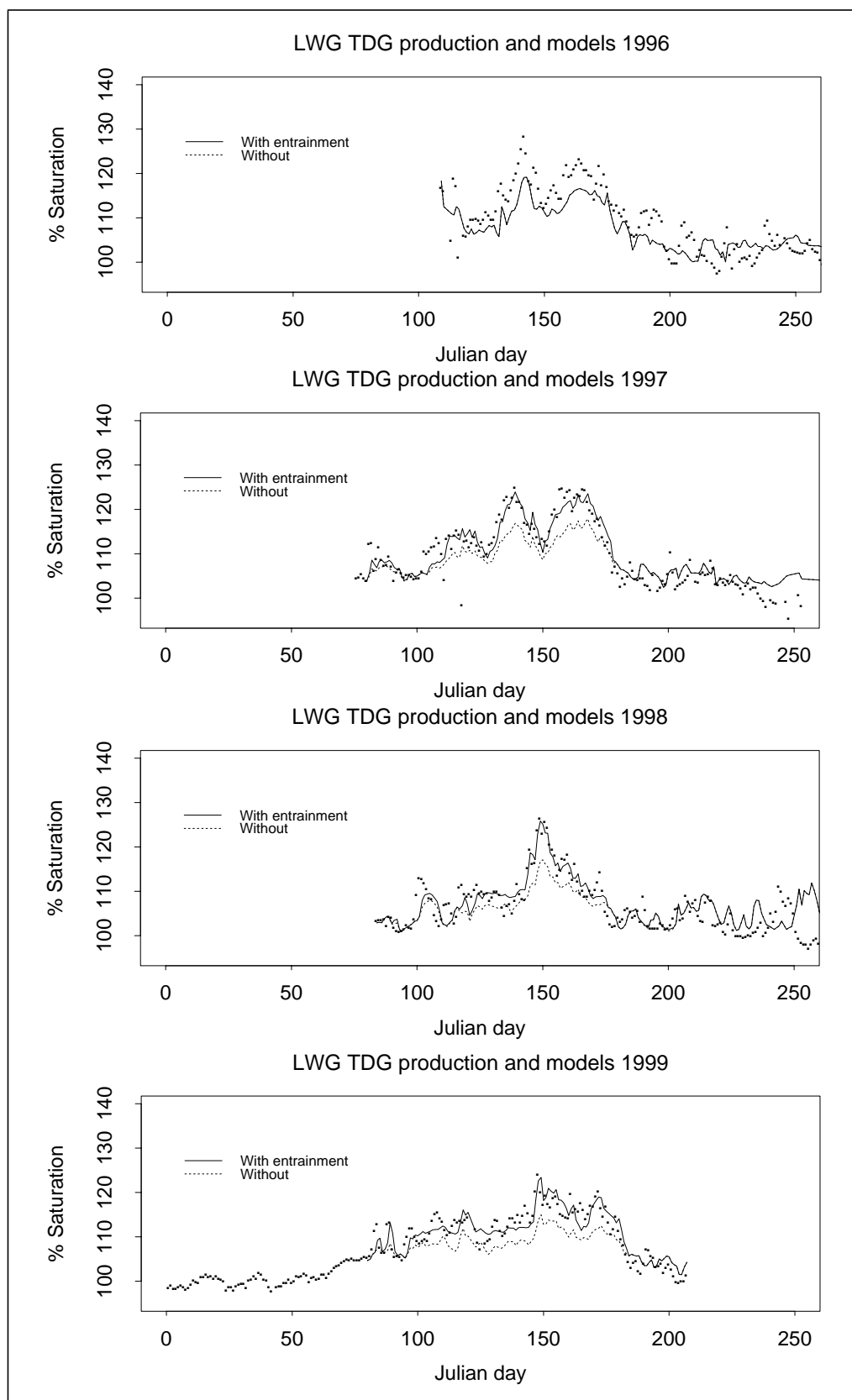


Fig. 40 LWG production values with and without entrainment and observed data (points).

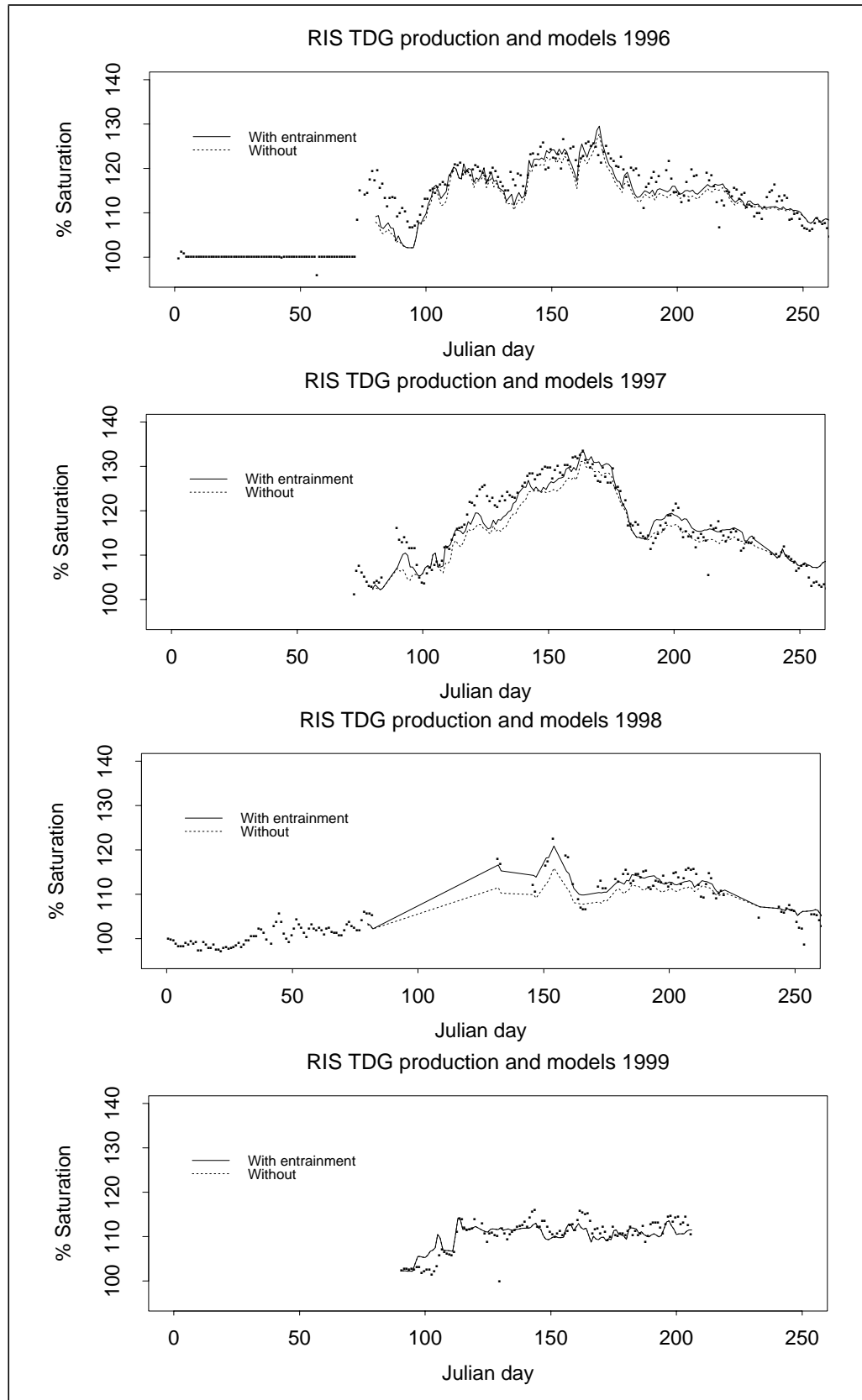


Fig. 41 RIS production values with and without entrainment and observed data (points).

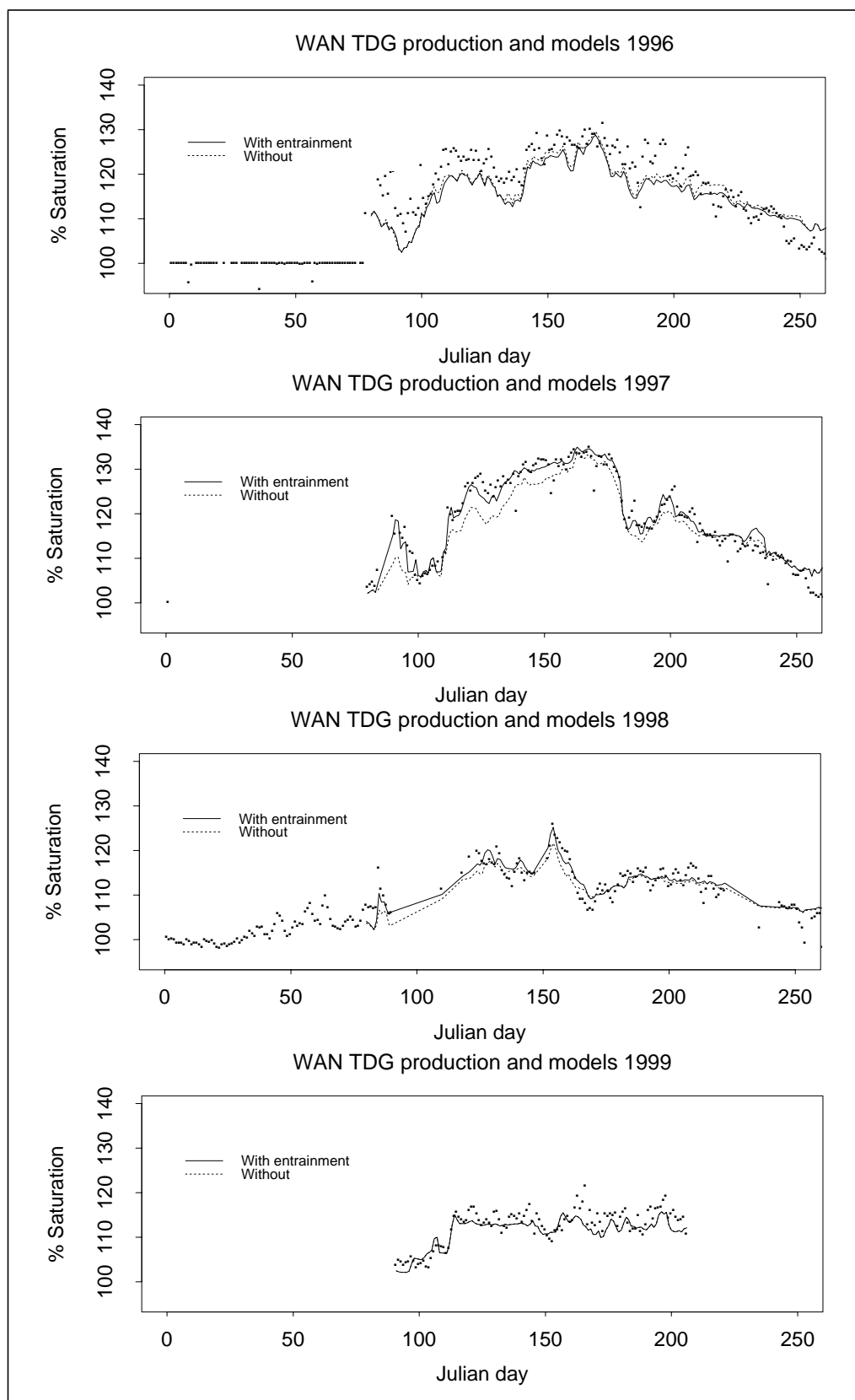


Fig. 42 WAN production values with and without entrainment and observed data (points).

II.5.4 -Reservoir Dissolved Gas Distributions

Theory

The CRiSP.1 reservoir gas model has been reworked to model the movement and mixing of parcels of water distinguished by different levels of total dissolved gas. A quasi-2D river model is used to describe the river as two flows, with each flow having its own TDG level. Looking downstream, there is the right bank and the left bank flow (see Fig. 43).

At a dam, the river is divided according to the proportion of spill from the nearest upstream dam and at a confluence by the proportion of flow from the two converging rivers. At a reach where there has been no spill or upstream confluences, the gas levels on either side of the river are simply set to be equal and there is essentially one flow in the reservoir. Fig. 44 represents the case downstream of a dam. The right bank flow in this case is just the spill flow, and the fraction of flow in the right bank flow is simply the spill fraction.

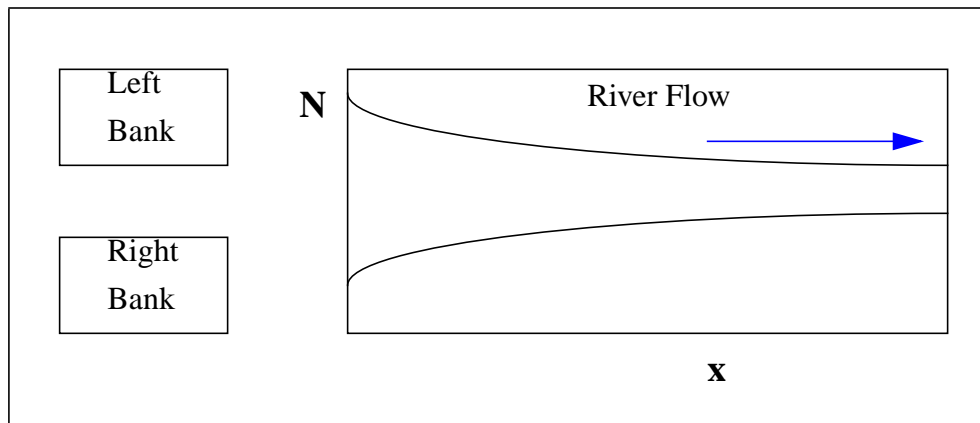


Fig. 43 A Divided Reservoir

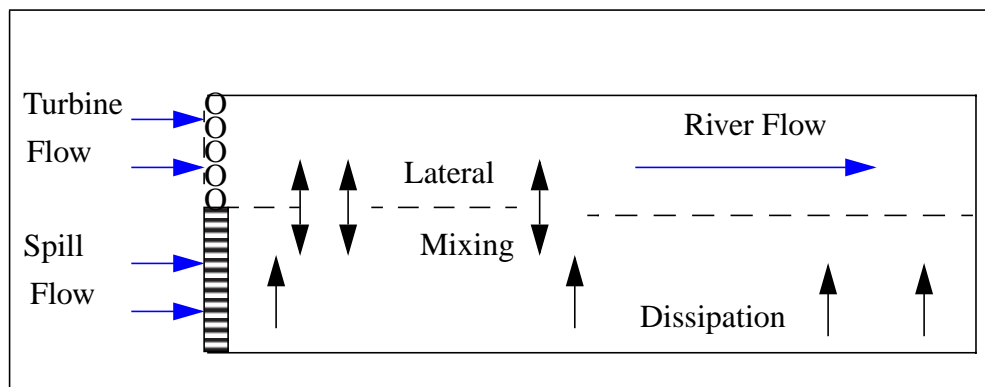


Fig. 44 Reservoir Gas Dynamics

TDG is mixed between the two flows and simultaneously dissipated as the water moves downstream, with the river velocity being estimated from the flow and reservoir geometry. In this manner, the model captures heterogeneous levels of gas. Fig. 44 also gives a diagram of the gas dynamics modeled in the reservoir.

Each of the flows has an initial mass of TDG which is then diffused through the boundary between them and also dissipated into the air. Both of these processes were achieved in the model using simple exponential functions. These models were also chosen for their simplicity; the sparseness of data and the added complexity discouraged the use of a full two-dimensional advection-diffusion model. Exponentials were also used because the rate of change of an exponential variable is proportional to its value; this is representative of many decaying substances in nature.

The 2-flow model is shown in equations below.

$$N_{right} = \left[N_{mix} - E + N_{dif} \cdot (1 - S_{fr}) \cdot e^{-\theta x} \right] \cdot e^{-k \cdot \frac{x}{v}} + E \quad (96)$$

$$N_{left} = \left[N_{mix} - E - N_{dif} \cdot S_{fr} \cdot e^{-\theta x} \right] \cdot e^{-k \cdot \frac{x}{v}} + E \quad (97)$$

where

- N_{right} , N_{left} = the %-TDG in the flow entering the reach on the respective sides
- S_{fr} = the percent of river in the right-bank flow
- N_{mix} = the flow weighted average of the TDG values in each flow

$$N_{mix} = S_{fr} \cdot N_{right} + (1 - S_{fr}) \cdot N_{left} \quad (98)$$

- N_{dif} = the difference between the original concentrations of the two flows

$$N_{Dif} = N_{right} - N_{left} \quad (99)$$

- W = width of the river channel, assumed to be constant
- E = %-TDG in water at equilibrium, 100% saturation or 0% supersaturation
- θ = diffusion rate constant in units of (mile)⁻¹, a model parameter set for each reach
- k = dissipation rate constant in units of (day)⁻¹ a model parameter calculated for each reach based on the river depth, velocity and a diffusion constant (see eq (100) below)
- x = longitudinal distance, where x is in miles
- v = river velocity, in miles per day.

Using Equation 96 and Equation 97:

$$N_{right} - N_{left} = N_{dif} \cdot e^{-\theta x} \cdot e^{-k \cdot \frac{x}{v}} \quad (100)$$

In other words, the difference between the two concentrations is decaying to zero due the diffusion factor $e^{-\theta x}$ and the dissipation factor $e^{-k \cdot \frac{x}{v}}$. Similarly, with a little algebra the total mass in the system can be shown to be:

$$S_{fr} \cdot N_{right} + (1 - S_{fr}) \cdot N_{left} = (N_{mix} - E) \cdot e^{-k \cdot \frac{x}{v}} + E \quad (101)$$

Thus the total mass (without the dissipation factor $e^{-k \cdot \frac{x}{v}}$ it remains at N_{mix}) is decaying to equilibrium level E . Hence the physical properties are captured with these two equations. N_{right} and N_{left} are computationally inexpensive and their simplicity results in an easy fitting and integration.

A given reservoir can have slugs of water which entered the reach under different initial conditions. Typically, these slugs are caused by varying spill conditions at an upstream dam. Conditions at a dam can vary on a “dam time-step” basis. Thus all water leaving the reach in a given dam-timestep is assumed to have the same initial conditions. At any given point in the reach, daily river velocities and the distance downstream in the reach are used to calculate the length of time the water has been in the reach. These travel times are used to capture the correct initial conditions and the amount of mixing and dissipation that have occurred in this slug of water. At any given point at the reach, the dissolved gas level is calculated by knowing the initial conditions for N_{right} and N_{left} , and S_{fr} along with x (distance downstream).

Parameter Determination

In transect studies completed by the Army Corps of Engineers, gas data from lateral cross sections of the Snake and Columbia river were sampled to gather information on mixing characteristics in each of the reservoirs from Lower Granite to Bonneville dam. These pools were sampled under high and low flow conditions and showed that while the dam introduced a heterogeneous flow, the reservoirs were well-mixed by the next downstream forebay.

Because mixing rates vary according to dam operations, river velocity, and other conditions such as wind, a conservative estimate for mixing was fixed for all reaches. A value of 0.075 was used to fix the mixing rate so that the flows were 95% mixed in 40 miles. The transect data from the 1996 and 1997 studies showed that the difference between the left-bank and right bank flows rarely differed by more than this in the downstream forebay.

II.5.5 -Other Gas Inputs

In the last several years more and more dissolved gas data has become available from the Army Corps of Engineers so that nearly every pool has at least 2 water quality monitors, one in the forebay of the dam and one in the tailrace of the previous dam. For this reason an input feature was added to CRiSP.1 to allow the direct input of dissolved gas data at any reach or dam in the model. This is achieved through a token called `output_gas` in the data file. By default this feature is turned off, but if the line “`output_gas on`” appears in a reach or dam profile, than a vector of dissolved gas data of length `num_days* num_dam_slices` (currently 366*4) should be supplied.

The intention of this feature was to allow total dissolved gas to enter the system above the dams. Thus, in most data files a vector of data is provided at two locations: Chief Joseph pool for gas entering from Columbia Headwaters, and Lower Granite pool, for the gas entering from the upper Snake and Clearwater. For a more accurate description of dissolved gas, historic data could be used for all reaches where it is available, but generally this is turned off since gas production and distribution is well modeled.

The output_gas token has the effect of setting gas values that exit the reach on both sides of the river to the same value.

Total Dissolved Gas in the Tailrace

Total dissolved gas supersaturation in the tailrace results from mixing spill water with water passing through turbines (Fig. 38). The equation is

$$N = N_{fb} + \frac{F_s}{F}(N_s - N_{fb}) \quad (102)$$

where

- F = total flow through the dam in kcfs
- F_s = spill flow in kcfs
- N = tailwater tdg supersaturation (in percent)
- N_{fb} = forebay tdg supersaturation (in percent)
- N_s = spill water tdg in percent saturation as defined by an empirical or mechanistic saturation equation.

Total Dissolved Gas at a Confluence

The tdg at a confluence is determined by the addition of two flows with different tdg levels. The equation is

$$N = \frac{F_1 N_1 + F_2 N_2}{F_1 + F_2} \quad (103)$$

where

- F_i = flow in kcfs in segment i
- N_i = tdg in percent supersaturation in segment i of the confluences.

Total Dissolved Gas Dissipation

Total dissolved gas levels above the saturation level are lost from the river as a first order process. This is defined by a total flux equation for a segment as

$$\Phi = AK_d(N_{eq} - N) \quad (104)$$

where

- Φ = flux of tdg across the air water interface
- N = tdg supersaturation concentration in the segment
- N_{eq} = tdg equilibrium concentration
- A = surface area of the segment
- K_d = transfer coefficient defined

$$K_d = \left(\frac{D_m U}{D} \right)^{0.5} \quad (105)$$

where

- D_m = molecular diffusion coefficient of tdg
- U = hydraulic stream velocity
- D = depth of the segment

To express the loss in terms of concentration we divided eq (104) by AD to give

$$\frac{dN}{dt} = \frac{\Phi}{AD} = (N_{eq} - N) \sqrt{\frac{D_m U}{D^3}} \quad (106)$$

To put the calculation in units of miles and days, note that one mile = 16.0934×10^4 cm = 5280 ft, and one day = 8.64×10^4 seconds. Expressing U in miles/day and D in feet and D_m in cm^2/s , the diffusion coefficient per unit square mile of river is

$$\frac{dN}{dt} = k(N_{eq} - N) \quad (107)$$

where the coefficient k is expressed

$$k = 700.75 \sqrt{\frac{D_m U}{D^3}} \approx 0.085 \text{ /day} \quad (108)$$

assuming:

- D_m = order¹ of $2 \times 10^{-5} \text{ cm}^2\text{s}^{-1}$
- U = order of 3 cm/s (20 miles/day), note this changes on a daily basis and for each reach in the model
- D = order of 900 cm, note this changes on a reach specific basis and is dependent on reservoir elevation
- the constant 700.75 gives the coefficient k in unit of day^{-1} .

Tdg loss rate due to degassing can be expressed as a function of the residence time since the water entered the tailrace as

$$N(t) = N_{eq} + [N(0) - N_{eq}]e^{-kt} \quad (109)$$

where

- N_{eq} = tdg equilibrium concentration
- $N(0)$ = tailrace concentration defined by eq (102)
- k = dissipation coefficient defined by eq (108)
- t = time in a river segment.

Noting that in the models N is in terms of percent above supersaturation we then set $N_{eq} = 0$.

1. F.A. Richards 1965.

Adjustments of k

The tdg dissipation coefficient depends on the average depth as defined in eq (108). The average depth is variable according to the geometry of the reservoir and the pool elevation. This depth is defined as

$$D = \frac{Volume}{WL} \quad (110)$$

where

- *Volume* = pool volume at a specific elevation
- *W* = average pool width at full pool
- *L* = length of pool.

II.6 - Dam Passage

Fish enter the forebay of a dam from the reservoir and experience predation during transit time and during delays due to diel and flow related processes. They leave the forebay and pass the dam mainly at night through spill, bypass or turbine routes, or are diverted to barges or trucks for transportation. Once they leave the forebay, each route has an associated mortality and fish returning to the river are exposed to predators in the tailrace before they enter the next reservoir. The details of passage through the regions of the dam are illustrated schematically in (Fig. 45).

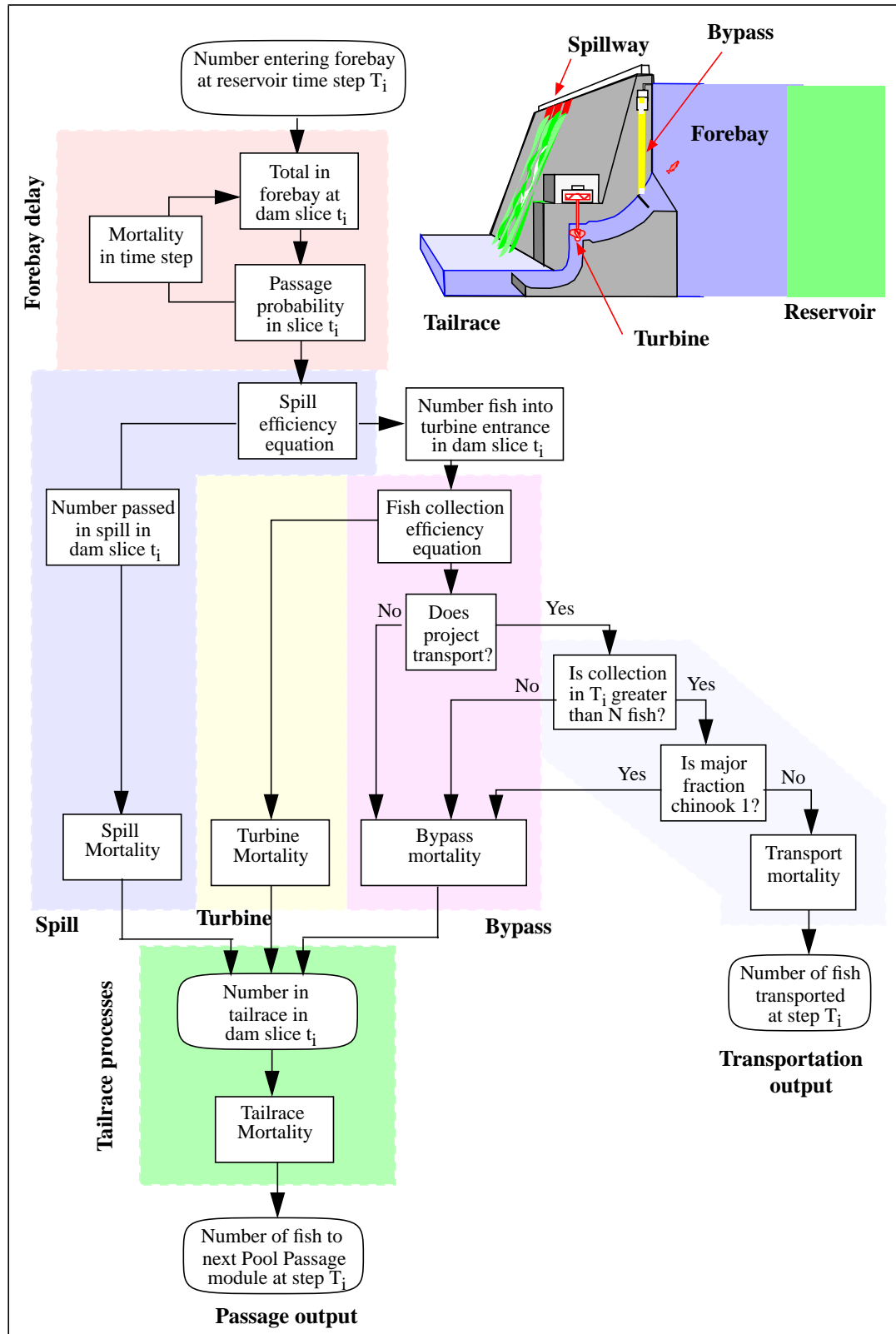


Fig. 45 Dam processes showing passage routes and mortality. Forebay delay is further illuminated in Fig. 46.

The movement and allocation of fish through the forebay is illustrated in Fig. 46. Fish exiting the reservoir in each reservoir time slice, currently two slices per day, are evenly allocated as input to the forebay across the dam time slices, currently four slices per day. Fish entering from the reservoir are subjected to possible predation for the duration of the forebay transit. The forebay transit is for mortality modeling and is not counted against travel time. Next, fish are either passed (through dam or spillway) to the tailrace or are delayed for one dam time slice in the forebay. Delayed fish are combined in the next dam time slice with fish completing the forebay transit. These are passed or are delayed, etc.

Output from the forebay in each dam time slice depends on flow and diel illumination. Allocation to the passage routes depends on spill schedules and passage efficiencies through the routes.

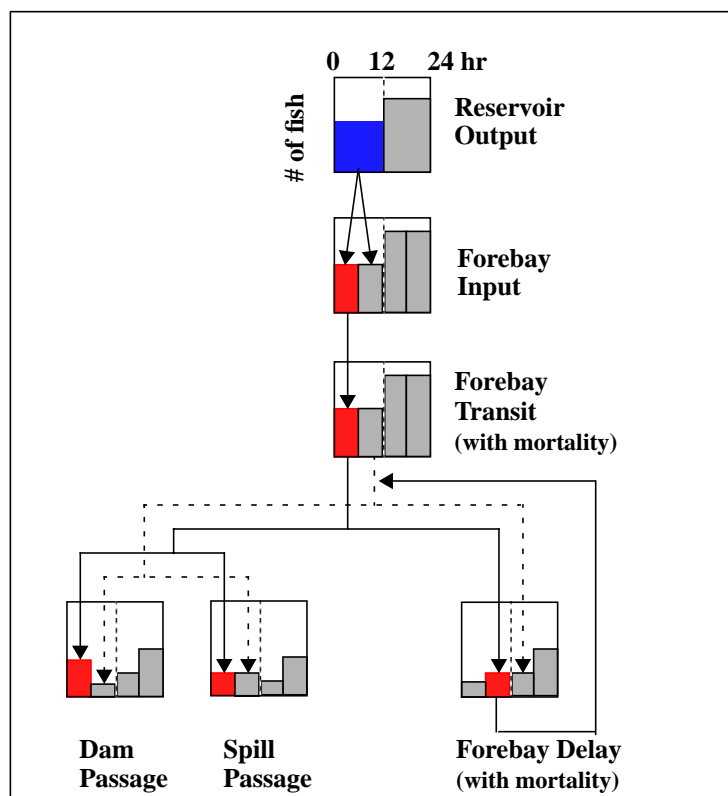


Fig. 46 Transfer of fish from reservoir to forebay to dam. Diagram shows allocation of fish from a reservoir time slice of 12 hours to dam time slices of 6 hours each. Mortality is associated with dam and spill passage as well as forebay transit and delay.

II.6.1 -Forebay Delay

Studies of the timing of fish passage at dams indicate that passage occurs mostly at night, with fish delaying passage during daylight hours. This delay process is represented in CRiSP.1 as a simple input-output submodel. Fish enter the forebay at a rate determined by reservoir passage factors. Fish are assumed to be more susceptible to being drawn into turbine intakes or spill at night than during the day, and this susceptibility is represented through the flow and the volume of the forebay area occupied by the fish. CRiSP.1 expands this volume in the day and contracts it at night.

The essential elements of this submodel include a forebay volume defined by the forebay depth H , a horizontal length scale L , which changes with illumination I , and river flow F (Fig. 47).

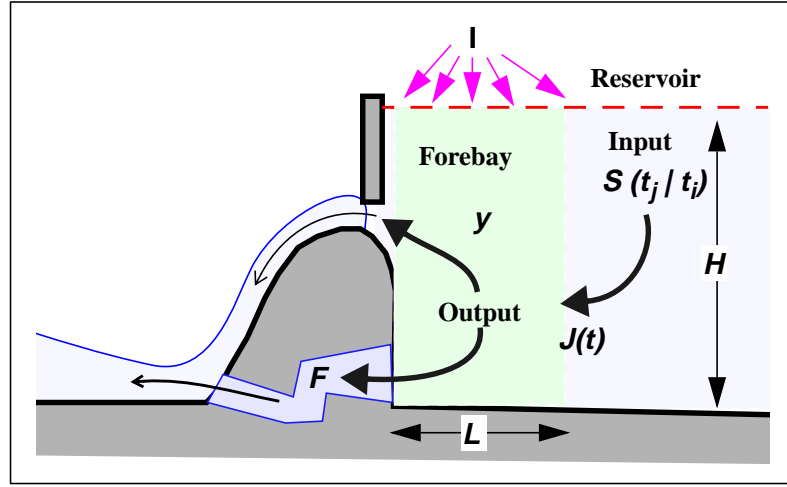


Fig. 47 Variables for dam passage delay model

Dam Delay Model

$$\lambda_t = p \cdot \alpha_{day} + (1 - p) \cdot \alpha_{night} + \beta_1 \cdot V_t + \beta_2 \cdot SP_t + \beta_3 \cdot D_t \quad (111)$$

where

- λ_t = instantaneous probability of passage
- p = proportion of time step during day
- $(1-p)$ = proportion of time step during night
- V_t = upstream river velocity in mi/day
- SP_t = proportion of river spilled
- D_t = julian date
- α 's and β 's = parameters that vary by dam and species.

Probability of remaining during a single time step:

$$P_1 = e^{-(\lambda_t \cdot \Delta t)} \quad (112)$$

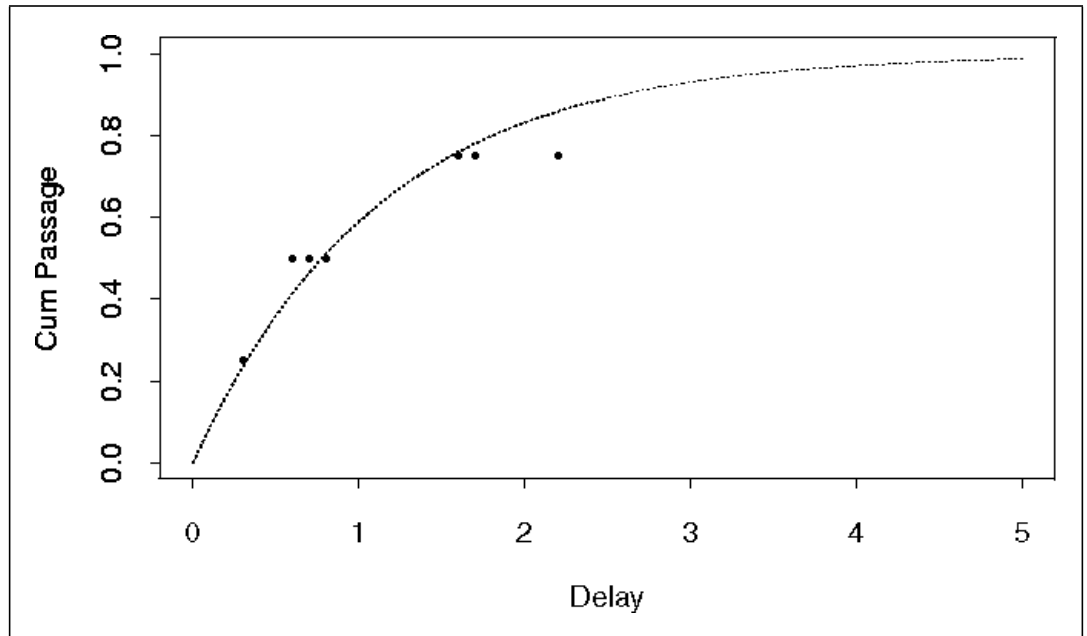


Fig. 48 Cumulative passage versus dam delay in days at Little Goose Dam

II.6.2 -Spill

The spill algorithm represents allocations of spill from flow models (HYDROSIM or HYSSR) through Flow Archive Files or the **Spill Schedule** window under the **Dam** menu.

Flow Archive Spill

When spill is allocated from Flow Archive files, it is identified as a percent of daily averaged flow over multi-day periods. Consequently, for use in CRiSP.1, archive derived spill must be allocated to specific days and hours of the day. Special adjustments to spill allocations in years of low and high water are not implemented at this time. CRiSP.1 considers three types of spill:

Planned Fish Spill is requested by the fisheries agencies. The schedule for this can be obtained from the Flow Archive Files or can be set in the Spill Schedule Window.

Overgeneration Spill occurs when electrical generation demand is less than that available in flow. This is obtained from the Flow Archive File only.

Forced Spill occurs when river flow exceeds powerhouse capacity. This is calculated by CRiSP.1.

CRiSP.1 allocates spill flows in the following order.

➔ First, **Planned Fish Spill** is allocated. For each period, planned spill is distributed over scheduled spill days and fish spill hours (within those days) using the following steps.

1. Total modulated flow in the period that occurs in fish spill hours on planned spill days is calculated and designated
flow_available (in kcfs units)
2. The requested spill in a period is designated
spill_request (in kcfs units)
3. Percent spill during Fish Hours is calculated as
$$\text{spill_daily_percent} = \text{spill_request} / \text{flow_available}$$
4. If $\text{spill_daily_percent} > 100\%$
then $\text{spill_daily_percent} = 100\%$ of the flow available in the request periods and the rest is discarded and a warning message is generated.

➔ Second, **Overgeneration Spill** identified in the flow models for 2 or 4 week periods is evenly distributed over all days in the periods. The following calculations are made on a daily basis.

1. Overgeneration Spill is added to Planned Fish Spill in Fish Hours every day in a period to yield total spill.
2. If Total Spill in Fish Hours is now greater than the total flow over the hours then the excess is distributed over the rest of the day.
3. If Total Spill for the entire day is greater than the total daily modulated flow then the spill is set to the total daily modulated flow.

→ Third, **Forced Spill** occurs when river flow exceeds powerhouse capacity. Forced Spill is calculated on the dam time slice periods. This is typically a 6 hour interval. CRiSP.1 uses the following logic:

1. Calculate the quantity

$$\text{flow} - \text{powerhouse capacity} / \text{flow} = \text{possible forced spill}$$
2. Then, if

$$\text{possible forced spill} > \text{total fish \& overgeneration spill}$$

$$\text{assign total spill} = \text{possible forced spill}.$$

Otherwise the forced spill is assimilated into fish and overgeneration spills.

Spill from Spill Schedule Tool

Planned Spill can be set by specifying spill information with the **Spill Schedule** Tool. The following information is entered:

- fraction of flow spilled
- days over which the spill fraction applies
- days in which actual spill occurs, i.e. the planned spill
- hours of planned spill for the indicated days.

Overgeneration Spill is only applied if a Monte Carlo Mode is used. Forced Spill is calculated as described above and is applied in both Scenario and Monte Carlo Modes.

Spill Caps

The maximum allowable planned spill is set by spill caps at each dam. If planned spill exceeds the cap then spill is limited to spill cap. Forced spill can exceed the spill cap. Spill cap is under the **Dam** menu.

Spill Efficiency

The fraction of fish passed with spilled water is defined by one of nine possible empirical equations that can be selected by the user. The following are the spill efficiency equations:

$$\begin{aligned}
 Y &= a + b \cdot X + e \\
 Y &= a + b \cdot X + X \cdot e \\
 Y &= b \cdot \exp(a \cdot X + e) \\
 Y &= b \cdot \exp(a \cdot X) + X \cdot e \\
 Y &= b \cdot X^{a+e} \\
 Y &= b \cdot (X/100)^a + X \cdot e \\
 Y &= a + b \cdot \ln X + e \\
 Y &= a \cdot X + b \cdot X^2 + c \cdot X^3 + e \\
 Y &= a \cdot (X/100) + b \cdot (X/100)^2 + c \cdot (X/100)^3 + e
 \end{aligned} \tag{113}$$

where

- Y = fraction of total fish passed in spill
- X = fraction of water spilled

- a and b = regression coefficients
- e = error term (var) selected from random distribution.

The equations and parameters defining spill efficiency (often called “effectiveness” in the literature) are indicated in Table 32. These values were used beginning with the SOR screening runs of CRiSP.1.

Table 32 Spill efficiency (% fish passed in spillway /% flow passed in spillway).

Dam	Spill equation	Reference
Wells	zero ^a	Erho et al. 1988; Kudera et al. 1991
Rocky Reach	% pass = 0.65 * (% spill)	Raemhild et al. 1984
Rock Island	% pass = 0.94 * (% spill) + 11.3	Ransom et al. 1988
Wanapum	% pass = 15.42 * ln (% spill)	Dawson et al. 1983
Priest Rapids	% pass = (% spill) ^ 0.82	
L. Monumental	% pass = 1.2 * (% spill)	Johnson et al. 1985. Ransom and Sullivan 1989
The Dalles	% pass = 2 * (% spill)	
all other dams	% pass = (% spill)	-

a. Wells Dam is designed to pass smolts preferentially through the spillway system: about 96% of all smolts pass via the spillway. This is modeled by assigning an FGE value of 96% (range 95-97%) at Wells with a zero spill efficiency for years 1991 on.

II.6.3 -Fish Guidance Efficiency (FGE) Theory

Guidance of fish into the bypass systems of dams is achieved by diverting fish into a bypass slot. Individual fge are specified for day and night at each dam and for each species. In addition, CRiSP.1 can treat fge as constant over time or vary fge with the age of the fish relative to the onset of smoltification.

Constant FGE

Fish guidance efficiency is fixed in time and set for day and night from the **fge** window selected from the **Dam** menu. This is activated by switching “off” the **age dependent fge** toggle in **Runtime Settings** from the **Run** menu (this is the default setting). Note that only the mean remains constant; FGE can still vary in a stochastic fashion if variance suppression is disabled.

Age Dependent FGE

Studies on fish guidance at several dams in the Columbia system indicate that fge varies with seasons from a number of factors including the water quality and the degree of smolt development in the fish, which changes with age. If the age dependent option is selected, fish depth in the forebay varies with age, which in turn alters the fge. The algorithm assumes that fish above some critical depth z enter the bypass system and fish below z enter the turbine (Fig. 49). Thus, to define age dependent fge, fish depth in the forebay is defined as a function of age. If the surface drops below the level of the bypass orifice fish bypass goes to zero.

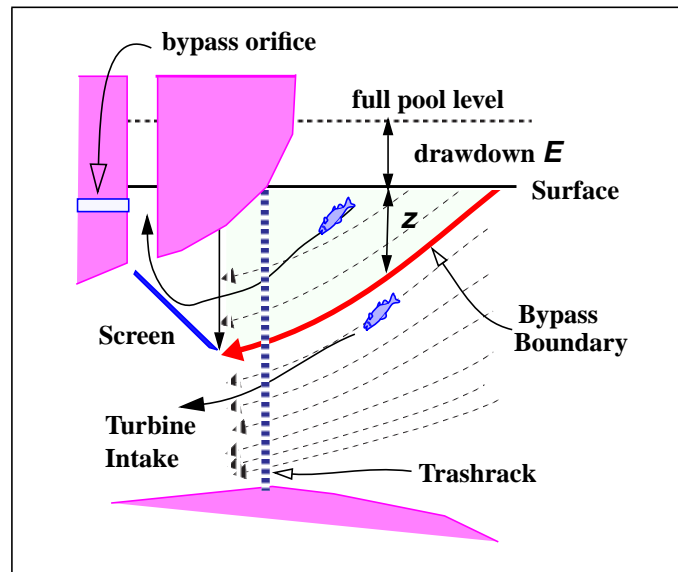


Fig. 49 Critical parameters in fish guidance are fish forebay depth z , screen depth D and elevation drop E . Only fish above z are bypassed. Bypass stops when the surface is below the bypass orifice depth.

The fge is based on the fge model of Anderson (1992). Behavioral and hydraulic factors affecting fge are combined into a calibration factor D_c . In addition, the affect of drawdown on fge can be expressed in terms of screen depth relative to the surface. The modified equation is

$$fge = 1 - \exp\left(\frac{-0.693}{z}(D - D_c - E)\right) \quad (114)$$

where

- fge = fish guidance efficiency
- z = median depth of fish in the forebay at a distance from the dam where fish are susceptible to being drawn into the intake
- D = screen depth relative to full pool forebay elevation
- D_c = fge calibration parameter
- E = amount the pool is lowered below full pool elevation.

Thus, changes in fge result from changes in fish depth and changes in reservoir elevation. The parameter D_c depends on physical and hydraulic properties of a dam, and behavioral properties of fish. As such, the term is specific to both a given species and a given dam. In addition, separate coefficients are defined for day and night dam passage.

Changes in fge with fish age are represented by changes in fish forebay depth which is described by a linear equation

$$\begin{aligned} t < t_0 & \quad z(t) = z_0 \\ t_0 < t < t_0 + \Delta t & \quad z(t) = z_0 + (z_1 - z_0)\left(\frac{t - t_0}{\Delta t}\right) \\ t > t_0 + \Delta t & \quad z(t) = z_1 \end{aligned} \quad (115)$$

To implement the fge equation define the calibration coefficient

$$K = \frac{\log(1 - fge_0)}{-0.693} = \frac{D - D_c}{z_0} \quad (116)$$

Combining eq (114), eq (115) and eq (116) the final fge equation is

$$fge(t) = 1 - \exp\left(-\frac{0.693}{z(t)}(z_0 K - E(t))\right) \quad (117)$$

where

- t = fish age since the onset of smoltification, see eq (56) on page 42
- t_0 = onset of change in fge relative to the onset of smoltification set in the release window
- Δt = increment of time over which fge changes
- z_0 = initial mean fish depth (at age t equals 0) in the forebay
- z_1 = final mean fish depth (at age t equals $t_0 + \Delta t$) in the forebay
- fge_0 = fge at onset of smoltification
- $E(t)$ = elevation drop.

The resulting fge and depth are illustrated in (Fig. 50).

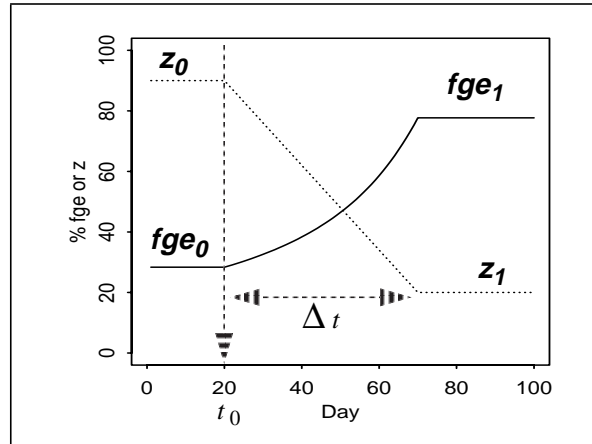


Fig. 50 Fge and fish depth over fish age

FGE Estimation

Spring Chinook

Fall Chinook FGE

Steelhead FGE

A similar approach was taken for juvenile steelhead PIT tagged from the Dworshak hatchery. These fish were detected at Lower Granite, Little Goose, and McNary Dams, and assuming travel time and mortality algorithms were calibrated, estimates of *FGE* could be obtained for these projects. *FGE* was estimated using data from 1989-1995 inclusive (Table 33). Because of the variation in year-to-year fits, the average of these years' *FGE* values was used. Note that the PIT tag-calibrated *FGE* value is close to that estimated by NMFS for coordination purposes, but at McNary, for spring chinook, the calibrated value is about 5/6 that of the coordination value in the System Operation Review. This makes sense in the context of the fyke net argument made above. Also note that 1994 and 1995 observations are complicated by the fact that slide gates were in operation at all three upper projects; this led, for example, to an astonishingly high collection rate at Lower Monumental Dam in 1995.

Table 33 CRiSP.1 estimated FGE for steelhead.

Year	LGR	LGS	LMN	MCN
1989	82%	89%	n/a	90%
1990	77%	66%	n/a	27%
1991	89%	99%	n/a	100%
1992	77%	63%	n/a	41%
1993	56%	88%	n/a	54%
1994	72%	58%	73%	50%
1995	81%	67%	100%	54%
average	76.3%	75.7%	86.5%	59.4%

Table 33 CRiSP.1 estimated FGE for steelhead.

Year	LGR	LGS	LMN	MCN
SOR value	79.0%	79.0%	76.0%	75.0%

Historical FGE Values

Time Variable FGE

The calibration of time varying FGE is not available for CRiSP.1.6.

Bypass orifice and FGE

Fish guidance goes to zero when the surface elevation drops below the bypass orifice elevation (Fig. 49). This parameter, designated `bypass_elevation`, is set in the **columbia.desc** file. If `bypass_elevation` is missing or commented out (with #) the bypass elevation is set to the pool floor_elevation and bypass will occur for all reservoir elevations. This function applies with or without selection of age dependent fge.

Bypass Elevations

The bypass elevations and forebay elevations in feet above sea level (obtained from the Army Corps of Engineers) are set in the **columbia.desc** file for each dam where a bypass system exists.

Table 34 Bypass and forebay elevations of dams with bypass systems

Dam	Bypass elevation (ft)	forebay elevation (ft)
Bon # 1 and 2	65.5	77
The Dalles	149	160
John Day	250.5	269
McNary	330	340
Wells	716	781
Ice Harbor	431.5	440
Lower Monumental	531.5	540
Little Goose	628.9	638
Lower Granite	729	738

Multiple Powerhouses

Bonneville Dam and Rock Island Dam each have two powerhouses that can be operated independently to optimize survival during the fish passage season since each project has a single spillway. Multiple-powerhouse dams can be represented schematically as shown in Fig. 51.

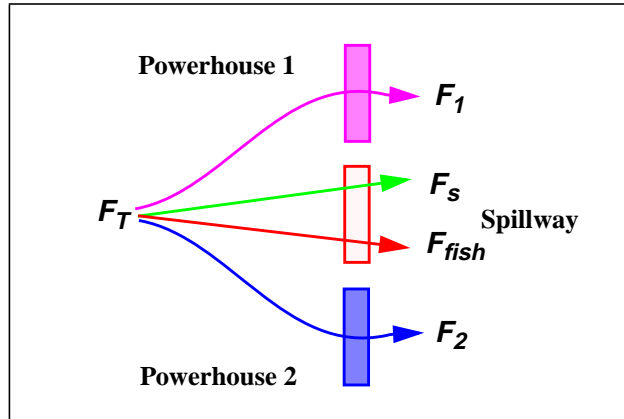


Fig. 51 Multiple powerhouse configuration showing allocation of spill and powerhouse flows.

In these cases, flow is allocated fractionally as follows:

- Flows are first allocated to planned spill in fish passage hours.
- Remaining flow is partitioned between the primary and secondary powerhouses and additional spill as follows:

The strategy is to:

- Operate highest priority powerhouse up to its hydraulic capacity.
- Spill water up to another level called the spill threshold.
- Above the threshold, use the second powerhouse.
- Over the second powerhouse hydraulic capacity, spill extra flow.

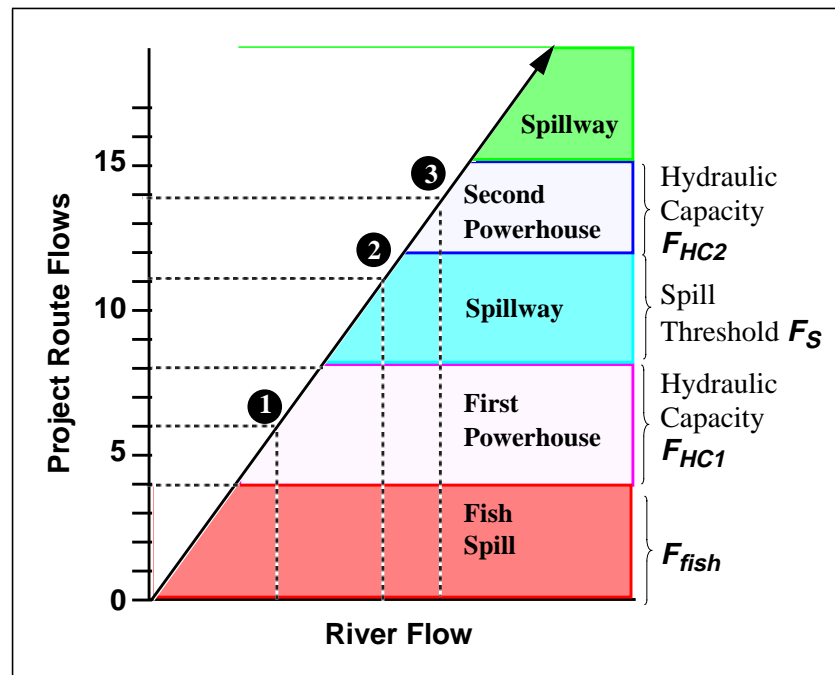


Fig. 52 Flow allocation through two powerhouse projects.

An example of flow allocations is described as follows (Fig. 52):

- At level ① 4 units of flow are put to Fish Spill and 2 units are put through the First Powerhouse.
- At level ② Fish Spill has four units of flow, the First Powerhouse is run at its hydraulic capacity, which is 4 flow units, and the spillway has 3 units of additional spill.
- At level ③ the First Powerhouse is at hydraulic capacity, spill flow includes Fish Spill and additional spill up to the Spill Threshold and 2 units of flow pass the Second Powerhouse.

Fish Passage Efficiency (FPE)

Fish passage efficiency is the percent of fish that pass a project by non-turbine routes (spill, bypass, and sluiceway passage). FPE considers that fish pass mostly during the night and spill generally occurs at night. The simple fish routing is illustrated below in Fig. 53. A fraction of the fish are first diverted in to spill water. What remains is diverted into the turbine intake and a fraction of this flux is diverted into the fish bypass system.

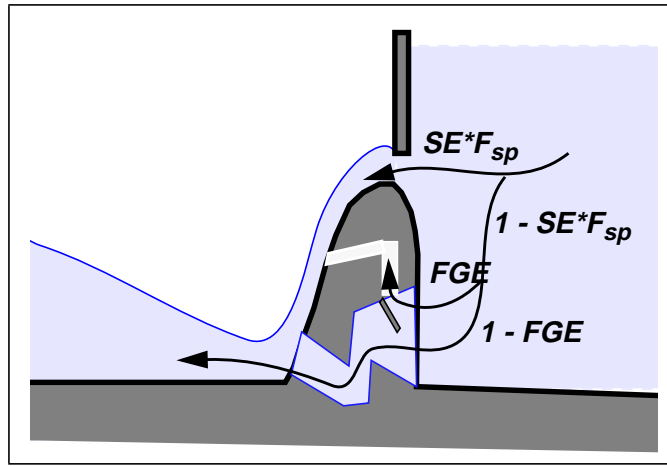


Fig. 53 Routing of fish for calculation of FPE

The formula expressing FPE considers these independent diversions and accounts for the fact that fish may be attracted to spill flow over flows into the turbine. The simplified formula for FPE which considers spill occurs at night and most of the fish pass at night can be expressed

$$FPE = \{D \cdot F_{sp} \cdot SE + D \cdot FGE \cdot (1 - F_{sp}SE) + (1 - D) \cdot FGE\} \cdot 100 \quad (118)$$

where

- D = fraction of fish that pass dam during spill hours
- F_{sp} = fraction of daily flow that passes in spill
- SE = fraction of fish that pass in spill relative to the fraction of flow passing in spill
- FGE = fraction of fish passing into turbine intake that are bypassed.

The spill flow, in percent of the total flow, required to generate a given FPE can be expressed by arranging eq (118) to give

$$F_{sp} = \frac{FPE - FGE}{D \cdot SE \cdot (1 - FGE)} \quad (119)$$

Dam Passage Survival

Fish passing through the dams can take several routes (depicted in Fig. 45). Equations describing the number of fish that pass through each route in terms of the number that enter the dam from the forebay on a particular dam time slice are given below. In each case the mortality and passage efficiencies have deterministic and stochastic parts.

For mortalities and fge, the random elements are represented by additive deterministic and stochastic parts in

$$x = \bar{x} + x' \quad (120)$$

where

- \bar{x} = deterministic part of the random parameter fixed for each species and dam
- x' = stochastic part of the parameter taken from a broken-stick distribution (see Stochastic Parameter Probability Density section on page 108) over each dam time slice.

For spill efficiency, each equation contains a random term. A typical equation is

$$y = a + bx + e \quad (121)$$

where

- y = spill efficiency
- x = percent flow
- a and b = deterministic parameters
- e = stochastic parameter selected from a normal distribution.

Turbine Survival

The equation for turbine survival can be expressed

$$N_{tu} = N_{fo} \cdot p \cdot (1 - Y) \cdot (1 - m_{fo}) \cdot (1 - m_{tu}) \cdot (1 - fge) \quad (122)$$

where

- N_{tu} = number of fish passing in a time increment (6 hrs)
- N_{fo} = number of fish in forebay ready to pass in the increment
- p = probability of passing during the increment ($1 - P_1$ from eq (112) on page 92)
- m_{fo} = mortality in forebay (see Predation Mortality section on page 47)
- m_{tu} = mortality in turbine passage
- fge = fish guidance efficiency for a day or night period
- Y = proportion of fish passage in spill defined by spill efficiency equation (see eq (113) on page 95).

Bypass Survival

The equation for bypass survival is

$$N_{by} = N_{fo} \cdot p \cdot (1 - Y) \cdot (1 - m_{fo}) \cdot (1 - m_{by}) \cdot fge \quad (123)$$

where

- m_{by} = mortality in the bypass.

Transport Survival

The equation for transport survival with fixed transport mortality is

$$V_{tr} = N_{fo} \cdot p \cdot (1 - Y) \cdot (1 - m_{fo}) \cdot (1 - m_{by}) \cdot fge \cdot m_{tr} \quad (124)$$

where

- m_{tr} = mortality in the transport.

Spill Survival

The equation for spill survival is

$$N_{sp} = N_{fo} \cdot p \cdot (1 - m_{sp}) \cdot Y \quad (125)$$

where

- m_{sp} = mortality in the spill passage.

Parameter Determination for Passage Mortality

II.6.4 -Transport Parameters

Transportation schedule

The schedule of transporting fish from each transport dam depends on the flow, number of each species passing the dam, and the efficiency of separating fish for return back into the river. The schedules for transportation, compiled from FTOT annual reports, for the historical years are given in Table 35.

Table 35 Transport operations for historical data files, 1975-1994.

Year	Project	Start Date	Stop Date	Separation @ (kcfs)	Criterion
1975	L. Goose	4/10	6/15	none	transport all
1976	L. Granite	4/12	6/15	none	transport to 50% of run
	L. Goose	4/10	6/15	none	transport to 50% of run
1977	L. Granite	4/15	6/5	none	transport all
	L. Goose	4/29	6/16	none	transport all
1978	L. Granite	4/4	6/21	none	transport all
	L. Goose	4/10	6/21	none	transport all
1979	L. Granite	4/11	7/4	none	transport all
	L. Goose	4/17	7/4	none	transport all
	McNary	4/9	8/24	none	transport all
1980	L. Granite	4/3	7/7	none	transport all
	L. Goose	4/7	7/7	none	transport all
	McNary	4/3	9/22	none	transport all
1981	L. Granite	4/2	7/30	none	transport all
	L. Goose	4/7	7/24	none	transport all
	McNary	3/30	9/11	none	transport all
1982	L. Granite	4/8	7/29	85	full trans @ 80% yearlings
	L. Goose	4/10	7/22	85	full trans @ 80% yearlings
	McNary	3/30	9/24	220	full trans @ 80% yearlings
1983	L. Granite	4/3	7/30	85	full trans @ 80% yearlings
	L. Goose	4/5	7/8	85	full trans @ 80% yearlings
	McNary	5/30	9/22	220	full trans @ 80% yearlings
1984	L. Granite	4/1	7/26	none	transport all
	L. Goose	4/5	7/28	85	full trans @ 80% yearlings
	McNary	4/16	9/28	220	full trans @ 80% yearlings

Table 35 Transport operations for historical data files, 1975-1994.

Year	Project	Start Date	Stop Date	Separation @ (kcfs)	Criterion
1985	L. Granite	3/28	7/23	none	transport all
	L. Goose	3/30	7/23	85	full trans @ 80% yearlings
	McNary	4/6	9/26	220	full trans @ 80% yearlings
1986	L. Granite	3/27	7/24	none	transport all
	L. Goose	4/5	7/3	85	full trans @ 80% yearlings
	McNary	3/27	9/26	220	full trans @ 80% yearlings
1987	L. Granite	3/29	7/31	none	transport all
	L. Goose	4/6	7/4	100	full trans @ 80% yearlings
	McNary	3/28	10/29	220	full trans @ 80% yearlings
1988	L. Granite	3/28	7/26	none	transport all
	L. Goose	4/12	7/23	100	full trans @ 80% yearlings
	McNary	3/29	9/22	220	full trans @ 80% yearlings
1989	L. Granite	3/29	7/30	none	transport all
	L. Goose	4/8	7/11	100	full trans @ 80% yearlings
	McNary	3/27	9/20	220	full trans @ 80% yearlings
1990	L. Granite	3/27	7/26	none	transport all
	L. Goose	4/12	7/21	100	full trans @ 80% yearlings
	McNary	4/1	9/14	220	full trans @ 80% yearlings
1991	L. Granite	3/27	7/26	none	transport all
	L. Goose	4/12	7/20	100	full trans @ 80% yearlings
	McNary	4/1	9/14	220	full trans @ 80% yearlings
1992	L. Granite	4/27	10/31	none	transport all
	L. Goose	4/3	8/31	100	full trans @ 80% yearlings
	McNary	3/25	9/30	220	full trans @ 80% yearlings
1993	L. Granite	4/14	10/31	none	transport all
	L. Goose	4/15	10/31	none	transport all
	L. Mo.	5/3	10/31	none	transport all
	McNary	4/15	11/24	none	transport all
1994	L. Granite	4/5	10/31	none	transport all
	L. Goose	4/5	10/31	none	transport all
	L. Mo.	4/6	10/31	none	transport all
	McNary	4/8	11/28	none	transport all

Transportation Separation

The above table indicates conditions under which fish are *separated* and returned to the river. While it is assumed that transportation always benefits steelhead juveniles, many people believe that smaller migrants (chinook, coho, sockeye) benefit from transportation when flows are low, but are better off in the river when flows are higher and conditions are presumably better.

If a dam has a *separation trigger*, when flows exceed that value, smaller fish are separated from the larger steelhead smolts and are returned to the river. This separation continues according to the *criterion* given in the table. For example, if the criterion is “full transport at 80% yearlings”, this means that fish are separated under high flow conditions until it is estimated that 80% of yearlings have already passed the dam. After that point, all collected fish are transported regardless of flow condition.

There is great variability in separator efficiency: the idea is to retain steelhead for transport and return other fish to the river. As a rule of thumb, CRiSP.1 uses the “80/20” criterion (Table 36), which means that 80% of steelhead are successfully retained, and 80% of smaller fish are successfully returned to the river, but 20% of steelhead also escape to the river, and 20% of smaller fish are retained for transport.

Table 36 Separation efficiencies at transport projects.

Stock	retained for transport	diverted to river
Steelhead	80%	20%
Yearling Chinook	20%	80%
Subyearling Chinook	20%	80%

II.7 - Stochastic Processes

CRiSP.1 provides the ability to vary parameters over a run. This allows a representation of random factors. The randomness is incorporated in different ways for flow, dam passage, reservoir mortality and travel time. The approach is to describe specific parameters as having a deterministic part and a stochastic part. A deterministic part may change with the independent variables that determine the parameter but the value obtained does not change from one model run to another if all factors are the same. The stochastic part changes each time it is calculated in CRiSP.1 or between model runs. The value of the stochastic part is obtained from a random number distribution function using a “broken-stick” distribution function. This is described along with deterministic and stochastic parts of the parameters.

II.7.1 - Stochastic Parameter Probability Density

Variation in many of the stochastic rate parameters is described by a *broken-stick* probability distribution function (pdf). This is a simple function based on a piecewise linear distribution. The probability density function and the cumulative density function are illustrated in Fig. 54. It is described using the 0, 50 and 100% cumulative probability levels.

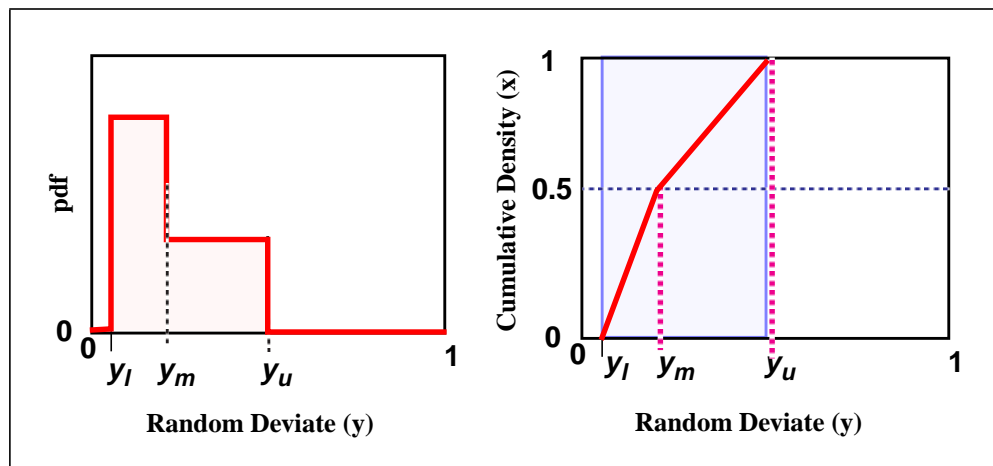


Fig. 54 Probability function (pdf) and cumulative function of the broken stick probability distribution

Random deviates for this broken stick density distribution are obtained from the following transformation formula

$$\begin{aligned} y &= y_l + 2x(y_m - y_l) & x \leq x_m \\ y &= y_m + 2(x - 0.5)(y_u - y_m) & x \leq x_m \end{aligned} \quad (126)$$

where

- x = unit uniform random deviate range $0 < x < 1$
- y_l = lower limit of the distribution range
- y_m = distribution of the median value
- y_u = upper limit of the distribution range.

Although the distribution uses the median, the broken-stick input windows in CRiSP.1 use the mean value since most data reports include a mean in addition to the minimum and maximum values. The median is estimated from these three measures as

$$y_m = \frac{4\bar{y} - y_l - y_u}{2} \quad (127)$$

assuming the mean of the distribution is equal to the average of the mean of the lowest 50% of the distribution and the highest 50%. These are simply the average of the minimum and median, and maximum and median, respectively.

Note that in a skewed distribution the mean and median are different. The result is that the mean specified by the user *must* fall in the middle two quartiles of the distribution, i.e. if the user specifies a minimum of 0 and a maximum of 100 for some distribution, the mean must lie between 25 and 75, inclusive. If the user specifies a distribution outside this range, CRiSP.1 will post a message to that effect in the message window and will direct the user to choose a mean that lies in the acceptable range.

II.7.2 - Stochastic Parameters

Migration

Variability in the migration rate is determined by the equation

$$r_i(t) = r(t)V(i) \quad (128)$$

where

- $r(t)$ = determined from eq (51) on page 39
- $V(i)$ = variance factor which is different for each release i .

The term $V(i)$ is drawn from the broken-stick distribution. The mean value is set at 100%, representing the deterministic $r(t)$ and the upper and lower values are set with sliders under the migration rate variance item in the **Behavior** menu.

The variance factor assumes that variability in migration velocity relative to water velocity is associated with a particular stock of fish. Studies of travel time support this assumption since particular stocks exhibit their own unique relationship with flow.

Flow

In the Scenario Mode, daily flow variations are described by a random process in headwater flow. Details of this process are described in the Headwater Modulation section on page 21.

Dam Passage

Variability in dam passage parameters is applied on each dam time slice, (typically 6 hours). The variability is generated from the broken-stick distribution and is applied to the following variables:

- bypass mortality
- spill mortality

- turbine mortality
- transportation mortality
- day / night fge
- spill efficiency.

II.7.3 - Scales of Stochastic Variability

The scales over which stochastic variability are applied is given in the table below.

Table 37 Model probability density functions

Process	Equation	pdf	Scale
Migration rate variance	eq (55)	broken-stick	release group
Flow in Scenario	eq (16)	Normal	12 hrs
FGE & dam mortality	eq (120)	broken-stick	6 hrs
Spill efficiency	eq (121)	Normal	6 hrs

III. Calibration

III.1 - Calibration Overview

CRiSP.1 is a composite of individual, integrated, process submodels that jointly determine smolt migration and survival.

The model has many parameters which must be determined. The parameters with ecological meaning can often be determined from data sets from other related studies and systems. For the empirical parameters, the model or a submodel are calibrated to lab and field data using a variety of mathematical (optimization) fitting methods. The end result is that through the parameter determination and calibration process, diverse theories and data sets are synthesized into a consistent picture of the process of fish migration and survival through the river system.

Environmental variables describe the observable state of the environment in which fish live. These variables have been determined from historical records dating back to 1970 for all variables and back as far as 1937 for some of the variables. Future values of these variables are assessed from runs of hydromodels and management-derived scenarios of river operations. The environmental variable sets must be determined before the model can be calibrated.

Fish passage observations involve a variety of data, extending back several decades, on the passage timing and survival of fish through various segments of the river and hydrosystem. This ranges from relatively small-scale information on the passage of individual groups of fish at individual dams to system-wide estimates of passage and survival of species over specific years. Observations include brand release studies conducted from 1970's and 80's and PIT tag studies conducted beginning in the late 80's. These data sets yield two levels of information. The direct observations provide passage numbers and timing at individual dams as well as returns of adults to dams and collection points. These raw numbers can be further reduced to estimates of migration rates and fish survival between points in the river and in some cases collection efficiencies at dams.

After all possible variables and parameters have been determined and after any submodels which can be calibrated externally to the model have been calibrated, the parameters related to reservoir passage survival and travel time are calibrated within the model. That is, the model-predicted survivals and travel times are calibrated to NMFS survival estimates and to PIT-tag passage data. In this way, the whole model is ultimately calibrated to data.

The CRiSP.1 model contains a number of different theoretical constructs that can be selected at run time. The selection of which construct to use depends on the available information, the effect of the feature on the calibration, and its ecological soundness. Any calibration of the model is only specific to a particular choice of theoretical constructs.

III.1.1 - Parameter Determination and Calibration techniques

Ecological model parameters are determined (estimated) from both field observations and laboratory studies. Estimates made from field observations (such as fish passage timing or mortality rates) are used with the corresponding environmental variables (Fig. 55). Estimates made from laboratory experiments are analyzed assuming the corresponding laboratory conditions and are used to infer the relevant ecological parameters. For example, the estimation of mortality from gas bubble disease is made based upon laboratory experiments.

Parameter determination involves mixing results from laboratory experiments, isolated field studies on aspects of migration, and system-wide studies of survival and timing. Parameters are determined directly from studies where possible. Then the calibration proceeds in a hierarchy of steps where submodels are calibrated first (where possible) and finally the migration (travel time parameters) and survival (predation parameters) submodels are calibrated. The sequence which is reflected in the chapter organization is: River and Environmental Description, Flow Processes, , Dam Processes and finally migration processes and Reservoir Mortality. The final two steps are in part connected (e.g. in the model, slower migration can result in higher predation mortality) and so are calibrated iteratively until both converge.

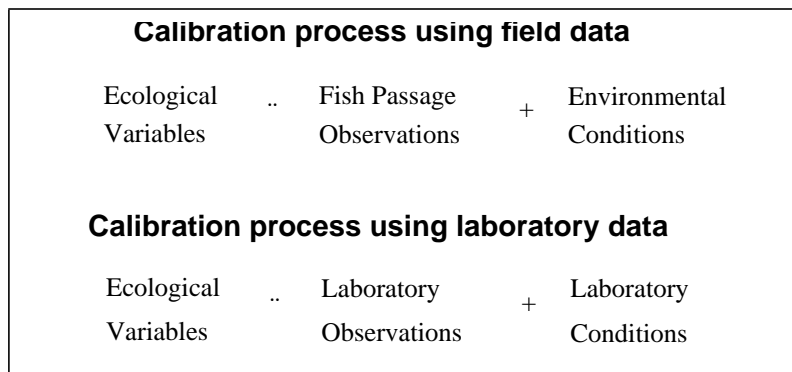


Fig. 55 Calibration process involves using passage and environmental data to estimate the model ecological parameters

Goodness-of-fit

In calibration, the parameters are adjusted so that the model (or a submodel) prediction best fits the observations according to statistical criteria within ecological constraints. A variety of goodness-of-fit measures are applied in the calibrations. The choice of method depends on the type and quantity of data and the dimensions of the data being fit. Where possible graphical examples are given along with statistical measures of the goodness-of-fit. The following approaches are used.

- Least Squares, 2 dimensional regressions (Press et al. 1992) used for
 - t_{dg} supersaturation mortality rates vs. time
 - size vs. mortality rate
 - spill efficiency equations
- Nonlinear regression using the Gauss-Newton algorithm to minimize sums of squares (SPLUS 1991) used for
 - t_{dg} supersaturation mortality rate vs. t_{dg} level
 - prediction of migration rate parameters vs. flow and fish age
- Hyperbolic “amoeba routine” (Press et al. 1992) used for
 - t_{dg} mortality rate vs. t_{dg} level
- Fourier series analysis (SPLUS 1991) used for
 - determining scenario mode flow modulators
- Maximum likelihood estimators via a Marquardt method or a Conjugate Gradient method are used for
 - determining migration rate parameters

- determining predation rate parameters

In cases with limited data, statistical techniques might not converge to a unique best fit solution. In this case the calibration is assisted by selecting one of the parameters within its range inferred from ecological constraints, and then calibrating the remaining parameters.

III.1.2 - Parameter Determination and Calibration status

The calibration process involves fitting the submodels to data using goodness-of-fit measures. First environmental condition variables are ascribed and ecological parameters are calibrated in a hierarchy that can be organized according to categories of similarity and interdependency.

Parameter Determination and Calibration Status by Type

Environmental variables and ecological parameters are listed below along with a description of the state of their calibration.

- Environmental conditions (define river condition)
 - River description parameters relating geometry of river and dams. These parameters are fairly well described and no further improvements of these parameters are expected at this time.
 - Headwater parameters define the river environment flow and temperatures. Flow data exist for years from 1960 through 1999. Temperature in headwaters exists from 1966 through 1999. These parameters are fairly well described and no improvements are expected at this time (other than adding new data for each new year).
- Passage observations (define movement and survival of fish)
 - Release parameters include the number of fish released at each site at each day, the beginning and end of smoltification onset
 - survival and passage timing: information on passage timing and survival of fish through the hydrosystem are adjusted according to model run specifics.
- Ecological parameters (characterize ecological interactions)
 - Total dissolved gas supersaturation parameters relate the buildup of gas as function of spill, flow, and temperature. These have been calibrated with data current through 1999.
 - Age at smoltification initiation (smolt_onset) and completion (smolt_finish) which are release-specific and also may depend on release date itself. Release information along with the predicted passage information at dams and reaches comprises the passage data in the model. These parameters are critical to survival estimates and are under further study.
 - Dam parameters describing passage mortality at dams and fish guidance efficiency have been derived from two decades of studies including results obtained from recent PIT tag studies.
 - Transportation mortality calibration depends on the transport benefit ratio and in-river survival estimates. Although initial estimates have been obtained, both of these factors are under further analysis.
 - Relative predator densities have been derived from CPUE data for the Snake and lower Columbia. This includes base densities for 1990 and prior as well as yearly

- updates to account for the effects of the pikeminnow removal program. Mid-Columbia densities are in progress. Densities for other reaches need work.
- Migration rate parameters have been calibrated for spring/summer and fall chinook and steelhead using data from PIT tag studies.
 - Predator activity has been derived from pikeminnow consumption information from John Day reservoir for spring and fall chinook and steelhead.
 - Predator temperature response parameters have been calibrated for spring/summer and fall chinook and steelhead using NMFS survival estimates.

Parameter Determination and Calibration Status by Submodel

The CRiSP.1 submodels have been calibrated individually or within the model. Data sources are mentioned in the following list. See also the relevant sections in Chapter 2 as well as the following sections on calibration of gas supersaturation and calibration of migration and predation rate parameters.

Travel Time (Migration Rate)

The travel time submodel was calibrated for fall chinook, spring chinook, and steelhead using tagging data from the entire river system and over the entire migration season. Two separate calibrations steps were applied: one to measure the spread of fish as they moved through the reservoir, and the other to measure the change in relative migration velocity with fish age. The first used marked, individual stock releases over a short period of time, and the second used marked and recaptured fish over entire seasons.

Predation Survival (Predation Rate)

Predator-prey interactions including predator temperature response were calibrated to NMFS survival estimates for fall chinook (1995 - 1999), spring chinook (1993 - 1999), and steelhead (1994 - 1999). Predator activities in the forebay and main reservoir were set to the ratio of smolt consumption by pikeminnow in those zones.

First, the predator densities were derived from predation studies in John Day Reservoir and information on the predation index for each of the major reservoirs.

Gas Bubble Disease

The rate of mortality was calibrated from dose-response studies conducted in both field and laboratory conditions.

Dam Passage

Diel passage elements of CRiSP.1 were calibrated from hydroacoustic and radio-tagging studies at dams. Fish guidance efficiency and spill efficiency were calibrated from a number of studies at a variety of dams. Fish guidance efficiency can be set to change with fish age and reservoir level or it can be set constant over the year. Mortalities in dam passage were determined from mark-recapture studies at dams.

Transportation Passage

Separation of large and small fish in transportation was applied from general information on the efficiency of the separators in the transportation facilities at dams. A transportation

mortality was estimated for each species. In addition, time to transport fish through the river system was specified.

Total Dissolved Gas Supersaturation

Total dissolved gas (tdg) supersaturation models were calibrated with data from the Army Corps and includes new information collected in the 1992 drawdown study in Lower Granite Reservoir and Little Goose Reservoirs and from total dissolved measurements from 1994 - 1999.

Flow

Headwater flows in the Scenario Mode were calibrated from information on stream flows provided by the USGS. In Monte Carlo Mode, modulators of the period average hydro-model flows were calibrated with daily flow records at dams.

Water Velocity

Water velocity requires information on reservoir and geometry. The relationship between geometry and elevation and free stream velocities were determined from Lower Granite Reservoir drawdown studies.

Stochastic Processes

The ranges for variables used in the Monte Carlo Mode have been calibrated to available data in the above mentioned studies.

III.2 - Total Dissolved Gas Calibration

WES linear and exponential curves

Most calibration work is based on published documents by WES (Waterways Experiment Station, U.S. Army Corps of Engineers). Some of WES's calibrations were not used because of structural modifications to the dam or more available data that suggested a different dynamic. These empirical equations depend on spill alone and hence if there are significant structural or operational changes to a specific dam, new calibrations would most likely be needed.

Table 38 Lower Snake and Lower Columbia Dams, gas production curves using linear or exponential models.

Project	%-TDG =		Reference
BON	$0.12 \cdot Q_s + 105.61$		WES Apr 1996
TDA	$124.3 - 9 \cdot \exp(-0.273 \cdot Q_s/12)$	juvenile pattern (night)	WES Feb 1997
	$124.3 - 9 \cdot \exp(-0.273 \cdot Q_s/23)$	adult pattern (day)	WES Feb 1997
JDA	$128.4 - 24.4 \cdot \exp(-0.00812 \cdot Q_s)$	juvenile pattern 1998 (with new deflectors)	Shaw 1998
	$124.6 - 26.2 \cdot \exp(-0.0209 \cdot Q_s)$	adult pattern 1998 (with new deflectors)	Shaw 1998
	$0.203 \cdot Q_s + 108.5$	Before 1998 ^a	WES Feb 1997
MCN	$0.0487 \cdot Q_s + 114.9$		WES Feb 1997
IHR	$120.9 - 20.5 \cdot \exp(-0.023 \cdot Q_s)$	1998 (with 2 additional deflectors)	Shaw 1998
	$130.9 - 26.5 \cdot \exp(-0.022 \cdot Q_s)$	1997 (with new deflec- tors)	Shaw 1997
	$138.7 - 79 \cdot \exp(-0.0591 \cdot Q_s)$	Before 1997	WES Feb 1997
LMN	$132.7 - 24.6 \cdot \exp(-0.022 \cdot Q_s)$	juvenile pattern (night)	Shaw 1998
	$131.2 - 36.1 \cdot \exp(-0.059 \cdot Q_s)$	adult pattern (day) ^a	Shaw 1998
LGS	$131.3 - 32.0 \cdot \exp(-0.01985 \cdot Q_s)$	juvenile pattern (night)	WES Feb 1997
	$0.53 \cdot Q_s + 100.5$	adult pattern (day) ^a	WES Apr 1996
LGR	$138.0 - 35.8 \cdot \exp(-0.10 \cdot Q_s/6)$	(1996)	WES Feb 1997
	$138.0 - 35.8 \cdot \exp(-0.10 \cdot Q_s/8)$	(1995)	WES Feb 1997

a. In CRISP.1 an upper bound of roughly 145% was added to these equations.

For LGR and TDA, the Feb 1997 WES reference gave the production curve in the terms of q_s = discharge per spillbay. Here q_s was converted to Q_s/n --assuming the total discharge, Q_s , was uniformly distributed between the number, n , of spillbays. In addition, the number of spillbays in use for Lower Granite was different for 1995 and 1996. In general, because of possible construction or repairs at a dam, the number of spill bays will have to be set separately for each year.

In the cases where the earlier WES reference was used, for Bonneville Dam, Lower Monumental juvenile pattern, and Little Goose juvenile pattern, there was no new recommendation in the 1997 documentation; the authors in fact felt that there was not a good fit available. The equations given in the older reference were nevertheless taken as a starting point for the new gas production model.

For the mid-Columbia dams, the “best” fitting of the three empirical gas production equations was chosen based on available hourly tailwater TDG data from 1995-1998. The bounded exponential performed well in all cases. The results of this calibration are shown below.

Table 39 Mid-Columbia Dams and Dworshak dam gas production curves using linear or exponential model

Project	%-TDG =
PRD	$130.4 - 25.2 \cdot \exp(-0.01045 \cdot Q_s)$
WAN	$139.4 - 26.9 \cdot \exp(-0.00915 \cdot Q_s)$
RIS	$141.1 - 26.9 \cdot \exp(-0.00874 \cdot Q_s)$
RRH	$137.6 - 21.4 \cdot \exp(-0.00733 \cdot Q_s)$
WEL	$0.47 \cdot Q_s + 107.9$ Night $0.15 \cdot Q_s + 107.2$ Day
CHJ	$140.1 - 34.8 \cdot \exp(-0.0241 \cdot Q_s)$
DWR	$135.9 - 71.1 \cdot \exp(-0.4787 \cdot Q_s)$

There was no data for Hells Canyon Dam and so a “generic” set of coefficients was used for this dam. The bounded exponential model, the one predominantly used for the other dams, was chosen and the coefficients were set for moderate gas production.

Table 40 Hells Canyon Dam gas production curves using exponential model

Project	%- TDG =
HCY	$138 - 36 \cdot \exp(-0.02 \cdot Q_s)$

These calibrations are based on spill and typically represent the river best in moderate to high levels of spill. All gas production curves break down when spill gets to be only a few *kcs*. In this case the spill flow retains the dissolved gas level of the forebay.

Exponential Empirical Equation

The parameters in Table 41 were obtained by fitting the exponential submodel to the rating curves. This is the backup model under some circumstances for certain dams.

Table 41 Values for exponential empirical tgd model and last year of its use

Dam	a	b	h
Default	30.0	.025	.030
Little Goose	45.48	0.0106	0.03
Dworshak	34.5	0.0073	0.03
Hells Canyon	32.35	0.025	0.03

Hyperbolic Empirical Equation

This model is retained for backward compatibility. The calibration is applied to the hyperbolic empirical model given by eq (90) on page 73 where

- N_s = percent supersaturation above 100%
- F_s = spillway flow volume in kcfs
- a , b and h = coefficients specific to each dam, derived from tgd rating curves provided by the Army Corps of Engineers.

Data for fitting these parameters were obtained from rating curves provided by Bolyvong Tanovan of the Army Corps of Engineers, North Pacific Division, Portland, OR. The graphs showing observed tgd concentrations in supersaturation for spill flows were copies of in-house documents (unreferenced and unpublished). The graphs were identified with the codes NPDEN-WC, DLL/KPA, 8MAR79. The ruling of the rating curves allowed a precision of ± 0.5 kcfs and ± 0.1 % saturation.

The parameters in Table 42 were obtained by fitting the hyperbolic submodel of eq (90) to the rating curves using a nonlinear “amoeba” routine from Press et al. (1992). Constraints on fitted parameters were

$$0 \leq a \leq 50$$

$$0 \leq b \leq 0.12$$

$$0 \leq h \leq 100.$$

The current values apply to the hyperbolic gas model

Table 42 Values for hyperbolic empirical tgd model

Dam	a	b	h
Default	30.0	0.025	6.00
John Day to 95	45	0.025	6.00
John Day 96, 97	36.11	0.025	6.00
John Day 98	25	0.0247	7.67

GasSpill 1 and GasSpill 2 Mechanistic Equations

The mechanistic tdg saturation submodel was calibrated using flow/spill/gas saturation data from the rating curve data 1984 to 1990 at most projects. (This data set was supplied by Tom Miller of the Walla Walla District of the U.S. Army Corps of Engineers.) The data originated from the Columbia River Operations Hydrological Monitoring System (CROHMS) data base. At each dam the data consisted of: hourly flow and spill, forebay saturation, forebay elevation, tailrace elevation, and temperature, all measured throughout the summer. Using the same gas dissipation mechanism as was used in earlier versions of CRISP.1, the tailrace gas saturation was back-calculated from the next dam downstream.

For each point in time the three parameters a , b , and c below were estimated using a multiple linear regression of the equation defining K_{20} in terms of the energy loss rate, the forebay concentration, and the entrainment coefficient. The mechanistic model for GasSpill 2 assumes that these parameters are related as is given by eq (92) on page 73 where

- K_{20} = entrainment coefficient
- E = energy loss rate
- C_f = forebay concentration
- a , b , and c = coefficients calculated from multiple linear regression of data in Table 43.

For each dam K_{20} is calculated from data using:

$$K_{20} = 1.028^{20-T} \cdot \frac{S}{W \cdot L \cdot \Delta} \cdot \log \frac{P - N_{fb}}{P - N_{sw}} \quad (129)$$

where

- T = water temperature in the forebay in degrees C.
- S = spill in kcfs
- W = spillway width (gates x width/gate)
- L = stilling basin length in feet
- N_{fb} = forebay gas saturation
- N_{sw} = back-calculated spillway gas saturation

$$P = B + (sgr \cdot \alpha \cdot 0.5 \cdot (d - y_0)) + (0.25 \cdot \alpha \cdot (d + y_0))$$

where

- sgr = specific gravity of roller (usually 1)
- $\alpha = 0.0295$
- d = stilling basin depth in feet
- $y_0 = S / (W \cdot \sqrt{2GH})$
- H = hydraulic head in ft is obtained from information in Table 44
- $G = 32.2$ (gravitational constant)

and

$$\Delta = \sqrt[3]{P + 0.25\alpha(d + y_0)} - \sqrt[3]{P - 0.25\alpha(d + y_0)}$$

No data were available for Wanapum Dam thus preventing calibration of both Wanapum and Rock Island, the dam immediately upstream. In these cases the initial calibration of Water Resources Engineers Inc. (WRE 1971) was used as the calibration.

The spill program of 1994 presented an opportunity to recalibrate GasSpill parameters using up-to-date data at a variety of spill levels, including some observations at very high levels that had not previously occurred. Daily average gas levels were compared to those estimated using previously calibrated GasSpill parameters, and parameters were adjusted on a dam by dam basis to bring model predictions into closer agreement with observed data. Required changes were quite small, but the improvement of fit was noticeable; current estimates and observed gas levels are shown for several points in the system in Fig. 56. Note that in all four graphs the predicted and observed saturation tracks do not differ significantly (chi-squared goodness-of-fit test, in all cases $p > 0.05$).

Table 43 Parameters for Gas spill model equations

Dam	L	Basin Floor Elev.	gate wd	# gates	sgr	a	b	c
Default BON GasSpill 1						2.47	1.11	-1.1
Default GasSpill 2						3.31	0.41	-0.032
TDA	170.0	55.0	60	23	0.50	37.00	3.255	-0.394
IHR	178.0	304.0	60	10	1.0	28.05	1.38	-0.28
LMN	218.7	392.0	50	8	1.0	-2.55	4.53	0.018
WEL	30.0	670.0	46	11	1.0	27.84	2.40	-0.28

Table 44 Variables for reservoir geometry, in feet. Dam abbreviations correspond to dams in Table 42.

Dam	Max. Forebay Elevation	Full Pool Depth at Head	Full Pool Forebay Depth	Elevation Spillway Crest	Normal Tailwater Elevation
BON	82.5	68	93	24	16
TDA	182.3	85	105	121	80
JDA	276.5	105	149	210	163
MCN	357	75	105	291	269
IHR	446	100	110	391	343
LMN	548.3	100	118	483	440
LGS	646.5	98	140	581	540
LWG	746.5	100	140	681	638
PRD	488	82.5	101.0		416
WAN	575	83.5	116		497
RIS	619	54	84		558
RRH	710	93	108.4		614
WEL	791	72	1111		707.4

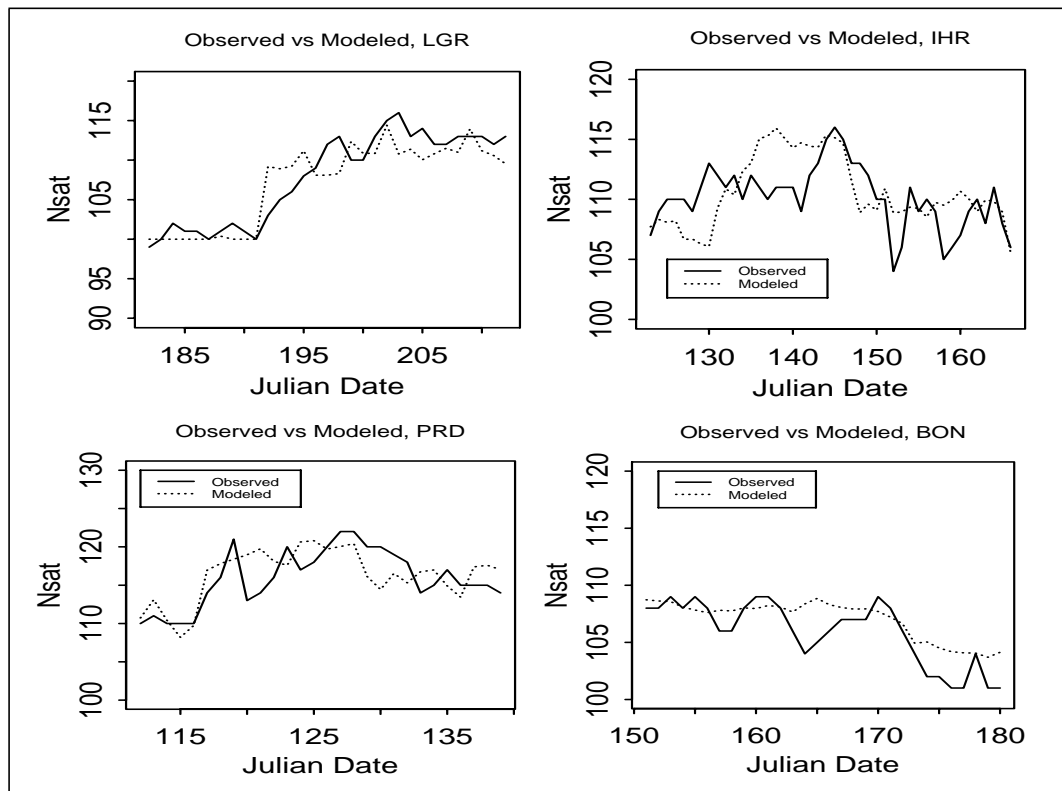


Fig. 56 Comparison of observed and modeled gas supersaturation for 1994 data. Lower Granite Pool Chi-square = 1.88, $p > 0.05$. Ice Harbor Pool Chi-square = 3.38, $p > 0.05$. Priest Rapids Pool Chi-square = 2.01, $p > 0.05$. Bonneville Pool Chi-square = 1.08, $p > 0.05$.

K Entrainment

CRiSP1.6 was used to determine the optimal value of the parameter. This method is computationally intensive, but has certain advantages over simpler regressions. In particular, water travel time is computed based on river geometry and input information on flows and elevations and does not need to be input into the regression for each simulation.

For each dam in turn, CRiSP.1.6 was run with historical data sets from 1995 through 1998, and for each year, a range of k_{entrain} values between 0 and 1 was used to obtain total dissolved gas (TDG) output at the forebay of the downstream dam. The output was compared to DART data on a day-by-day basis. CRiSP.1 produces values for the left and right side of the segment. These values were averaged to produce a single value for the downstream forebay.

To examine the k_{entrain} values at PRD and IHR, both of them were varied simultaneously since they both contribute to mixed waters at the confluence of the Snake and Columbia.

The overall success of the k_{entrain} parameter for each of the model runs was determined by taking the mean sum of squares for all days when there was both an observation and a model prediction:

$$MSS = \frac{\sum_{days} (N_{obs} - N_{model})^2}{n} \quad (130)$$

A second test examined the sensitivity of θ_{dam} to a range of changes in $k_{entrain}$. This involved a series of runs for various levels of θ_{dam} and $k_{entrain}$.

$K_{entrain}$ values change from year to year. In the tables that follow, the optimized $k_{entrain}$ values for each year and dam are shown. In Table 31 on page 78, the analysis was restricted to values of TDG > 100% for both the observed DART values and the CRiSP.1 model predicted. IHR, PRD and BON were not evaluated.

$K_{entrain}$ is an important parameter in some cases. Where CRiSP.1 is poor at fitting the data, even with $k_{entrain}$, other avenues need to be explored: values of other gas parameters, accuracy of flow and spill archives, accuracy of gas archives, functional form of the entrainment coefficient etc.

Examples of the optimization profiles for 1998 are shown in Fig. 57.

Sensitivity of gas production to the θ_{dam} values is very limited. Variation in the MSS was 1% or less across the range of theta from 0 to 10 for all the dams tested in 1997 and 1998. The only significant sensitivity was for WAN in 1995 (11%) and 1997 (7.5%).

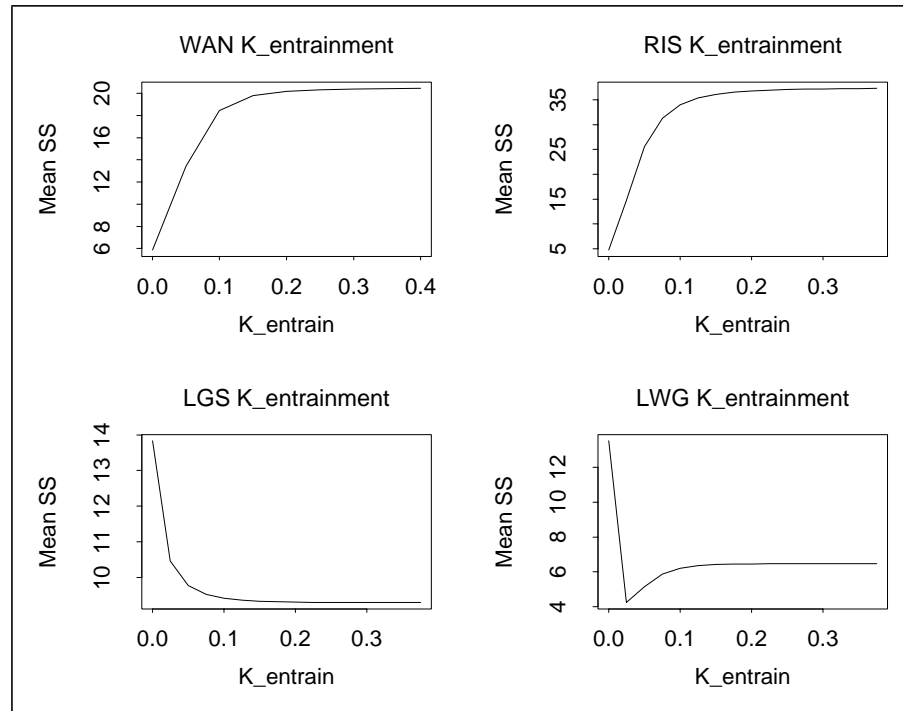


Fig. 57 Example of optimization of $k_{entrain}$ values for 1998.

III.3 - Predation Rate Parameter Calibration

The final parameter sets to be calibrated are those for predation rate (including temperature response) and migration rate. Both of these sets are calibrated by using optimization routines to adjust parameters so as to *best fit* the model to relevant data.

Though travel time is not explicitly represented in the predation rate, it clearly factors into overall predation mortality in the model (since slower migrants have more opportunity to become prey). In the same way, predation rate implicitly effects median travel time in the model (since a higher predation rate has greater effect on the slower migrants). For this reason, the travel time and predation rate calibrations are run alternately until both calibrations have converged. Since we only have survival data for one stock from each species (spring chinook, fall chinook, steelhead), the predation rate parameters found by this process are then used for all stocks in that species.

For each stock, the predation rate equation is based on the following parameters (see equations (64) and (66)):

- $\alpha_{forebay}, \alpha_{reach}$ and $\alpha_{tailrace}$ = predator activity in the river zones
- C_{max}, α and T_{inf} = temperature response equation parameters
- P = predator density (by zone in each river segment)
- T = water temperature in the river segment.

Note that C_{max} multiplies the three activity coefficients (depending on river zone) and thus can be thought of as scaling them. It was never intended that $C_{max}, \alpha_{forebay}, \alpha_{reach}$ and $\alpha_{tailrace}$ be calibrated simultaneously (as that would confound the optimization).

Survival Calibration Process

For survival/predation parameter calibration, we produce a *modeled survival* S^m corresponding to each point S^o of the observed NMFS survival data. This relationship can be expressed as

$$S^o_{i,j} = S^m_{i,j}(\Theta_{fixed}, \Theta_{pred}) + \epsilon_{i,j}. \quad (131)$$

The model-estimated survivals depend both on parameters that are fixed (Θ_{fixed} e.g. flows, temperatures, predator densities as well as the migration rate parameters) and on the predation rate parameters (Θ_{pred}) that are adjusted to calibrate the modeled survival to the survival data.

The calibration process utilizes a conjugate gradient method (an optimization technique) to minimize the sum-of-squares difference between the survival data and the model-predicted survival in each *survival reach* j for each cohort (or release) i in each year:

$$SS = \sum_{year} \sum_{i,j} W_{i,j} \cdot (S^o_{i,j} - S^m_{i,j})^2 \quad (132)$$

where the weights are given (as they are in Hockersmith et al. 1999) as

$$W_{i,j} = w_{i,j} / \left(\sum_i w_{i,j} \right) \text{ for each } j, \text{ where } w_{i,j} = \frac{(S_{i,j}^o)^2}{Var_{i,j}}. \quad (133)$$

The survival data in the numerator of the weighting counteracts the tendency of lower survivals having lower variances. This weighting also diminishes the relative weight of the lower survivals (which are thought to be less accurate).

Survival Data

The data consists of NMFS survival estimates and standard errors for both wild and hatchery released fish released.

The survival estimates for spring chinook consists of fish released above the Lower Granite Reservoir on multiple days in 1993 - 1995 and for releases regrouped (by week) in the LGR tailrace for 1995 - 1998. Estimates for survival are given from release (RLS) to Lower Granite (LGR), LGR to Little Goose (LGS), LGS to Lower Monumental (LMN) and LMN to McNary (MCN). A *survival reach* is defined as being from tailrace to tailrace. Not all data exists for all years.

The survival estimates for fall chinook consists of fish releases regrouped (by week) in the LGR tailrace for 1995 - 1998 with estimates to LGS and LMN.

The survival estimates for steelhead consists of fish releases regrouped (by week) in the LGR tailrace for 1995 - 1998 with estimates to LGS, LMN and MCN and for releases regrouped (by week) in MCN tailrace for 1997 - 1998 with estimates to John Day (JDA) and Bonneville (BON) tailrace.

III.3.1 - Parameter Determination and Calibration

Predator Densities

The predator densities have been determined (by zone and reach) from CPUE indices as described in Section II.4.2. We will revisit this below in Section III.3.2 because of difficulties encountered in the calibration process due, in part, to the high variability of the predator densities between reaches.

Predator Activity Coefficient Determination

Since the survival data is given by reach, from tailrace to tailrace, there is currently no data to differentiate predation occurring in the forebay from that occurring in the reach (pool) and tailrace (or from mortality due to nitrogen supersaturation or dam passage). If we were to calibrate the three activity coefficients α_{reach} , $\alpha_{forebay}$, $\alpha_{tailrace}$ simultaneously, it is likely that the calibration tool would allocate all of the predation activity to the one segment of the model (e.g. forebay) that most closely mimics the survival data.

To avoid this problem, we set $\alpha_{forebay}$, and α_{reach} in the *ratio* of consumption rates (per predator) of smolt by pikeminnow as found by Vigg et. al (1991). That is we set $\alpha_{forebay} = 15.6$, and $\alpha_{reach} = 12.7$ for spring migrants (chinook and steelhead) (see Table 17 on page 52). and we set $\alpha_{forebay} = 20.0$, and $\alpha_{reach} = 12.4$ (see Table 18 on

page 52) for fall chinook. Calibration of the parameter C_{MAX} then scales the activity coefficients.

The tailrace mortality is handled differently in the model (see Zone Specific Formulations of the Predation Model section on page 48). In the calibration, we set $\alpha_{tailrace}$ so that tailrace mortality would be 1% for spring migrants and 2% for fall migrants (set by PATH) if the temperature was at its mean (10.9°C for Spring, 17°C for Fall) and the tailrace predator density was at its mean (15000 preds/km²). The tailrace predations will, of course, vary since the actual temperatures and densities vary.

Temperature Response

Vigg and Burley (1991) provide laboratory results showing the activity response of predators (pikeminnow) to temperature. We thought it is important to try to see this temperature response in the survival data and so did not wish to use their parameter values.

However, the survival data for spring chinook and steelhead, for example, corresponds only to temperatures in the 7°C - 14°C range (mostly 8°C - 12°C) and so cannot be used to predict the upper asymptote of the sigmoidal response. It turned out that many sigmoidal curves would produce a nearly-optimal fit. To counter this problem, we chose that the 95% level of consumption should correspond to a temperature of 15°C (22°C for Fall). This is reasonable given the temperature range of the survival data.

The results from these fixed 95% level runs were used to provide good initial values for our final calibration runs (without the fixed point). But those runs also can provide justifiable results.

III.3.2 - Predator Density - Temperature Response Interaction

The most challenging problem of the spring chinook calibration effort related to the interaction between the predator density data and the temperature response equation and parameters in the spring chinook calibration. Three factors combined to cause the difficulty:

- lower than expected (by the model) survival data from Lower Monumental through McNary
- lower than average predator densities in Ice Harbor and McNary reaches
- slightly higher water temperatures in Ice Harbor and McNary than between Lower Granite Reservoir and Lower Monumental dam.

We observed that the calibration tool was trying to jack up the temperature response, using slightly higher downstream temperatures (*i.e.* higher activity) to make up for lower densities but higher predation in Ice Harbor and McNary reaches. To do this, the calibration tool was producing an extremely steep temperature response function -- one with a predation rate as much as 50 times higher at 15°C than at 10°C for a given predator density. For comparison, Vigg and Burley's (1991) laboratory study found the predation rate to be approximately a 5.5 times higher at 15°C than at 10°C.

As a result, the late-season modeled survival rates were very low compared to the data. Also, the model was decimating the smolt downstream in the Columbia where both temperatures and densities are high.

Density Data Revised

In reaction to this problem of overly steep temperature response, we decided to level out the predator densities -- either by averaging the densities for all reaches, all forebays and all tailraces, or by finding an average for each separately in the Snake, Columbia and Estuary regions.

The five predator density options we studied were:

- River-wide density averages (from 1990 data) for reach, forebay and tailrace.
- Separate density averages (from 1990 data) in the Snake, Mid-Columbia and below Bonneville.
- River-wide averages adjusted (after 1990) for the pikeminnow reduction program.
- Separate averages in the Snake, Mid-Columbia and below Bonneville; adjusted (after 1990) for the pikeminnow reduction program.
- Original densities adjusted (after 1990) for the pikeminnow reduction program.

When the averaged density options (first four) were used, the calibrated sum-of-squares was in the range of 145 to 151. Also, the temperature response curves were of similar steepness to those found by Vigg and Burley (1991) (with $\alpha = 0.4$). It would be meaningless to compare our temperature response curve to Vigg and Burley's directly, since our C_{max} is scaled by the activity coefficient as well as by the (relative) predator density in each reach, forebay and tailrace.

When the full original density data (fifth option) was used, the minimum sum-of-squares was 174 and the temperature response curve was *unreasonably* steep (α much too large).

We opted for the 4th option as most reasonable: separate averages in the Snake, Mid-Columbia and below Bonneville; adjusted (after 1990) for the pikeminnow reduction program. The predator densities in the data files (for spring chinook and steelhead) reflect this simplification. At this time, the predator densities for the fall chinook migration have not been averaged in this way.

III.3.3 - Results

Tables 45, 46 and 47 compare CRiSP.1 model yearly average survivals to NMFS yearly average survivals in the research reach (for which NMFS estimates are given) and for the extended reach. It should be noted that:

- The model is calibrated to weekly or daily survival estimates, not to the yearly average.
- The NMFS survival *projections* are made by assuming that survival is equivalent in each reach during that year. This is an extremely simplistic model. We do not calibrate the model to those results and do not strive to reproduce those results.
- The 1997 and 1998 projections to BON are actually the product of the LGR-MCN and MCN-BON survivals.
- The distribution of release numbers across a season can effect CRiSP.1 model survivals. In most cases, we do not have actual release numbers and so have estimated a release distribution across the season based on release distributions from the few years with known release distributions.
- At the time of this writing, we did not have NMFS survival estimates for the 1999 migrations and so the model was not calibrated to the estimates for those years. Those

results are given for comparison. 1998 fish releases were used with 1999 temperature, flow and other river condition data to produce those results.

Table 45 Spring chinook CRiSP.1 survivals and NMFS survivals for the research reach and down to Bonneville for each year.

Year	Survival Through Research Reach			Extrapolated Survival		
	Research Reach	NMFS Estimates	CRiSP.1 Survivals	Reach	NMFS Projections	CRiSP.1 Survivals
1993	RES-LGO	.75	.76	RES-BON	.32	.41
1994	RES-LMO	.64	.72	RES-BON	.31	.38
1995	RES-MCN	.66	.60	RES-BON	.51	.40
	LGR-MCN		.67	LGR-BON		.46
1996	LGR-MCN	.65	.73	LGR-BON	.47	.57
1997	LGR-MCN	.65	.76	LGR-BON	.48	.59
1998	LGR-MCN	.77	.68	LGR-BON	.63	.49
1999	LGR-BON	.56	.54			

Figures 58, 59 and 60 show modeled versus observed (NMFS estimated) weekly survivals for spring and fall chinook and steelhead over all years for which data exists.

For fall chinook in particular (Fig. 60), the model has difficulty explaining variations in the data. Notice first that for the late season releases (after Julian day 230, August 18) the NMFS estimates tend to be particularly low. An explanation for this might include fish residualizing. Also, the 1997 survivals tended to be low. This may be partially explained by the fact that 1997 was an extremely high flow year.

In fitting the predation parameters for the fall chinook, we found no temperature response. Since CRiSP.1 ultimately models changes in migration and predation due to changes in flow and temperature, the model has a particularly difficult time mimicking variations in the fall chinook survival estimates.

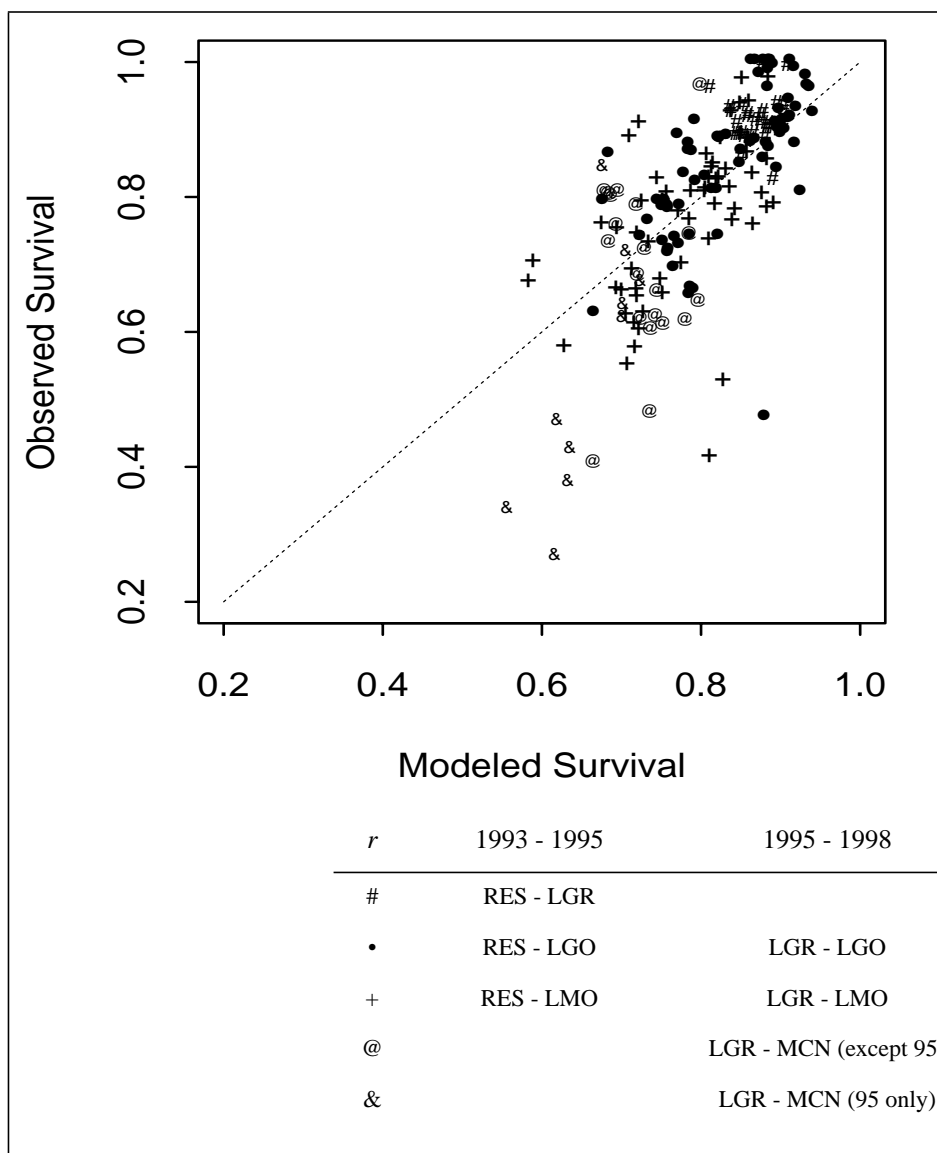


Fig. 58 Spring chinook, modeled vs. observed survivals. The LGR - MCN survivals for 1995 were singled out to highlight the poor behavior of (the late season portion of) that data.

Table 46 Steelhead CRiSP.1 survivals and NMFS survivals for the research reach and down to Bonneville for each year.

Year	Survival Through Research Reach			Extrapolated Survival		
	Research Reach	NMFS Estimates	CRiSP.1 Survivals	Reach	NMFS Projections	CRiSP.1 Survivals
1994	LGR-LMO	.77	.77	LGR-BON	.40	.35
1995	LGR-LMO	.86	.80	LGR-BON	.59	.42

Table 46 Steelhead CRiSP.1 survivals and NMFS survivals for the research reach and down to Bonneville for each year.

Year	Survival Through Research Reach			Extrapolated Survival		
	Research Reach	NMFS Estimates	CRiSP.1 Survivals	Reach	NMFS Projections	CRiSP.1 Survivals
1996	LGR-MCN	.69	.67	LGR-BON	.52	.47
1997	LGR-MCN	.73	.71	LGR-BON	.47	.52
	MCN-BON	.65	.73			
1998	LGR-MCN	.65	.66	LGR-BON	.50	.45
	MCN-BON	.77	.69			
1999	LGR-BON	.50	.44			

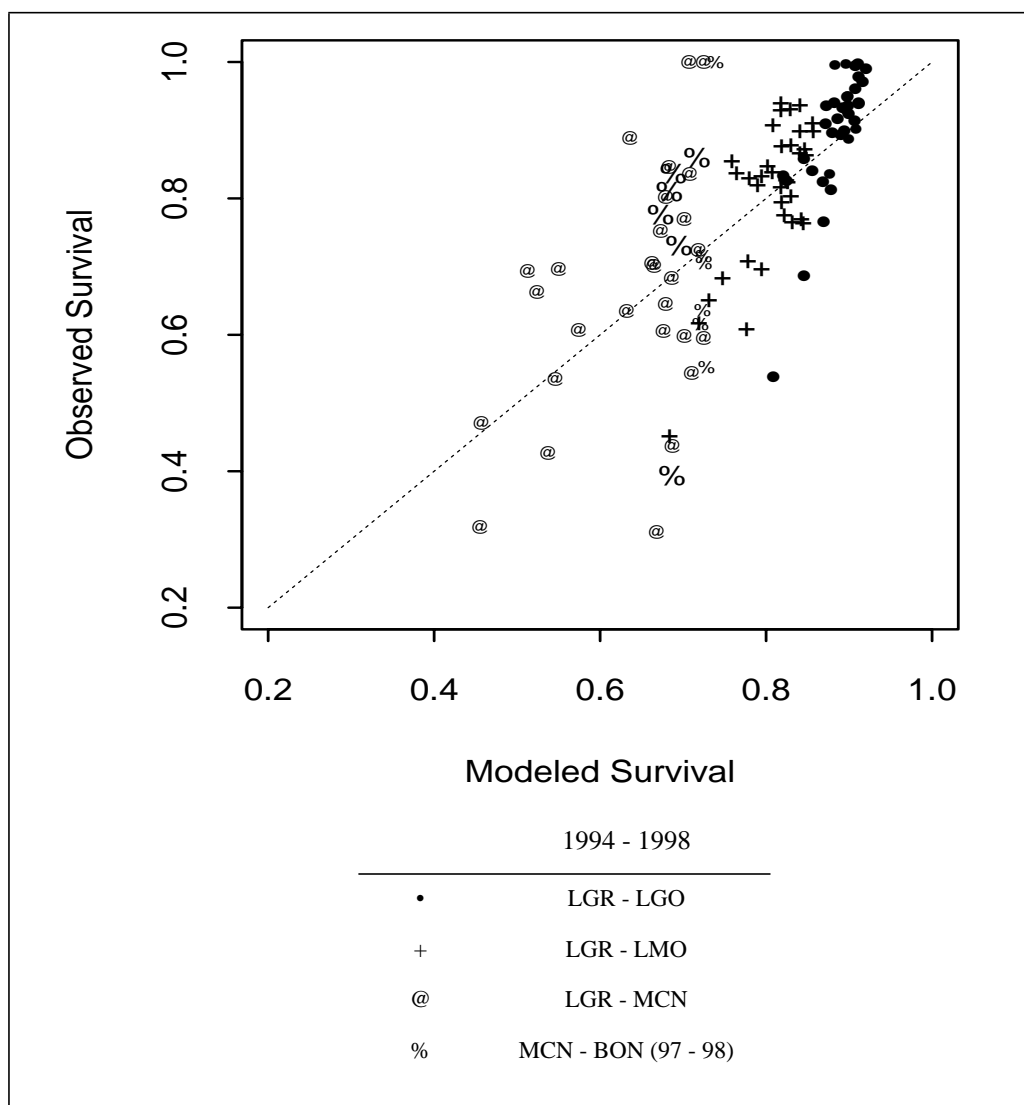


Fig. 59 Steelhead, modeled vs. observed survival.

Table 47 Fall chinook CRiSP.1 survivals and NMFS survivals for the research reach and down to Bonneville for each year.

Year	Survival Through Research Reach			Extrapolated Survival	
	Research Reach	NMFS Estimates	CRiSP.1 Survivals	Reach	CRiSP.1 Survivals
1995	LGR-LMO	.69	.66	LGR-BON	.32
1996	LGR-LMO	.67	.65	LGR-BON	.33
1997	LGR-LMO	.37	.63	LGR-BON	.31
1998	LGR-LMO	.73	.57	LGR-BON	.29

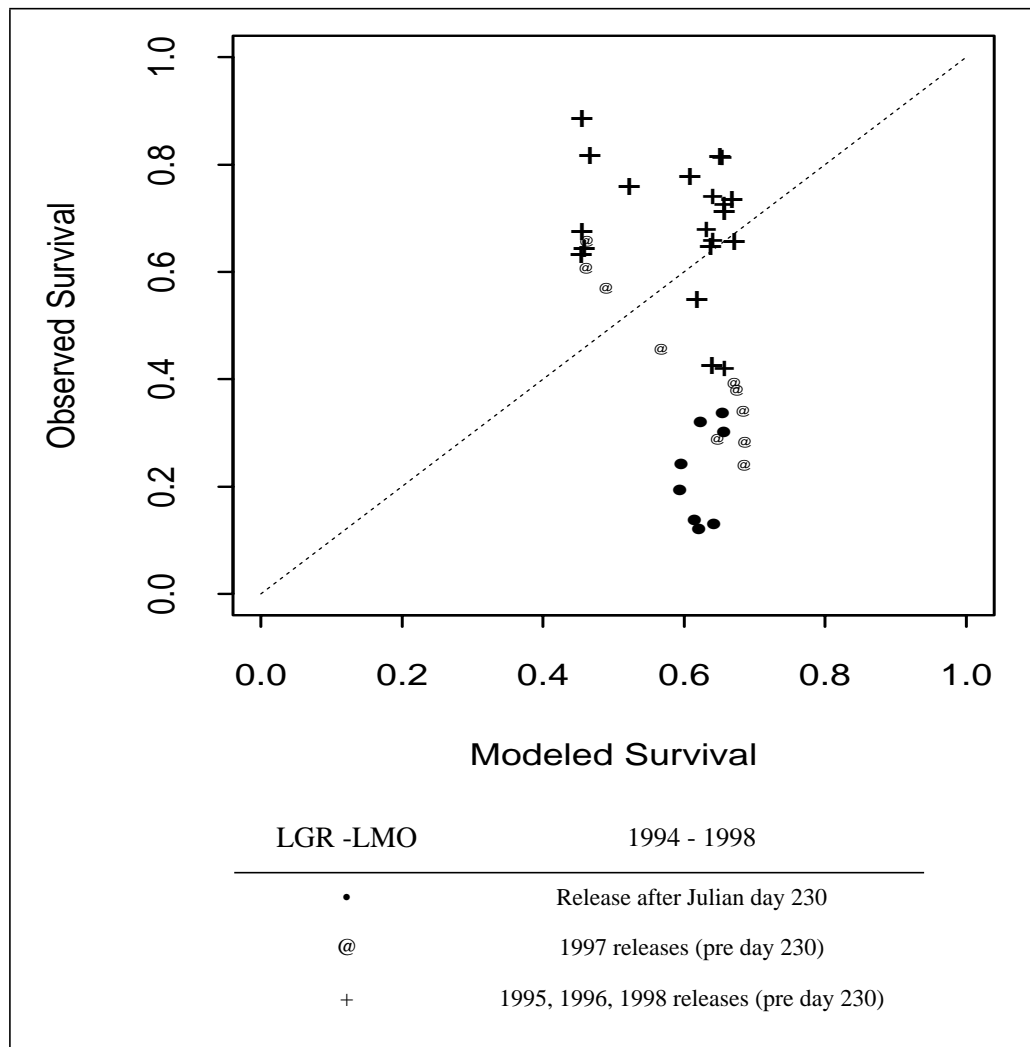


Fig. 60 Fall chinook, modeled vs. observed survivals. The late season releases have been singled out as have the 1997 releases.

III.4 - Calibration of Fish Travel Time Algorithms

After the combined survival -- travel time calibrations are performed for (one stock) in each species, the travel time parameters for the remaining stocks in each species are calibrated. The predation rate parameters found in the combined runs for each species are used in these additional stock runs.

The migration rate equation (eq (51) on page 39) has the following coefficients:

- $r(t)$ = migration rate (miles/day)
- t = Julian date
- $\beta_0, \beta_1, \beta_{\text{flow}}$ = migration rate regression coefficients
- V_f = average river velocity during the average migration period
- α = slope parameter
- T_{SEASN} = inflection point of flow dependent term (in Julian date)
- T_{RLS} = release date (in Julian date).

Other, models containing a subset of these parameters are also used when appropriate (see eq (53) and eq (54) on page 40).

Travel Time Calibration Process

The procedure is to first organize fish into cohorts, which comprise fish released on the same day or on several consecutive days. Based on these cohorts, the following equation is minimized with respect to the migration rate parameters:

$$SS = \sum_{i=1}^n \sum_{j=1}^k (\overline{tt_{mod}} - \overline{tt_{obs}})^2 \quad (134)$$

where n is the total number of cohorts, and k is the total number of observation sites. This equation is fit using a conjugate gradient routine or a Levenberg-Marquardt routine (Press et al. 1992), with derivatives calculated numerically using a finite difference method (Gill, Murray, and Wright 1981).

In the following sections, the estimated migration rate parameters are provided, along with plots that compare the model-predicted average travel times to observed average travel times.

Estimating Vvar

Vvar determines the rate of spreading of the cohort of fish and requires more detailed information to estimate than the migration rate parameters, which just require average travel time information. Estimating *Vvar* requires the distribution of travel times for a cohort; thus the unit of information for calibration is the daily counts. Since there is a great deal of variability in the variances associated with the daily counts, generalized least squares (Draper and Smith 1981) is used to estimate *Vvar*. Zabel (1994) provide the details of this procedure.

Smolt Start/Stop Date

The smolt dates determine when fish initiate migration. Before smolt start date, no migration occurs. After smolt start date and before smolt stop date, a proportion of the release initiate migration on a daily basis. After smolt stop date, all fish in the release have initiated migration. Note that these dates are only relevant if fish are released before they are ready to migrate. If the fish are active migrants, then smolt start and stop dates should be set to dates previous to release dates.

In order to estimate these dates, we require data of fish released before they are ready to migrate. Based on the arrival distribution at the first observation point and the travel time to reach that point, smolt start and stop dates can be estimated.

Travel Time Data

Several criteria are used to select appropriate data sets. First, because migration rate is related to date in season and date of release, it is essential that the calibration data sets have fish released over long periods of time so these effects can be measured. Also, it is desirable to have fish released from the same site over multiple years so that a variety of river conditions are encountered. Sufficient numbers of fish must be observed at downstream observation sites, and fish must be observed at multiple sites. Finally, data sets are selected to represent as many stocks of fish and sections of the river as possible.

Variance in Migration Rate

Variability in plots of observed versus modeled average travel times result from variations among particular releases. To account for this a multiplicative variance is introduced by eq (55) on page 41 where

- r = determined
- $V(i)$ = variance factor that varies *between* releases only.

$V(i)$ is drawn from the broken-stick distribution. The default values for spring and fall chinook and steelhead are mean = 1 low = 0.7 and high = 1.3.

III.4.1 - Results

IV. Testing the Model with Data

IV.1 - Overview

IV.2 - FGE Validation

IV.3 - Travel Time Validation

IV.4 - Survival Validations

V. Sensitivity Analysis

V.1 - Description

V.2 - Results

V.3 - Summary

VI. Parameter Definitions

VII. References

Bypass Survival

- Ceballos, J., S. Pettit, and J. McKern. 1991. *Fish transportation and oversight team annual report - FY 1990*. NMFS.
- Ledgerwood, R. et al. 1990. *Relative survival of subyearling chinook salmon which have passed Bonneville Dam via the spillway or the second powerhouse turbines or bypass system in 1989, with comparisons to 1987 and 1988*. Research report to USACOE, NMFS.
- Ledgerwood, R. et al. 1991. *Relative survival of subyearling chinook salmon which have passed through the turbines or bypass system of Bonneville Dam second powerhouse, 1990*. Research report to USACOE, NMFS.

Fish Depth

- Brege, D.A., Grabowski, S.J., Muir, W.D., Hirtzel, S.R., Mazur, S.J., and Sandford, B.P. 1992. Studies to determine the effectiveness of extended traveling screens and extended bar screens at McNary Dam, 1991.
- Columbia River Biological Service, NBS. 1994. Preliminary Lower Granite Reservoir juvenile salmon distribution and behavior.
- Dauble, D.D., T.L. Page, and Hanf, R.W. 1989. Spatial distribution of juvenile salmon in the Hanford Reach, Columbia River. *Fishery Bulletin* 87: 775-790.
- Erho, M. 1964. Vertical distribution of coho smolts in the forebay of Merwin Dam in 1964. Prepared for Puget Power and Light Co.
- Johnson, L., Murphy, A., and Rawlinson, C. 1985. Hydroacoustic Assessment of Downstream Migrating Salmonids at Lower Monumental Dam in Spring 1985. Prepared for Bonneville Power Administration, contract number DE-A C79-85 BP23174.
- Krcma, R.F. Brege, D.A., and Ledgerwood, R.D. 1986. Evaluation of the rehabilitated juvenile salmonid collection and passage system at John Day Dam, 1985. Prepared for US Army Corps of Engineers, contract number DACW57-85-H- 0001.
- Ledgerwood, R.D., Swam, G.A., and Krcma, R.F. 1987. Fish guiding efficiency of submersible traveling screens at Lower Monumental Dam, 1986. Prepared for National Marine Fisheries Service, Seattle, WA and US Army Corps of Engineers, contract number DACW68-84-4-0034.
- McComas, R.L., Sandford, B.P., and Dey, D.B. 1994. Studies to evaluate the effectiveness of extended-length screens at McNary Dam, 1993. Prepared for National Marine Fisheries Service, Seattle, WA and US Army Corps of Engineers, contract number E86910060.
- Raemhild, G.A., Kuehl, S., and Murphy, A. 1984. Hydroacoustic assessment of downstream migrating juvenile salmonids at Priest Rapids Dam in summer 1983. Prepared for Grant County Public Utility District No.2, and Bonneville Power Administration, Portland, Oregon.
- Smith, J.R. 1974. Distribution of seaward-migrating chinook salmon and steelhead trout in the Snake River above Lower Monumental Dam. *Marine Fisheries Review* 36: 42-45.
- Wright, R.J., Johnson, L., and Schadt, T.H. 1986. Hydroacoustic evaluation of juvenile fish passage at Lower Monumental Dam in Spring 1986.
- Zabel, R.W. 1994. Spatial and temporal models of migrating juvenile salmon with applications. Doctoral dissertation. University of Washington, Seattle.

FGE

Bonneville Dam

- Gessel, M.H., D.A. Brege, B.H. Monk and J.G. Williams. April 1990. *Continued studies to evaluate the juvenile bypass systems at Bonneville Dam-1989*. U.S. Army Corps of

- Engineers, and Coastal Zone and Estuarine Studies report.
- Muir, W.D., A.E. Giorgi, W.S. Zaugg, and B.R. Beckman. May 1989. *An assessment of the relationship between smolt development and fish guidance efficiency at Bonneville Dam*. NMFS/Coastal Zone Report.
- Gessel, M.H., B.H. Monk, D.A. Brege, and J.G. Williams. January 1989. *Fish guidance efficiency studies at Bonneville Dam first and second powerhouses-1988*. NMFS/Coastal Zone Report.
- Gessel, M.H., B.H. Monk, and J.G. Williams. August 1988. *Evaluation of the juvenile fish collection and bypass systems at Bonneville Dam-1987*. NMFS/Coastal Zone Report.
- Gessel, M.H., L.G. Gilbreath, W.D. Muir, B.H. Monk and R.F. Krcma. May 1987. *Evaluation of the juvenile salmonid collection and bypass systems at Bonneville Dam-1986*. NMFS/Coastal Zone Report.
- Gessel, M.H., L.G. Gilbreath, W.D. Muir and R.F. Krcma. June 1986. *Evaluation of the juvenile collection and bypass systems at Bonneville Dam-1985*. NMFS/Coastal Zone Report.
- Gessel, M.H., R.F. Krcma, W.D. Muir, C.S. McCutcheon, L.G. Gilbreath and B.H. Monk. May 1985. *Evaluation of the juvenile collection and bypass systems at Bonneville Dam-1984*. NMFS/Coastal Zone Report.
- Krcma, R.F., M.H. Gessel, W.D. Muir, C.S. McCutcheon, L.G. Gilbreath and B.H. Monk. May 1984. *Evaluation of the juvenile collection and bypass system at Bonneville Dam-1983*. NMFS/Coastal Zone Report.
- Krcma, R.F., D. DeHart, M. Gessel, C. Long, and C.W. Sims. May 1982. *Evaluation of submersible traveling screens, passage of juvenile salmonids through the ice-trash sluiceway, and cycling of gatewell-orifice operations at the Bonneville first powerhouse, 1981*. NMFS/Coastal Zone Report.
- Krcma, R.F., W.E. Farr, and C.W. Long. April 1980. *Research to develop bar screens for guiding juvenile salmonids out of turbine intakes at low head dams on the Columbia and Snake Rivers, 1977-79*. NMFS/Coastal Zone Report.
- Krcma, R.F., C.W. Long, C.S. Thompson, W.E. Farr, T.W. Newcomb, and M.H. Gessel. April 1979. *The development of an improved fingerling protection system for low-head dams, 1978*. NMFS/Coastal Zone Report.

The Dalles Dam

- Monk, B.H., W.D. Muir, and M.H. Gessel. May 1987. *Studies to evaluate alternative methods of bypassing juvenile fish at The Dalles Dam--1986*. NMFS/Coastal Zone Report.
- Monk, B.H., W.D. Muir and R.F. Krcma. June, 1986. *Studies to evaluate alternative methods of bypassing juvenile fish at The Dalles Dam--1985*. NMFS/Coastal Zone Report.

John Day Dam

- Brege, D.A., D.R. Miller, and R.D. Ledgerwood. May 1987. *Evaluation of the rehabilitated juvenile salmonid collection and passage system at John Day Dam--1986*. NMFS/Coastal Zone Report.
- Krcma, R.F., D.A. Brege, and R.D. Ledgerwood. 1986. *Evaluation of the rehabilitated juvenile salmonid collection and passage system at John Day Dam--1985*. NMFS/Coastal Zone Report.
- Krcma, R.F., M.H. Gessel and F.J. Osslander. 1983. *Research at McNary Dam to develop and implement a fingerling protection system for John Day Dam*. NMFS/Coastal Zone Report.
- Swan, G.A., R.F. Krcma and C.W. Long. 1982. *Research to develop an improved fingerling-protection system for John Day Dam, 1981*. NMFS/Coastal Zone Report.

McNary Dam

- Brege, D.A., W.T. Norman, G.A. Swan and J.G. Williams. 1988. *Research at McNary Dam to improve fish guiding efficiency of yearling and subyearling chinook salmon, 1987*. NMFS/

Coastal Zone Report.

- Cramer, S.P., C. F. Willis and K.L. Witty. 1995. Assessment of negative impacts from spill on survival of anadromous salmonids in the Columbia Basin. Submitted to Direct Service Industries, Inc.
- Krcma, R.F., G.A. Swan and F.J. Ossiander. 1985. *Fish guiding and orifice passage efficiency tests with subyearling chinook salmon, McNary Dam, 1984*. NMFS/Coastal Zone Report.
- Krcma, R.F., M.H. Gessel and F.J. Ossiander. 1983. *Research at McNary Dam to develop and implement a fingerling protection system for John Day Dam*. NMFS/Coastal Zone Report.
- Krcma, R.F., W.E. Farr, and C.W. Long. 1980. *Research to develop bar screens for guiding juvenile salmonids out of turbine intakes at low head dams on the Columbia and Snake Rivers, 1977-79*. NMFS/Coastal Zone Report.
- Krcma, R.F., C.W. Long, C.S. Thompson, W.E. Farr, T.W. Newcomb, and M.H. Gessel. 1979. *The development of an improved fingerling protection system for low-head dams, 1978*. NMFS/Coastal Zone Report.
- McCabe, G.T., Jr., and R.F. Krcma. 1983. *Effects of the intermittent operation of submersible traveling screens on juvenile salmonids, 1982*. NMFS/Coastal Zone Report.
- Swan, G.A. and W.T. Norman. 1987. *Research to improve subyearling chinook salmon fish guiding efficiency at McNary Dam--1986*. NMFS/Coastal Zone Report.
- Stuehrenberg, L. and O.W. Johnson. 1990. *Evaluation of factors affecting collection efficiency estimates of chinook salmon and steelhead smolts at McNary Dam*. NMFS/Coastal Zone Report.

Upper Columbia Projects

No fge estimates are available for dams above McNary on the Columbia (Priest Rapids, Wanapum, Rocky Reach, Rock Island, and Wells), despite the fact that at least some of these dams have bypass systems installed (e.g. Rock Island).

Lower Snake Projects

Limited fge estimates are available for some stocks at each of Ice Harbor, Lower Monumental, Little Goose, and Lower Granite Dams.

Ice Harbor Dam

Brege, D.A., G.A. Swan, and J.G. Williams. 1988. *Fish guiding efficiency studies at Ice Harbor Dam, 1987*. NMFS/Coastal Zone Report.

Lower Monumental Dam

Ledgerwood, R.D., G.A. Swan and R.F. Krcma. 1987. *Fish guiding efficiency of submersible traveling screens at Lower Monumental Dam--1986*. NMFS.

Little Goose Dam

Swan, G.A., A.E. Giorgi, T. Coley and W.T. Norman. 1987. *Testing fish guiding efficiency of submersible traveling screens at Little Goose Dam; is it affected by smoltification levels in yearling chinook salmon?* NMFS/Coastal Zone Report.

Lower Granite Dam

- Swan, G.A., B.H. Monk, J.G. Williams and B.P. Sandford. 1990. *Fish guidance efficiency of submersible traveling screens at Lower Granite Dam--1989*. NMFS/Coastal Zone Report.
- Ledgerwood, R.D., W.T. Norman, G.A. Swan, and J.G. Williams. 1988. *Fish guiding efficiency of submersible traveling screens at Lower Granite and Little Goose Dams--1987*. NMFS/Coastal Zone Report.
- Muir, W.D., A.E. Giorgi, W.S. Zaugg, W.W. Dickhoff, and B.R. Beckman. 1988. *Behavior and*

physiology studies in relation to yearling chinook salmon guidance at Lower Granite and Little Goose Dams, 1987. NMFS.

- Swan, G.A., R.F. Krcma and F.J. Ossiander. 1986. *Continuing studies to improve and evaluate juvenile salmonid collection at Lower Granite Dam--1985. NMFS/Coastal Zone Report.*
- Kiehl, S. 1986. *Hydroacoustic evaluation of fish collection efficiency at Lower Granite Dam in Spring 1985. NMFS/Coastal Zone Report.*
- Swan, G.A., R.F. Krcma and F.J. Ossiander. 1985. *Development of an improved fingerling protection system for Lower Granite Dam 1984. NMFS/Coastal Zone Report.*
- Swan, G.A., R.F. Krcma and F.J. Ossiander. 1984. *Research to develop an improved fingerling protection system for Lower Granite Dam. NMFS/Coastal Zone Report.*
- Swan, G.F., R.F. Krcma and F. Ossiander. 1983. *Studies to improve fish guiding efficiency of traveling screens at Lower Granite Dam. NMFS/Coastal Zone Report.*
- McCabe, G.T. Jr., and R.F. Krcma. 1983. *Effects of the intermittent operation of submersible traveling screens on juvenile salmonids, 1982. NMFS/Coastal Zone Report.*
- Iwamoto, R.N. W.D. Muir, B.P. Sandford, K.W. McIntyre, D.A. Frost, J.D. Williams, S.G. Smith, and J.D. Skalski 1994. Survival estimates for the passage of juvenile chinook salmon through Snake River dams and reservoirs. Annual Report 1993. Bonneville Power Administration, Project No. 93-29 Contract No. DE-AI79-93BP10891.

Gas Bubble Disease

- Bentley, Wallace W. and Earl M. Dawley, NMFS. 1981. *Effects of Supersaturated Dissolved Gases on Northern Squawfish, Ptychocheilus oregonensis. Northwest Science, Vol. 55, No. 1.*
- Dawley, Earl M. and Wesley J. Ebel, NMFS. 1975. *Effects of Various Concentrations of Dissolved Atmospheric Gas on Juvenile Chinook Salmon and Steelhead Trout. Fishery Bulletin: Vol. 73, No. 4.*
- Dawley, Earl, Bruce Monk, Michael Schiewe, Frank Ossiander, and Wesley Ebel, NMFS. 1976. *Salmonid Bioassay of Supersaturated Dissolved Air in Water. EPA Ecological Research Series, Report #EPA-600 / 3-76-056, July 1976.*
- Ebel, Wesley J., Earl M. Dawley, and Bruce H. Monk, NMFS. 1971. *Thermal Tolerance of Juvenile Pacific Salmon and Steelhead Trout in Relation to Supersaturation of Nitrogen Gas. Fishery Bulletin: Vol. 69, No. 4.*
- Ebel, Wesley J., Richard F. Krcma, and Howard L. Raymond. 1973. *Evaluation of fish protection facilities at Little Goose Dam and review of other studies relating to protection of other salmonids in the Columbia and Snake Rivers, NOAA, NMFS NWFC, Seattle Washington Progress Report to U.S. Army Corps of Engineers, Contract DACW68-71-0093. 62 p (Processed.)*
- Ebel, Wesley J. and Howard L. Raymond, NMFS. 1976. *Effect of Atmospheric Gas Supersaturation on Salmon and Steelhead Trout of the Snake and Columbia Rivers. - MFR Paper 1191. Marine Fisheries Review, Vol. 39, N0.7, July 1976*
- Fidler, L.E. and S.B. Miller. 1994. *British Columbia Water Quality Guidelines for Dissolved Gas Supersaturation. Draft report to B.C. Ministry of Environment, February 1994. 93 pp. + appendices.*
- Richards, F. A. 1965. *Dissolved gases other than carbon dioxide. In "Chemical Oceanography," J.P. Riley and G. Skirrow (eds.) Academic Press, New York. pp712.*
- Scully, Richard, Edwin. Buettner and Clay Cummins 1983. *Smolt condition and timing of arrival at Lower Granite Reservoir. Bonneville Power Administration Project No. 83-323B. Annual Report 1983*
- Smith, Jim Ross, NMFS. 1974. *Distribution of Seaward-Migrating Chinook Salmon and Steelhead Trout in the Snake River above Lower Monumental Dam. - MFR Paper 1081. Marine Fisheries Review, Vol. 36, No. 8, August 1974.*
- U.S. Army Corps of Engineers, 1994. *Dissolved Gas Abatement Interim Letter Report. COE Portland and Walla Walla District, December 1994.*

White, P.G. et al. 1991. Effects of supersaturation of dissolved gases on the fishery of the Bighorn River downstream of the Yellowtail afterbay Dam. Prepared for the U.S. Department of the Interior Bureau of Reclamation Missouri Basin Region 6.

Hatchery Release Sites

- Chaney, Ed et al. 1988. *Umatilla Subbasin*. Columbia Basin System Planning Drafts. Northwest Power Planning Council and the agencies and tribes of the Columbia Basin Fish and Wildlife Authority.
- Columbia Basin Inter-agency Committee. 1962-1966. *River Mile Indices*. Hydrology Subcommittee.
- Feist, Blake. 1991. *Hatchery Listing*. Fisheries Research Institute, School of Fisheries, University of Washington.
- Fish Passage Center. 1991. *Hatchery Release Site Locations*. Fish Passage Data System file containing hatchery releases for the Columbia Basin from 9/01/90 to 9/11/91.
- Jonasson, Brian et al. 1988. *Deschutes Subbasin*. Columbia Basin System Planning Drafts. Northwest Power Planning Council and the agencies and tribes of the Columbia Basin Fish and Wildlife Authority.
- Parker, Steve et al. 1988. *Klikitat Subbasin*. Columbia Basin System Planning Drafts. Northwest Power Planning Council and the agencies and tribes of the Columbia Basin Fish and Wildlife Authority.
- Seidel, Paul et al. 1988. *Snake Subbasin*. Columbia Basin System Planning Drafts. Northwest Power Planning Council and the agencies and tribes of the Columbia Basin Fish and Wildlife Authority.
- Seidel, Paul et al. 1987. *Lower Snake River Compensation Plan, Lyons Ferry Evaluation Program, Annual Report*. WA Dept. of Fisheries report to the Lower Snake River Compensation Plan office in Boise, ID.
- Water Budget Center. 1991. *Site Definitions Listing*. Supplied by D. Anderson of the BPA to CRISP staff.

Hydraulic Capacities at Dams

- Corps of Engineers. 1989. *Columbia River and Tributaries Review Study: Project Data and Operating Limits. CRT 49 (Revised), Book No. 1*. US Army Corps of Engineers, North Pacific Division, Power Section.
- Corps of Engineers. 1989. *Columbia River and Tributaries Review Study: Project Data and Operating Limits. CRT 69, Book No. 2*. US Army Corps of Engineers, North Pacific Division, Power Section.

Modulators

- Chatfield, C. 1989. *The Analysis of Time Series - An Introduction*. 4th Edition. Chapman and Hall.
- Goel, Narendra S. and Nira Richter-Dyn. 1974. *Stochastic Models in Biology*. Academic Press.
- S-PLUS Manual*, Statistical Sciences, Inc., 1990.

Total Dissolved Gas Supersaturation

- 1996 Field Data Line Plots*. Waterways Experiment Station, Columbia Basin Limnological Research Facility, Dallesport, WA, 1996.
- 1997 Field Data Line Plots*. Waterways Experiment Station, Columbia Basin Limnological Research Facility, Dallesport, WA, 1997.
- 1996 Water Management Plan for FCRPS. Attachment 1. List of Spill Caps*. Bolyvong Tanovan. Army Corps of Engineers North Pacific Division. May 30 1996.
- Boyer, Peter B. 1974. *Lower Columbia and Lower Snake Rivers Nitrogen (Gas) Supersaturation*

- and Related Data Analysis and Interpretation.* NMFS/Coastal Zone Report
- Corps of Engineers. 1989. *Project Data and Operating Limits, CRT Report #49, Book 1.* US Army Corps of Engineers, North Pacific Division, Power Section.
- Corps of Engineers. 1986. *Gasspill: A System Spill Allocation Model for the Control of Dissolved Gas Saturation in the Columbia River Basin.* Corps of Engineers, North Pacific Division, Water Quality Section, Water Management Branch, Engineering Division.
- Corps of Engineers. 1978. *Report on Modeling of Dissolved Nitrogen Gas Data for the Lower Columbia and Lower Snake Rivers, Appendix A.* US Army Corps of Engineers, North Pacific Division, Water Management Branch, Water Quality Section.
- Ebel, Wesley J. H., G. E. Monan, W. E. Farr and G. K. Tanonaka. 1975. Effect of Atmospheric Gas Supersaturation Caused by Dams on Salmon and Steelhead Trout of the Snake and Columbia Rivers. Northwest Fisheries Center Processed Report.
- Evaluation and Analysis of Historical Dissolved Gas Data from the Snake and Columbia Rivers.* ACOE Dissolved Gas Abatement Study Phase 1 Technical Report, Appendix K. April 1996.
- Roesner, L.A. and W.R. Norton. 1971. *A Nitrogen Gas Model for the Lower Columbia River, Final Report.* Water Resources Engineers, Inc.
- Total Dissolved Gas Production at Spillways on the Snake and Lower Columbia Rivers. Memorandum for Record.* Waterways Experiment Station. February 1997 (To be published in ACOE Dissolved Gas Abatement Study Phase II Report).
- Total Dissolved Gas Abatement at Chief Joseph Dam. ACOE Initial Appraisal Report, Seattle District. May 1998.
- Weast, Robert C. and Samuel M. Selby. 1967. *Handbook of Chemistry and Physics.* The Chemical Rubber Co.

Predation Mortality

- Beamesderfer, R.C. and B.E. Rieman. 1988. Predation by Resident Fish on Juvenile Salmon in a Mainstem Columbia Reservoir: Part III. Abundance and Distribution of Northern Squawfish, Walleye, and Smallmouth Bass. In *Predation by Resident Fish on Juvenile Salmonids in John Day Reservoir. Volume I- Final Report of Research.* Final Report 1983-1986. Bonneville Power Administration Report Project No. 82-3 and 82-12. July 1988.
- Beamesderfer R.C. and B.E. Rieman 1991. Abundance and distribution of northern squawfish, walleye and smallmouth bass in John Day Reservoir, Columbia River. *Trans. Am. Fish. Soc.* 120:439-447.
- Burley, C. C. A.C. Klaybor, G. W. Short and G.J. Hueckel 1991. Report E. Evaluation of the North Squawfish Sport-Reward Fishery in the Columbia and Snake Rivers. Washington Department of Wildlife 600 Capitol Way N.E. Olympia WAS 98501-1091. December 3 1991.
- Fish Passage Center, 1986. Smolt Monitoring Program Annual Report 1985. Part I: Estimation of survival for the Columbia Basin Fish and Wildlife Agencies and Tribes, under contract to the Bonneville Power Administration, Contract No. DE-A179-83BP11797, Project No. 80-1.
- Fish Passage Center, 1987. Smolt Monitoring Program Annual Report 1986. Volume I: Migrational Characteristics of Columbia Basin Salmon and Steelhead Trout, 1986. For the Columbia Basin Fish and Wildlife Agencies and Tribes, under contract to the Bonneville Power Administration, Contract No. DE-A179-86BP61747, Project No. 86-60.
- Giorgi, A. E., D. M. Miller and B. Sandford. 1990b. Migratory behavior and adult contribution of summer out-migrating subyearling chinook salmon in John Day Reservoir 1981-1983. Annual Report of Research Financed by Bonneville Power Administration (Agreement DE-A179-88BP50301) and Coastal Zone and Estuarine Studies Division. Northwest Alaska Fisheries Center, National Marine Fisheries Center, National Oceanic and Atmospheric Administration.
- Loch, J. L., Ballinger, D. Christofferson, G. J.A. Ross, M. Hack, C. Foster, D. Snyder and D. Schultz. 1994 (DRAFT May 1994). Significance of Predation in the Columbia River from

- Priest Rapids Dam to Chief Joseph Dam: Abundance and Predation Indexing. Report B. In Significance of Predation in the Columbia River from Priest Rapids Dam to Chief Joseph Dam, Editors C. C. Burley and T.P. Poe. Contract 430-486. Prepared for Chelan County Utility district No. 1 P.O. box 1231. Wenatchee, Washington 98807, and Douglas County and Grant County Public Utilities. Draft January 1994.
- McConnaha, W.E. and L.R. Basham. 1985. Survival of Wells Hatchery Steelhead in the Mid-Columbia River. Part 1: Smolt Monitoring Program, Annual Report, 1985.
- Oregon Dept. of Fish and Wildlife (1988). "Predation by resident fish on juvenile salmonids in John Day Reservoir 1983-1986", Vol.1 U.S. Department of Energy Bonneville Power Administration Division of Fish and Wildlife, U.S. Fish and Wildlife Service Nat. Fishery Research Center, Ore. Dept. of Fish and Wildlife. July 1988. (Referred to as "ODF&W (1988)").
- Parker, R. M. Zimmerman, and D. Ward 1994. Report G. Development of a system wide program: Indexing and Fisheries Evaluation. In: Development of a System wide program: Stepwise Implementation of a Predation Index,. Predator Control Fisheries, and Evaluation Plan in the Columbia River Basin, Volume II. Annual Report 1992. Bonneville Power Administration Report project No. 90-077. June 1994
- Peters, C.N., D.R. Marmorek, and I. Parnell (eds). 1999. PATH Decision Analysis Report for Snake River Fall Chinook. Prepared by ESSA Technologies, Ltd., Vancouver, BC, 322pp.
- Petersen, J.H., D.M. Gadomski, T.P. Poe. 1994. Differential predation by northern squawfish (*Ptychocheilus oregonensis*) on live and dead juvenile salmonids in the Bonneville Dam tailrace (Columbia River). Canadian Journal of Fisheries and Aquatic Science. 51(5):1197.
- Poe, T. P. and B. Rieman. 1988. Predation by Resident Fish on Juvenile Salmonids in John Day Reservoir. Volume I- Final Report of Research. Final Report 1983-1986. Bonneville Power Administration Report Project No. 82-3 and 82-12. July 1988.
- Rieman, B.E., R.C. Beamesderfer, S. Vigg, and T.P. Poe. 1991. Estimated loss of juvenile salmonids to predation by northern squawfish, walleyes and small mouth bass in John Day Reservoir, Columbia River. Trans. Am. Fish Soc. 120:448-458.
- Rieman, B.E., and R.C. Beamesderfer. 1990. Dynamics of a Northern Squawfish population and the potential to reduce predation on juvenile salmonids in a Columbia River reservoir. North American Journal of Fisheries Management 10:228-241.
- Stevenson, J. and D. Olsen. 1991. Yearling chinook travel time and flow regime relationships in the John Day Pool, 1989 and 1990. Pacific Northwest Utilities Conference Committee, Portland OR. Internal report.
- Vigg and Burley. 1991. *Temperature dependent maximum daily consumption of juvenile salmonids by norther squawfish (Ptychocheilus oregonensis) from the Columbia River.* Canadian Journal of Fisheries and Aquatic Resources, Vol. 48, pp 2491-2498.
- Vigg, S., C. Burley, D. Ward, C Mallette, S. Smith, and M. Zimmerman 1990. Development of a system-wide predator control program: Stepwise implementation of a Predation index, predator control fisheries, and evaluation plan in the Columbia River Basin. Annual report 1990. Bonneville Power Administration Report. Project 90-77.
- Vigg S., T.P. Poe, L.A. Pendergast and H.C. Hansel. 1991. Rates of consumption of juvenile salmonids and alternative prey fishes by northern squawfish, walleyes, smallmouth bass and channel catfish in John Day Reservoir, Columbia River. *Trans. Am. Fish. Soc.* 120:421-438
- Ward, D.L. M.P. Zimmerman, R. M. Parker and S. S. Smith. 1994. Report G. Development of a system-wide predator control program: Indexing, fisheries evaluations and harvesting technology development. In: Development of a Systemwide program: Stepwise Implementation of a Predation Index,. Predator Control Fisheries, and Evaluation Plan in the Columbia River Basin, Annual Report 1991. Bonneville Power Administration Report project No. 90-077. February 1993
- Ward, D.L. and J. H. Peterson (in press) Index of Predation of Juvenile Salmonids by Northern Squawfish in the Lower Columbia and Snake Rivers. Transactions of the American Fisheries Society.

Reservoir Survival

- Hilborn, R. R. Donnelly, M. Pascual, C. Coronado-Heranadez. 1993. Draft the relationship between river flow and survival for Columbia River chinook salmon. Draft report to BPA by University of Washington. Project manager Pat Poe.
- Iwamoto, R. E., W.D. Muir, B.P. Sandford, K.W. McIntyre, D.A. Frost, J.G. Williams, S.G. Smith and J. R. Skalski. (1994) Survival estimates for the passage of juvenile chinook salmon through Snake river dams and reservoirs, 1993. US. Dept. of Energy Bonneville Power Administration Division of Fish & Wildlife. October 1993.
- Muir, W.D., S. G. Smith, Iwamoto, R. E., D. J. Kamikawa, K.W. McIntyre, E.E. Hockersmith, B.P. Sandford, P.A. Ocker, T.E. Ruehle and J. R. Skalski. (1995) Survival estimates for the passage of juvenile chinook salmon through Snake river dams and reservoirs, 1994. US. Dept. of Energy Bonneville Power Administration Division of Fish & Wildlife. October 1995.
- Muir, W.D., S.G. Smith, E.E. Hockersmith, S. Achord, R.F. Absolon, P.A. Ocker, B. Eppard, T.E. Ruehle, J.G. Williams, R.N. Iwamoto and J.R. Skalski. (1996) Survival estimates for the passage of yearling chinook salmon and steelhead through Snake River dams and reservoirs, 1995. US. Dept. of Energy, Bonneville Power Administration, Division of Fish and Wildlife. January 1996.
- Raymond, H. L. 1979. Effects of dams and impoundments on migrations of juvenile chinook salmon and steelhead from the Snake river, 1966 to 1975. Transactions American Fisheries Society 108(6): 505-529.
- Raymond, H. L. and C.W. Sims. 1980. Assessment of smolt migration and passage enhancement studies for 1979. National Marine Fisheries Service, Northwest and Alaska Fisheries Center, Coastal Zone and Estuarine Studies Division.
- Schreck, C.B., L.E. Davis, D. Klsey and P.W. Wood. 1994. Evaluation of facilities for collection, bypass and transportation of outmigrating chinook salmon. Draft annual report to U.S. Army Corps of Engineers by Oregon Coop. fish. Res. Unit, Oregon State University, Corvallis
- Sims, C. W, R.C. Johnsen, W. W. Bentley. 1976. Effects of power peaking operations on juvenile salmon and steelhead trout migrations, 1975. National Marine Fisheries Service, Northwest and Alaska Fisheries Center, Coastal Zone and Estuarine Studies Division.
- Sims, C. W, W. W. Bentley, R.C. Johnsen, 1978. Effects of power peaking operations on juvenile salmon and steelhead trout migrations - Progress 1977, National Marine Fisheries Service, Northwest and Alaska Fisheries Center, Coastal Zone and Estuarine Studies Division.
- Sims, C. W. W. W. Bentley, and R. C. Johnsen. 1978 Effects of power peaking operations on juvenile salmon and steelhead trout migrations: progress 1977. National Marine Fisheries Service, Northwest and Alaska Fisheries Center, Coastal Zone and Estuarine Studies Division.
- Sims, C. W., A. E. Giorgi, R. C. Johnsen, and D. A. Brege. 1983. Migrational characteristics of juvenile salmon and steelhead trout in the Columbia River Basin- 1982. National Marine Fisheries Service, Northwest and Alaska Fisheries Center, Coastal Zone and Estuarine Studies Division.
- Sims, C. W., A. E. Giorgi, R. C. Johnsen, and D. A. Brege. 1984. Migrational characteristics of juvenile salmon and steelhead trout in the Columbia River Basin- 1983. National Marine Fisheries Service, Northwest and Alaska Fisheries Center, Coastal Zone and Estuarine Studies Division.
- Sims, C. W., J. G. Williams, D. A. Faurot, R. C. Johnsen, and D. A. Brege. 1981. Migrational characteristics of juvenile salmon and steelhead trout in the Columbia River Basin and related passage research at John Day Dam. Volumes I & II. National Marine Fisheries Service, Northwest and Alaska Fisheries Center, Coastal Zone and Estuarine Studies Division.
- Sims, C. W. and F. J. Ossiander. 1981 Migrations of juvenile chinook salmon and steelhead in the Snake River, from 1973 to 1979: a research summary. National Marine Fisheries Service, Northwest and Alaska Fisheries Center, Coastal Zone and Estuarine Studies

Division.

- Steward, C.R. 1994. Assessment of the flow-survival relationship obtained by Sims and Ossiander (1981) for Snake River spring/summer chinook salmon smolts. US. Dept. of Energy, Bonneville Power Administration Division of Fish & Wildlife. April 1994.
- Williams, J.G. and G.M. Matthews. 1995. A review of flow and survival relationships for spring and summer chinook salmon, *Oncorhynchus tshawytscha*, from the Snake River Basin. Fish. Bull. 93: 732-740.

Spill Efficiency

- Dawson, J., A. Murphy, P. Nealson, P. Tappa, and C. Van Zee. 1983. *Hydroacoustic assessment of downstream migrating salmon and steelhead at Wanapum and Priest Rapids Dams in 1983*. Report to Grant Co. PUD No. 2 (BioSonics, Inc.).
- Erho, M.W., G.E. Johnson, and C.M. Sullivan. 1988. *The salmonid smolt bypass system at Wells Dam on the Columbia River*. Proceedings: Fish Protection at Steam and Hydroelectric Power Plants (EPRI): I-55 - I-69.
- Johnson, L., A. Murphy, and C. Rawlinson. 1985. *Hydroacoustic assessment of downstream migrating salmonids at Lower Monumental Dam in Spring 1985*. BPA report, Contract DE-A C79-85 BP23174, Project Number 84-15 (BioSonics, Inc.).
- Kudera, E.A., C.M. Sullivan, G.E. Johnson, and A.G. Birmingham. 1991. *Evaluation of the smolt bypass system at Wells Dam in 1991*. Draft report; Douglas Co. PUD. (BioSonics, Inc.)
- Raemhild, G., T. Steig, R. Riley, and S. Johnston. 1984. *Hydroacoustic assessment of downstream migrating salmon and steelhead at Rocky Reach Dam in 1983*. Report to Chelan Co. PUD No. 1 (BioSonics, Inc.).
- Ransom, B.H., G.A. Raemhild, and T.W. Steig. 1988. *Hydroacoustic evaluation of deep and shallow spill as a bypass mechanism of downstream migrating salmon and steelhead at Rock Island Dam*. Proceedings: Fish Protection at Steam and Hydroelectric Power Plants (EPRI): I-70 - I-84.
- Ransom, B.H., and A.E. Sullivan. 1989. *Hydroacoustic evaluation of juvenile fish passage at Lower Monumental Dam in 1989*. Final Report (to Army Corps; BioSonics, Inc.).
- Parametrix 1987. Hydroacoustic evaluation of the spill program for fish passage at the Dalles Dam in 1986, final Report. March 1987, Parametrix, Inc. for Portland District COE contract no. DACW57-86-0062.

Transportation

- Fisher, T.R. 1993. Modeling effects of transportation assumptions on the population trends of Snake River chinook salmon: A risk analysis. Bonneville Power Administration manuscript July 1993.
- ANCOOR (Analytical Coordination working Group) 1994. A Preliminary Analysis of the Reasons for Differences Among Models in the 1994 Biological Opinion Prepared by the National Marine Fisheries Service. Final draft report. Prepared by ANCOOR for the National Marine Fisheries Service. 87. pp.

Travel Time

- Dawley, E. M., L.G. Gilbreath, R.D. Ledgerwood, P.J. Bentley, B.P. Sanford, and M.H. Schiewe. 1989. Survival of subyearling chinook salmon which have passed through the turbines, bypass system, and tailrace basin of Bonneville Dam Second Powerhouse, 1988. NOAA, NWFSC, NMFS, Seattle, WA.
- Giorgi, A.E., Stuehrenberg, L.C., Miller, D.R., and Sims, C.W. 1986. *Smolt Passage Behavior and Flow-Net Relationship in the Forebay of John Day Dam*. Bonneville Power Administration, Contract No. DE-A179-84BP39644.
- Giorgi, A. E., D. M. Miller and B. Sandford. 1990b. Migratory behavior and adult contribution of summer out-migrating subyearlings chinook salmon in John Day Reservoir 1981-1983.

- Annual Report of Research Financed by Bonneville Power Administration (Agreement DE-A179-88BP50301) and Coastal Zone and Estuarine Studies Division. Northwest Alaska Fisheries Center, National Marine Fisheries Center, National Oceanic and Atmospheric Administration.
- Stuehrenberg, L.C., Giorgi, A.E., Sims, C.W., Ramonda-Powell, J., and Wilson J. 1986. Bonneville Power Administration, Project No. 85-35.
- Stevenson, J. and D. Olsen. Yearling chinook salmon travel time and flow regime relationships in the John Day Pool, 1989 and 1990. Report to the Pacific Northwest Utilities Conference Committee, Portland, Oregon.
- Fish Passage Managers. 1989. Annual Report. Fish Passage Center, Portland, Oregon.
- Fish Passage Managers. 1990. Annual Report. Fish Passage Center, Portland, Oregon.
- Fish Passage Managers. 1991. Annual Report. Fish Passage Center, Portland, Oregon.
- Ledgerwood, R.D., E.M. Dawley, L.G. Gilbreath, P.J. Bentley, B.P. Sanford, and M.H. Schiewe. 1990. Relative survival of subyearling chinook salmon which have passed Bonneville Dam via the spillway or the second powerhouse turbines or bypass system in 1989, with comparisons to 1987 and 1988. NOAA, NWFSC, NMFS, Seattle, WA.
- Ledgerwood, R.D., E.M. Dawley, L.G. Gilbreath, P.J. Bentley, B.P. Sanford, and M.H. Schiewe. 1991. Relative survival of subyearling chinook salmon that have passed through the turbines or bypass system of Bonneville Dam second powerhouse. NOAA, NWFSC, NMFS, Seattle, WA.
- Smolt Monitoring Program Annual Report. 1985. Brand Release Data. Fish Passage Center, Portland, Oregon.
- Smolt Monitoring Program Annual Report. 1986. Brand Release Data. Fish Passage Center, Portland, Oregon.
- Smolt Monitoring Program Annual Report. 1987. Brand Release Data. Fish Passage Center, Portland, Oregon.
- Smolt Monitoring Program Annual Report. 1988. Brand Release Data. Fish Passage Center, Portland, Oregon.
- Smolt Monitoring Program Annual Report. 1989. Brand Release Data. Fish Passage Center, Portland, Oregon.
- Smolt Monitoring Program Annual Report. 1990. Brand Release Data. Fish Passage Center, Portland, Oregon.
- Stevenson, J. and D. Olsen. 1991. Yearling chinook travel time and flow regime relationships in the John Day Pool, 1989 and 1990. Pacific Northwest Utilities Conference Committee, Portland OR.
- Zabel, R.W. (1994) Spatial and temporal models of migrating juvenile salmon with applications. University of Washington Ph.D dissertation. 223 pp.

Supporting Evidence

- Brawn, V.M. 1982. *Behavior of Atlantic Salmon (Salmo salar) during suspended migration in an estuary, Sheet Harbour, Nova Scotia, observed visually and by ultrasonic tracking.* Can. J. Fish. Aquat. Sci. 39: 248-256.
- Hiramatsu, K.; Ishida, Y. 1989. *Random movement and orientation in pink salmon (Oncorhynchus gorbuscha) migrations.* Can. J. Fish. Aquat. Sci. 46:1062-1066.
- Holm, Marianne, Ingvar Huse, Erlend Waatevik, Kjell B. Doving and Jan Aure. 1982. *Behavior of Atlantic salmon smolts during seaward migration. I: Preliminary report on ultrasonic tracking in a Norwegian fjord system.*
- Saila, S. B., and Shappy, R.A. 1963. *Random movement and orientation in salmon migration.* J. Cons. Int. Explor. Mer. 128: 153-166.
- Stasko, A.B. 1975. *Progress of migrating Atlantic salmon (Salmo salar) along an estuary, observed by radio-tracking.* J. Fish Biol. 7:329-338.
- Tyler, P., J. E. Thorpe, and W. M. Shearer. 1978. *Ultrasonic tracking of the movements of*

atlantic salmon smolts (Salmo salar L.) in the estuaries of two Scottish rivers. J. Fish Biol. 12: 575-586.

Turbine Survival/Mortality

Direct Measure Estimates

- Oligher, Raymond C. and Ivan J. Donaldson. 1966. *Fish passage through turbines tests at Big Cliff hydroelectric plant.* Progress Report #6, USACOE.
- Weber, Kinsley G. 1954. *Testing the effect of a Bonneville draft tube on fingerling salmon.* Unpublished research report. Bureau of Commercial Fisheries (now NMFS), Seattle.
- RMS Environmental Service, Inc. and J.R. Skalski. (1994). Survival of yearling fall chinook salmon smolts (*Oncorhynchus tshawytscha*) in passage through a Kaplan turbine at the Rocky Reach hydroelectric dam, Washington. Prepared for Public Utility district No. 1 of Chelan county. October 1993.
- RMS Environmental Service, Inc. and J.R. Skalski. (1993). Turbine passage survival of spring migrant chinook smolts (*Oncorhynchus tshawytscha*) at Lower Granite Dam, Snake river, Washington. Prepared for Department of the Army. July 1994.

Indirect Measure Estimates

- Holmes, Harlan. 1952. *Loss of fingerlings in passing Bonneville Dam as determined by marking experiments.* USF&W unpublished manuscript.
- Schoeneman, Dale E., Richard T. Pressey, and Charles O. Junge. 1961. *Mortalities of downstream migrant salmon at McNary Dam.* Transactions of the American Fisheries Society, Vol. 90 (1), pp. 58-72.
- Long, Clifford W. 1968. *Research on fingerling mortality in Kaplan turbines.* Unpublished research report, Bureau of Commercial Fisheries (now NMFS), Seattle.
- Long, Clifford W., Frank J. Osslander, Thomas E. Ruehle and Gene Mathews. 1975. *Survival of coho salmon fingerlings passing operating turbines.* Unpublished research report, NMFS, Seattle.
- Ledgerwood, R.D. et al. 1990. *Relative survival of subyearling chinook salmon which have passed Bonneville Dam via the spillway or the second powerhouse turbine or bypass system in 1989, with comparisons to 1987 and 1988.* Unpublished research report, NMFS, Seattle.
- Iwamoto, R. E., W.D. Muir, B.P. Sandford, K.W. McIntyre, D.A. Frost, J.G. Williams, S.G. Smith and J. R. Skalski. (1994) Survival estimates for the passage of juvenile chinook salmon through Snake river dams and reservoirs, 1993. US. Dept. of Energy Bonneville Power Administration Division of Fish & Wildlife. October 1993.
- Muir, W.D., S. G. Smith, Iwamoto, R. E., D. J. Kamikawa, K.W. McIntyre, E.E. Hockersmith, B.P. Sandford, P.A. Ocker, T.E. Ruehle and J. R. Skalski. (1995) Survival estimates for the passage of juvenile chinook salmon through Snake river dams and reservoirs, 1994. US. Dept. of Energy Bonneville Power Administration Division of Fish & Wildlife. October 1995.
- Muir, W.D. S.G. Smith, E. E. Hockersmith, S. F. Achord, R. F. Absolon, P. A. Ocker, T. E. Ruehle, J. G. Williams, R. N. Iwamoto, and J. R. Skalski. Survival estimates for the passage of yearling chinook salmon and steelhead through the Snake River dams and reservoirs, 1995. US. Dept. of Energy Bonneville Power Administration Division of Fish & Wildlife. January 1996.

River Geometry and Velocity

- Nigro, Anthony A. 1989. *Developing a Predation Index and Evaluating Ways to Reduce Salmonid Losses to Predation in the Columbia River Basin*, Table A-2. US Dept. of Energy, Bonneville Power Administration, Division of Fish & Wildlife and Oregon Dept. of Fish and Wildlife, Report #DOE/BP-92122-1.

US Geological Survey provided data from individual field stations using either USGS Form # 9-207 or "Summary of Discharge Measurement Data" forms.

Project Data and Operating Limits: Columbia River Tributaries Review Study. US Army Corps of Engineers North Pacific Division. CRT 49 Book No. 1 1989.

Project Data and Operating Limits: Columbia River Tributaries Review Study. US Army Corps of Engineers North Pacific Division. CRT 69 Book No. 2 1989.

Lower Granite & Little Goose Projects Draft. US Army Corps of Engineers Walla District, October 1992.

Miscellaneous

- Beamesderfer, R.C. B.E. Rieman, L.J. Bledsoe and S. Vigg. 1990. Management implication of a model of predation by a resident fish on juvenile salmonids migrating through a Columbia River reservoir. *North American Journal of fisheries Management* 10:290-304.
- Ebel, W.J., R. W. Krcma and H.L. Raymond. 1974. Evaluation of fish protection facilities at Little Goose Dam and Review of other studies relating to protection of juvenile salmonids in the Columbia and Snake Rivers, 1973. National Marine Fisheries Service, Northwest and Alaska Fisheries Center, Coastal Zone and Estuarine Studies Division.
- Hinrichsen, R. T. Frever, J. Anderson, G. Swartzman and B. Sherer 1991. Columbia River Salmon Passage (CRiSP) Model. Documentation for CRiSP.0. University of Washington, unpublished report. May 1991.
- Henderson, F.M. 1966. Open Channel Flow. Macmillan Publishing Co. New York. Macmillan Series in Civil Engineering-Gene Norby, Editor. 522 p
- Oreskes, N, K. Shrader-Frechette and K. Belitz. 1994. Verification, validation and confirmation of numerical models in the earth sciences. *Science* vol 263 4 February 1994. p 641-646.
- Matthews, G. V. T. 1966. *Book Reviews*, *Animal Behavior*, 14:593-4.
- Press, W. H., S. A. Teukolsky, W. T. Vetterling, and B. P. Flannery. 1992. *Numerical Recipes in C, Second Edition*. Cambridge University Press, Cambridge.
- Norman, W.T. (1992). Factors controlling variations of naturally spawning fall chinook salmon in the Upper Columbia River. Masters Thesis University of Washington 239 pp.
- Rieman. B.E., R.C. Beamesderfer, S. Vigg, and T.P. Poe. 1991. Estimated loss of juvenile salmonids to predation by northern squawfish, walleyes and small mouth bass in John Day Reservoir, Columbia River. *Trans. Am. Fish Soc.* 120:448-458.I
- Richards, F.A. 1965. Dissolved Gases Other than carbon dioxide. Chapter 6 (p 211) in *Chemical Oceanography* Eds. J.P. Riley and G. Skirrow. Volume 1. Academic Press London.
- Smith, J.R., G.M. Matthews, R. Basham, S. Achord, and G. T. McCabe. 1980. Transportation operations on the Snake and Columbia rivers 1979. National Marine Fisheries Service, Northwest and Alaska Fisheries Center, Coastal Zone and Estuarine Studies Division.
- Skalski, J.R., A. Hoffman and S. G. Smith. 1993. Development of survival relationships using concomitant variables measured from individual smolt implanted with PIT-tags. Annual Report 1990-1991. US. Dept. of Energy Bonneville Power Administration Division of Fish & Wildlife. October 1993.
- Spain, G. (1994) Federal mismanagement at heart of salmon decline. *Seattle Times* 7.14.94. Glen Spain is the Northwest Regional director of the Pacific Coast Federation of Fishermen's Associations (PCFFA), an organization of commercial fisherman on the West Coast.
- Ward, D.L. J.H. Peterson, T.P. Poe (1993). Index of predation on juvenile salmonids by northern squawfish in the lower Columbia and Snake Rivers. Report US. Dept. of Energy Bonneville Power Administration Division of Fish & Wildlife. October 1993